



Sterlet Monitoring in the Austrian Danube – A Feasibility Study Using Acoustic Telemetry and Net Fishing

Jakob Neuburg

supervised by:

Univ. Prof. DI Dr. Stefan Schmutz

DI Dr. Thomas Friedrich

DDI Dr. Kurt Pinter

April 2, 2021

Ich erkläre eidesstattlich, dass ich die Arbeit selbständig angefertigt habe. Es wurden keine anderen als die angegebenen Hilfsmittel benutzt. Die aus fremden Quellen direkt oder indirekt übernommenen Formulierungen und Gedanken sind als solche kenntlich gemacht. Diese schriftliche Arbeit wurde noch an keiner Stelle vorgelegt.

Abstract

Due to human impacts, the sterlet (*Acipenser ruthenus*) is critically endangered in the Austrian Danube and the need for action to preserve it arises. To gather missing fundamental knowledge about its ecology, a combined monitoring using telemetry and net fishing shall examine the behavior and structure of the local population.

This study reveals the feasibility of receivers of the Juvenile Salmon Acoustic Telemetry System (JSATS, frequency = 416.7 kHz) and Lotek's Mobile Acoustic Processor system (MAP, 76 kHz) to detect tags and potential differences between a free flowing section, a head of the impoundment and an impoundment and among receivers from two manufacturers. Smaller tags available in the JSATS allow for monitoring of juvenile sterlets.

Detection range and detection efficiency (DE) of receivers were tested with static and drifting tests using test tags. A decision tree analysis showed that at receiver-tag distances of 120 m, 30 % or less of the signals were detected in all habitats. No receiver is able to cover the river width in the study area. Confidence intervals revealed higher detection efficiencies until 90 m of the SR3017 than for both other JSATS receivers. Isolated values of high DE at high distances indicate better suitability of the MAP system.

During net fishing 42 sterlets were caught; 30 females, 8 males and 4 unsexed. With a mean length and weight of 794 mm and 3 440 g females were larger and heavier. Relative condition factors of 1.07, 0.97 and 0.93 indicate good condition. A population size of ca 50 individuals in the study area was estimated using the Chapman estimator and Jolly-Seber method.

A monitoring with acoustic telemetry demands precise planning to cover the river width. The quality of information gained through net fishing paired with insights into the behavior potentially collected by telemetry reasons to combine both methods in the monitoring. Larger tags of the MAP system can be used to monitor occurring large sterlets.

Acknowledgements

First I want to thank my supervisors Prof. Stefan Schmutz, Dr. Kurt Pinter and Dr. Thomas Friedrich for their encouragement and excellent mentoring through the process of data acquisition and analysis and their precious suggestions during the writing process.

I appreciate the great support of my family and the amount of patience they granted me and, especially Laura, who had to endure a good amount of "fishtalk".

Also many thanks to the large number of people who assisted during many days on the boat despite unfavorable weather conditions during some sessions. Thanks to Alex Auhser, Andi Cosma, Chris Witt, Daniel Pelz, Gabriel Schmid, Jay Morgan, Leo Sonten, Lina Florian, Lukas Kaspar, Lukas Walser, Max Brandner, Max Loimer, Max Müller, Michi Grohmann, Roman Burtscher, Ruamruedee Panchan and Stefan Auer.

I further appreciate the great technical support Christian Dorninger and Martin Seebacher offered me during field work and the writing process and the support and advice Prof. Erwin Lautsch gave, in order to apply a sound statistical analysis of the telemetry data.

This thesis was financed with the contribution of the LIFE program of the European Union.

Contents

1	Introduction	1
1.1	Net Fishing as a Tool for Fisheries Research	5
1.1.1	Research Questions - Net Fishing	5
1.2	Telemetry as a Tool for Fisheries Research	5
1.2.1	Research Questions - Telemetry	8
2	Study Sites	9
2.1	Wachau	9
2.1.1	Free Flowing Section	10
2.1.2	Head of the Impoundment	10
2.1.3	Impoundment	10
2.2	Freudenau	11
3	Material and Methods	13
3.1	Telemetry	13
3.1.1	JSATS	13
3.1.2	MAP Series	14
3.1.3	Receivers	15
3.1.4	Tags	16
3.1.5	Test Design	16
3.1.5.1	Detection Range	16
3.1.5.2	Detection Efficiency	18
3.1.6	Abiotic Parameters	18
3.1.7	Data Analysis - Telemetry	19
3.2	Net Fishing	22
3.2.1	Net Deployment and Fish Handling	22
3.2.2	Data Analysis - Net Fishing	25
4	Results	27
4.1	Telemetry	27
4.1.1	Detection Range	27
4.1.2	Detection Efficiency	27
4.1.3	Overall Performance	29
4.1.4	Performance among Habitats	32
4.1.5	Abiotic Parameters	34
4.1.6	Performance of JSATS in other studies	36

4.2	Net Fishing	38
4.2.1	Catch Per Unit Effort	38
4.2.2	Total Catches	39
4.2.3	Sterlets	41
4.2.3.1	Condition Factors	44
4.2.3.2	Recaptures	45
4.2.4	Population Estimation	46
5	Discussion	49
5.1	Telemetry	49
5.1.1	Overall Performance	49
5.1.2	Performance among Habitats	53
5.1.3	Performance of JSATS in other studies	56
5.1.4	Abiotic Parameters	61
5.1.5	WHS3250	63
5.2	Net Fishing	65
5.2.1	Catch Per Unit Effort	65
5.2.2	Sterlets	65
5.2.3	Population Estimation	68
6	Conclusions	70
	References	75
	Online References	84
	Appendix	85

Abbreviations

- 20DE - the distance at which detection efficiency is 20 %
- CI - confidence interval
- CPUE - catch per unit effort in Ind/h/net
- CRT - Classification and Regression Tree
- DE - detection efficiency
- DE100m - DE at 100 m
- DE200m - DE at 200 m
- DE_{mig} - "probability of detecting a tag moving past a specific location" (Melnychuk, 2012)
- DE_{mobile} - "probability of detecting tags present within the area sampled by mobile surveys" (Melnychuk, 2012)
- DE_{single} - "probability of detecting a single transmission of a tag" (Melnychuk, 2012)
- DR - detection range
- ff - free flowing stretch
- f_r - female with ripe gametes
- f_u - female with unripe gametes
- himp - head of the impoundment
- HPP - hydropower plant
- imp - impoundment
- JSATS - Juvenile Salmon Acoustic Telemetry System
- JS-model - Jolly-Seber-model
- K_F - Fulton's condition factor
- K_n - relative condition factor

- MAP - Mobile Acoustic Processor, telemetry system manufactured by Lotek
- N - estimated population size
- N_i - estimated population size at sampling day (i) after Manly (1984)
- n_1 - number of animals captured at the first visit
- n_2 - number of animals captured at the second visit
- n_i - caught sterlets at sampling day (i) after Manly (1984)
- n_M - number of recaptured animals that were marked
- PIC - pulse interval coding
- PIT - passive integrated transponder
- PSL - Power Spectrum Level
- p_i - sampling intensity at sampling day (i) after Manly (1984)
- Q - discharge in m^3/s
- Sd - Secchi depth in cm
- SNR - Signal to Noise Ratio
- SPL - Sound Pressure Level
- T - water temperature in $^{\circ}C$
- TL - total length in mm
- W - weight in g

1 Introduction

Sturgeons (*Acipenseridae* Bonaparte, 1831) are an old group of animals with fossil findings from the Northern Hemisphere (Bemis *et al.*, 1997) dating back 200 million years (Billard and Lecointre, 2001). Currently, 25 species of *Acipenseridae* inhabit the Holarctic region (Bemis and Kynard, 1997), where they are often the largest freshwater fish in a fauna (Bemis *et al.*, 1997). Due to their size, sturgeons can occupy central parts of large rivers where they reside at the bottom and mostly feed benthically. Exceptions are the beluga (*Huso huso* Linnaeus, 1758) and kaluga (*Huso dauricus* Georgi, 1775) which feed on fish. Their, relatively to the body size, small eyes do probably not contribute much to the location and capture of prey (Billard and Lecointre, 2001). Sturgeons use their rostrum, which is equipped with tactile barbels, to dig in search of food. With a thick-lipped, protactile mouth, where the upper jaw can be projected out, prey is caught (Bemis *et al.*, 1997). Maturity is reached late in life and spawning does not take place annually but repeatedly (Bemis and Kynard, 1997).

The smallest species among the Danube sturgeons is the sterlet (*Acipenser ruthenus* Linnaeus, 1758) which is potamodromous and, therefore, fulfills its whole life cycle in freshwater habitats of the Danube and its tributaries (Hensel and Holčík, 1997; Billard and Lecointre, 2001; Friedrich *et al.*, 2014; Bănăduc *et al.*, 2016). Normally, it does not outgrow a size of 100 cm, a weight of 6.5 kg and 24 years. However, exceptional fish can reach 125 cm and a weight of 16 kg at an age of up to 27 years (Holčík, 1989). Males reach puberty at 3-5 years, females at 4-7 years, respectively (Billard and Lecointre, 2001) and show a high fecundity by producing between 15 000-20 000 eggs per kg body weight. Sterlets spawn during high water periods in spring at temperatures between 12-17 °C. If spawning occurs every year is not entirely solved, possibly it depends on the latitude whereas fish show later maturity in higher latitudes (Holčík, 1989). After hatching sterlets grow very fast. An increase in weight from 0.65 g to 88.5 g in only four months could be observed in the Danube (Holčík, 1989).

To support a sterlet population it is necessary that, depending on the season and life stage, different habitats are available (Ratschan *et al.*, 2017). Descriptions of spawning habitats in literature are rough and diverse. Reported are gravel or rocky bottom in the main channel (Friedrich, 2013) with high flow velocities, flooded floodplains and the head of impoundments at a depth range of 2-15 m (Holčík, 1989). For spawning success, however, the availability of a suitable spawning habitat is a critical factor (Bemis and Kynard, 1997). Optimal spawning conditions occur during moderate water levels in spring (Friedrich, 2013). Juvenile sterlets are reported to be found in sandy shallows (Holčík, 1989) or e.g. at the Drava River a small sterlet with 2.5 cm was found at the head of the impoundment Völkermarkt in a benthic sample 200 m downstream of a small tributary at a depth of 8 m with small gravel (microlithal), overgrown with algae

and a flow velocity of 0.1 m/s (Honsig-Erlenburg and Friedl, 1999). If available, sterlets patrol very different habitats in search of food like the main channel, backwaters and impoundments (Friedrich, 2013). However, if sufficient food is available, sterlets showed less movement in the Volga river (Kalmykov *et al.*, 2010). Strelnikova (2012) reported sterlets changing their feeding behavior between seasons depending on the availability of prey organisms. The presence of prey organisms related to different sediment and habitat types in the stomachs of sterlets further strengthen the assumption of high mobility. At low water levels, spawning and feeding habitats are the same (Friedrich, 2013) and it is also possible that spawning habitats are located close to the wintering habitats, which are usually deep areas where a good oxygen supply is guaranteed (Friedrich, 2013) like depressions in the river bed (Holčík, 1989), bends and areas protected from the current (Kalmykov *et al.*, 2010) or behind bridge piers (Friedrich, 2013).

Nevertheless, little is known about the life history and habitat requirements of the sterlet (Lenhardt *et al.*, 2010; Friedrich *et al.*, 2014) and for most sturgeons also little was known before populations declined (Acolas *et al.*, 2017). Basic information about life history is fundamental and helps in decision making regarding conservation measures (Cooke *et al.*, 2013). Furthermore, populations can show differing habitat preferences (Pollock *et al.*, 2015) and even different life history patterns (Bemis and Kynard, 1997) and behavior (Holčík, 1989; Kalmykov *et al.*, 2010), which supports the demand for further research on the required habitat for all stages of the life cycle (Billard and Lecointre, 2001; Lenhardt *et al.*, 2010; Ratschan *et al.*, 2017) and especially the very early life stages (Pollock *et al.*, 2015).

Although sturgeons show similarities in biology and behavior, meaningful biological generalizations are difficult because of the large range in size and differences in migration patterns (Bemis *et al.*, 1997; Acolas *et al.*, 2012). Since the sterlet usually stays in freshwater, long migrations are not observed frequently (Holčík, 1989). In the Danube, the documented maximum distance migrated by sterlets is 322 km (Hensel and Holčík, 1997), but usually migration distances are below 200 km (Holčík, 1989). During downstream migrations, daily migrations between 7 to 23 km were reported during a tagging experiment (Holčík, 1989). Those distances let assume that different populations within the Danube were in contact and exchanged with each other (Friedrich *et al.*, 2014). For spawning, sterlets migrate upstream during spring floods, whereby they migrate further when floods are stronger and vice versa (Holčík, 1989). In the River Volga, migrations of sterlets correlate with water temperature (Kalmykov *et al.*, 2010). Acolas *et al.* (2012) observed different migration patterns among stocked juvenile European sturgeons (*Acipenser sturio* Linnaeus, 1758) in the river Gironde, which were released during different flow conditions. Downstream migrations of sturgeons are usually related to feeding (Bemis and Kynard, 1997). Ratschan *et al.* (2017) observed downstream migrations of sterlets when the water level was lower and also strong vertical diurnal migrations. Sterlets stayed in deep areas during the day and migrated to shallower areas at night, which were still between 8-12 m deep and probably served as feeding habitat. In summer, sequences of long residence at certain points, which were interpreted as feeding habitats, were observed (Friedrich *et al.*, 2016). Ratschan *et al.* (2017) reported that during warm months upstream migrations ended at the hydropower plant Jochenstein.

The authors conclude that if there were no obstacles, migratory fish would use a very extended habitat. Therefore, the restoration of sterlet migrations should be prioritized to make habitats for all life stages accessible. Moreover, populations can show specifically timed migrations from wintering to feeding habitats depending on the availability of prey. Thus, for proper management it is necessary to understand such complexities at both, the species and the population level (Nelson *et al.*, 2013).

From historically six sturgeon species that occurred in the Danube, all except the European sturgeon, which is meanwhile extinct in the Danube River basin (Bănăduc *et al.*, 2016), resided in Austrian waters (Friedrich, 2013) and were common in the Danube (Hensel and Holčík, 1997). Nowadays, all sturgeons except the sterlet are classified as regionally extinct in the Austrian Danube (Wolfram and Mikschi, 2007). Hence, populations of those species do not occur in the upper Danube. The sterlet is currently classified as critically endangered (Wolfram and Mikschi, 2007) due to a very limited distribution in the upper and middle Danube (Hensel and Holčík, 1997).

Currently, sterlet populations are at historic low levels (Ludwig *et al.*, 2009) and various human impacts are responsible for declining sturgeon populations. A major threat is the construction of hydropower plants resulting in damming of the river, hindering sturgeons in their migrations and making key habitats unaccessible (Bemis and Kynard, 1997; Hensel and Holčík, 1997; Sandu *et al.*, 2013; Friedrich, 2013; Friedrich *et al.*, 2014; Bănăduc *et al.*, 2016; Ratschan *et al.*, 2017). After the construction of the hydropower plant Freudenu at Vienna, upstream spawning habitats were lost (Friedrich, 2013).

Sturgeons were an important food source and of great economical value along the Danube since ancient times (Bănăduc *et al.*, 2016). They were caught with harpoons or fences which blocked the whole river width (Friedrich, 2013). In Vienna, sterlets were caught until stocks declined and the trade with other countries only ceased with the beginning of World War I (Friedrich *et al.*, 2014). First regulations on sturgeon fisheries came up already in the 5th century and further management restrictions were formulated for the whole Danube basin in 1895 (Friedrich, 2013). Holčík (1989) summarized sterlet fisheries in the 20th century. Between 1935 to 1939, the world-wide harvest amounted to almost 800 tons annually, 700 tons in the former U.S.S.R alone. The largest numbers were caught in the Volga River System. Between 1963 to 1979, 63.5 tons were harvested annually from the Danube System, mainly in former Yugoslavia and Bulgaria. In the late 1980s, most sterlet catches came from the Danube system. In the former U.S.S.R., bans of sterlet fisheries in most water bodies followed the harvest of mainly immature fish (Holčík, 1989). Due to low numbers, Romania banned sturgeon fishing for 10 years in 2006 followed by Bulgaria (Friedrich, 2013).

Lenhardt *et al.* (2010) summarize the development of the sterlet fisheries catches in the Serbian part of the Danube. From the second half of the 20th towards the early 21st century, commercial sterlet captures developed towards younger age classes (mostly 0+ and 1+). However, even though the data on sterlet catch for this period was unreliable, the authors attribute the fishery of this time period as unsustainable. Fish below the prescribed length and outside the allowed time window were caught. Meanwhile, sterlet fishery in Serbia is prohibited (Friedrich, pers. comm.).

Due to their way of life oriented at the bottom of rivers, sterlets are exposed to both, pollution of water and sediments (Lenhardt *et al.*, 2010). Sources are discharge of industrial, agricultural and domestic wastewater (Lenhardt *et al.*, 2006). Effects of pollution can also affect whole populations as observed in the Volga River, where poor water quality is responsible for low survival of juveniles and, therefore, a constant decline of sturgeons (Lenhardt *et al.*, 2006). On the other hand, the reappearance of sterlets in the Slovakian part of the Danube in the 1970s was attributed to increasing water quality (Hensel and Holčík, 1997).

Sturgeon species tend to hybridize easily (Billard and Lecointre, 2001; Bănăduc *et al.*, 2016) and hybridization might increase due to anthropogenic alterations of river habitats (Bemis *et al.*, 1997). Ludwig *et al.* (2009) were the first to describe hybridization between sterlets and Siberian sturgeons (*Acipenser baerii* Brandt 1869) in the Danube. The hybridizations occurred within the last self-reproducing sterlet population in the upper Danube and pose a huge threat through loss of adopted alleles. More hybrids were caught between 2013 and 2015, but numbers decreased because caught Siberian sturgeons were removed (Ratschan *et al.*, 2017). However, increasing numbers of Siberian sturgeons in aquaculture correlate strongly with catches in the wild because of escapes during flood events and releases from ponds and aquariums after they reach a certain size (Ludwig *et al.*, 2009).

Currently, different programs supporting sturgeon populations are being implemented. The goal of the Sturgeon 2020 program is to ensure viable sturgeon populations in the Danube by 2020. In the upper Danube, due to the lack of basic knowledge, planned measures for supporting the sterlet are population analysis and life cycle assessment (Sandu *et al.*, 2013). The goal of the Interreg project at the border between Austria and Germany is to gather basic knowledge about the local sterlet population with the use of acoustic telemetry methods (Friedrich *et al.*, 2016). The aim of the Life Sterlet project is the reestablishment of viable sterlet populations of over 2 000 mature specimen in the river Morava and in two stretches of the Danube, namely the Wachau and along the National Park Donauauen (Friedrich, 2017). Hence, 10 000 juvenile sterlets reared in a hatchery under near-natural conditions are stocked yearly in all stretches until 2021. In general, most stocking measures take place in the Ponto-Caspian area and stocking of juveniles is considered as contributing significantly to sustained populations (Billard and Lecointre, 2001). Furthermore, high survival rates and different migration patterns in stocked juvenile European sturgeon highlight their adaptive capacity to different food items and salinity (Acolas *et al.*, 2012). Stocking should take place with native genetic material because non-native alleles may dilute or cause losses of locally adapted alleles (Ludwig *et al.*, 2009). In the Life Sterlet project, an additional monitoring program shall yield information about habitat use and behavior. The findings will be used to conserve key habitats and to develop a management plan for the sterlet in the upper Danube (Friedrich *et al.*, 2016). However, in the United States conservation measures which did not address habitat degradation generally failed to restore healthy sturgeon populations. Moreover, should habitat requirements for each species and life stage be known before conservation programs targeting habitat enhancement are implemented (Billard and Lecointre, 2001).

1.1 Net Fishing as a Tool for Fisheries Research

In order to collect information about the remnants of the sterlet population in the river section below Vienna, different methods are available. Since sterlets are reportedly being caught in the Danube with the use of nets (mainly directly below hydropower plants (Friedrich, 2013; Ratschan *et al.*, 2017)), net fishing evidently is an adequate method to capture sterlets. According to Friedrich *et al.* (2016), information like photographs, morphological and meristic characteristics of the fish, as well as DNA samples can be gathered. Additionally, when fish are marked using passive integrated transponder (PIT) tags, they can be identified to analyze recaptures and to estimate the population size. In the past, data from sterlets captured with nets even revealed long migrations with the passage of several hydropower plants from sterlets stocked in Germany (Friedrich, 2013). Moreover, does Friedrich (2013) refer to a personal communication with ZAUNER (s.a.) that, in comparison to other fish species, sturgeons cope well with the stress of being entangled in a net and show no injuries or odd behavior.

Hence, net fishing is part of the monitoring program in the course of the Life Sterlet project, where gathered information about captured sterlets will be analyzed. Therefore, one aim of this master thesis is to answer the following research questions:

1.1.1 Research Questions - Net Fishing

- What is the structure of the sterlet population in the sampled area and are there differences between males and females regarding size, weight and condition?
- What is the size of the sterlet population in the sampled area calculated based on recaptures with the Chapman estimator and the Jolly-Seber method?

1.2 Telemetry as a Tool for Fisheries Research

Additional tools, which are widely used to study various biological questions, such as the habitat use and migration behavior of a variety of freshwater taxa, are active telemetry tools like radio and acoustic telemetry (Melnychuk, 2012; Cooke *et al.*, 2013). Their application helped e.g. in collecting important information about habitat use, migrations and spawning of the meanwhile well-studied gulf and green sturgeon and, nowadays, telemetry data is often used as the basis for conservation regulations in the United States (Nelson *et al.*, 2013). Furthermore, it helped in rapidly closing some information gaps (Nelson *et al.*, 2013). To estimate survival, fewer fish (than with conventional methods) need to be tagged using radio and acoustic telemetry, which helps to reduce impacts from scientific studies imposed on valuable and already protected resources (McMichael *et al.*, 2010). However, few telemetry studies focused on the sterlet (none of the 55 reviewed in Nelson *et al.* (2013)), even though it is a widely used technology (Lenhardt *et al.*, 2010). Telemetry tools and their ability to observe animals in their natural environment might be especially useful to acquire insights about the behavior and needs of endangered animals (Acolas *et al.*, 2012). Further telemetry studies on

juvenile sturgeons could gather important information about life history aspects (Gessner *et al.*, 2006). Nowadays, acoustic telemetry is routinely applied in large rivers to assess migration patterns (Cooke *et al.*, 2013) of various fish species. The research of Ratschan *et al.* (2017) indicate that it might be a well-suited research tool for the Danube, where more research on sterlets using telemetry is required.

In freshwater, the optimal choice between radio and acoustic telemetry is often less clear because freshwater habitats represent a wide range of abiotic conditions, whose negative effects on detection distances have often been ignored (Shroyer and Logsdon, 2009). In shallow water (<3-10 m), radio telemetry is the method of choice (McMichael *et al.*, 2010; Cooke *et al.*, 2012, 2013), whereas acoustic telemetry is mainly used in deeper areas (Cooke *et al.*, 2013). Nevertheless, it was already successfully applied in very shallow areas (<2 m) too (Niezgoda *et al.*, 2002).

Regarding acoustic telemetry, lower frequencies are considered capable to achieve higher detection distances (McMichael *et al.*, 2010) because absorption losses increase with frequency (Stasko and Pincock, 1977). One acoustic telemetry system which operates with low frequencies (76 kHz) is Lotek's Mobile Acoustic Processor (MAP) system. Transducers need larger diameters to emit low frequency signals, which limits tag size and, therefore, their use for small fish (Stasko and Pincock, 1977; McMichael *et al.*, 2010; Cooke *et al.*, 2013). Even though heavily discussed, most researchers apply the rule-of-thumb that the tag to fish weight ratio should not exceed 2 % of the body mass of the fish (hereafter referred to as the 2 % rule) (Jepsen *et al.*, 2005). Another factor limiting tag size is the size of the battery used, which results in a shorter life span of smaller tags (McMichael *et al.*, 2010; Cooke *et al.*, 2013; Lu *et al.*, 2016). The battery in tags also lasts shorter at faster burst intervals (McMichael *et al.*, 2010; Lu *et al.*, 2016). The problem of achieving high detection distances and at the same time having tags available small enough to study early life stages over long periods of time is a topic of current research (Lu *et al.*, 2016).

Currently, the Juvenile Salmon Acoustic Telemetry System (JSATS) is a suitable system for the monitoring of small fish. It is an acoustic tracking system, which was developed to answer questions related to migration behavior and survival of small fish migrating through relatively fast flowing and shallow waters (McMichael *et al.*, 2010, 2013). It works at a high frequency of 416.7 kHz which requires smaller transducers and, hence, tags are smaller. The JSATS was used to answer a wide range of questions in a variety of different environments like studying migrations of juvenile salmonids over long distances (McMichael *et al.*, 2010, 2013) or to monitor fine-scale movements in 2D (Tétard *et al.*, 2019) and 3D (Li *et al.*, 2015b,a, 2018).

However, in order to successfully monitor tagged fish, it is important to estimate the probability of detecting them (Melnychuk, 2012) because many factors can influence detection range and efficiency (Simpfendorfer *et al.*, 2008; Melnychuk, 2012; Brownscombe *et al.*, 2019; Cooke *et al.*, 2013). Despite its variability, detection range is often assumed or obtained from published literature rather than tested in situ (Huvneers *et al.*, 2016), but researchers should not assume that published values will hold for their particular study site (Melnychuk, 2012). Therefore, the combination of receivers and tags (hereafter referred to as telemetry system), which will be used in the study, should be tested

before (Melnychuk, 2012) and across habitats and study sites (Huvneers *et al.*, 2016). Also variability in performance of receivers over time should be considered during the design phase in order to better understand uncertainty in data collected (Simpfendorfer *et al.*, 2008). Tests typically aim to assess the distance between a tag and receiver at which still a serviceable amount of signals is detected (Weiland *et al.*, 2011; Ingraham *et al.*, 2014; Kessel *et al.*, 2014; McMichael and Kagley, 2015; Steig, 2017). During many tests typically the detection efficiency (DE), which is the probability of detecting transmissions of a tag at a given distance, is measured (Melnychuk, 2012).

Next to technical features of the telemetry system, also environmental conditions are known to have major impacts on its performance (Shroyer and Logsdon, 2009; Pincock and Johnston, 2012; Gjelland and Hedger, 2013; Huvneers *et al.*, 2016). In stagnant water, wind, wind speed, rain and the thermocline among others are known to seriously affect telemetry systems (Gjelland and Hedger, 2013; Huvneers *et al.*, 2016). In rivers, background noise, which is mostly a combination of several noise sources (Amoser and Ladich, 2010), is reported to strongly affect the performance of telemetry systems and to inhibit successful decoding of signals and, therefore, detection range (Simpfendorfer *et al.*, 2008; Ingraham *et al.*, 2014; Jung *et al.*, 2015). Also turbulent currents can present major problems (Shroyer and Logsdon, 2009; Melnychuk, 2012). However, acoustic telemetry systems were already successfully used in fast flowing rivers (Bergé *et al.*, 2012). Other factors influencing the performance of telemetry systems are receiver depth (Huvneers *et al.*, 2016; Pinter *et al.*, 2019) and orientation (Huvneers *et al.*, 2016), signal distortion through Doppler shift (Pincock and Johnston, 2012) and the time since deployment (Huvneers *et al.*, 2016) because a growing amount of biofouling organisms on the receiver can cause interferences (Simpfendorfer *et al.*, 2008). Hence, the need of a well considered and planned experimental design is essential when using all forms of biotelemetry (Brooks *et al.*, 2017).

Aside of technical and environmental limitations, the application of biotelemetry will only answer specific questions. Hence, it is recommended to use a combination of telemetry and conventional research methods to acquire the most complete picture of fish behavior and physiology in relation to the environment (Bridger and Booth, 2003).

Due to the lack of basic knowledge about life history aspects of juvenile sterlets such as their habitat use or migration behavior, a monitoring program will be implemented in order to identify habitats as base for guidelines for the protection of sterlets (Friedrich, 2017). To guarantee the functionality of the telemetry system used in the monitoring program, this master thesis serves as a feasibility study with the aim to answer the following questions:

1.2.1 Research Questions - Telemetry

- Are detection range and detection efficiency of three JSATS based receivers, namely the WHS4250, the WHS4350 and the SR3017, from two different manufacturers suitable to locate juvenile sterlets in the Upper Danube in order to monitor migration and movement patterns?
- Do measured detection range and detection efficiency of three different JSATS based receivers vary between the free flowing section, the head of the impoundment and the impoundment of the study area?
- What are the differences between three different JSATS based receivers to a MAP based receiver in the impoundment section?
- How do selected abiotic parameters influence the distance at which signals are detected and what are the differences between habitats?

2 Study Sites

2.1 Wachau

With a length of 2 826 km the Danube river is the second longest European waterway. Its drainage basin extends up to 801 093 km² and brings around 827 km³ water per year to the Black Sea, which is approximately 50 % of its tributaries water flow (Bănăduc *et al.*, 2016). The Danube is divided into three major sections, the Lower Danube from the Black Sea to the Cerna river, the Middle Danube from the Cerna to the Morava river and the Upper Danube from the Morava to its source in the Black Forest (Hensel and Holčík, 1997). Therefore, the whole stretch in Austria belongs to the Upper Danube and is characterised by a nival flow regime. The fluvial valley digs through several bioregions namely the Bohemian Massif, the Alpine foreland and the Pannonian lowland (Wimmer *et al.*, 2012). Due to recurring catastrophic events, a growing population and growing importance of navigation, countless regulation measures to straighten the river were implemented starting in the late 18th century, with the highest intensity during the 19th century. Additional damming for hydropower in the 20th century (Jungwirth *et al.*, 2014) led to a major loss of free flowing sections with only two remaining, one past Vienna between the hydropower plant Freudenua and the Austrian-Slovakian border and the other in the Wachau valley between the hydropower plants Melk and Altenwörth.

The Wachau valley is located in Lower Austria between the cities Melk and Krems (Figure 1). Its South-Western part belongs to the Mostviertel, whereas its North-Eastern part belongs to the Waldviertel region. The stretch East of Krems belongs to the region Tullnerfeld. In this area, the Danube flows through the Southern end of the Bohemian Massif, which is characterized by highlands, hilly expanses and plateaus with forested valleys and mainly metamorphic rocks (Krenmayr *et al.*, 2002). In 2019, the annual mean discharge at the gauging station Kienstock was 1 734 m³/s and water temperatures ranged between 2-21.2°C with an annual mean of 11.3°C (data retrieved from eHYD (www.ehyd.gv.at)).

The study site Wachau is located between the hydropower plants Melk (river-km 2 038.1) and Altenwörth (river-km 1 980.1) and contains a diverse set of habitats, namely a free flowing section (ff), the head of the impoundment (himp) and the impoundment (imp) section. This allows for testing in very different environments.

Measurements of river widths and lengths of sections were retrieved from Google Earth (earth.google.com), whereas depth measurements were taken from depth charts from Navionics (www.navionics.com). Flow velocities at the surface were retrieved in the field with a GPS device on the floating boat.

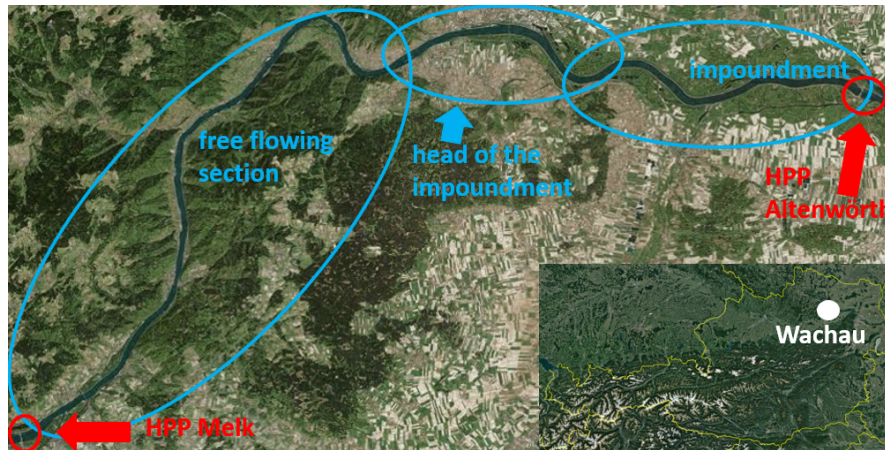


Figure 1: The study site Wachau with the hydropower plants Melk and Altenwörth (red) and the different habitats (blue). The map is based on maps retrieved from Google Earth (earth.google.com).

2.1.1 Free Flowing Section

The free flowing section, with an approximate length of 35 km, is located between the hydropower plant Melk and the city of Krems. Its widest part is directly below the dam with around 460 m and its narrowest part lies in the bend before Dürnstein with around 210 m. The average depth is around 4.5 m with several deeper sites down to 8-9 m for example at Aggsbach, Schwallenbach, Dürnstein and Rossatz. River banks are characterized by some left over and new gravel banks, but mainly by fixed banks with rip-rap. Nevertheless, in the course of the EU Life+ Auenwildnis Wachau project, a sidearm connection will be further improved as well as adjacent alluvial forests.

The current in the free flowing section is very strong with flow velocities of 2-2.5 m/s at the surface.

2.1.2 Head of the Impoundment

The head of the impoundment extends along the city of Krems for 4-6 km. Its width ranges between 280 m at Krems and 420 m at the port of Krems. Depths vary between 7-9 m with a rather fast increase at the beginning from 5 to around 8 m. In the outer banks of river bends, water depths down to 9 m can be found. From here on the river banks consist of only rip-rap and flow velocities are slower with 0.5-1 m/s at the surface.

2.1.3 Impoundment

The impoundment section starts approximately at the port of Krems and extends until the hydropower plant Altenwörth at a length of around 17 km. Its width varies between 350-400 m with depths around 10-12 m but with deep holes down to 18 m water depth. In this part, the Danube is confined by a dam on both sides and the banks consist out



Figure 2: Hydropower plant Freudenau South-East of Vienna. This picture was retrieved from Verbund AG (www.verbund.com).

of rip-rap only. Here, again, the deepest areas are located in the outer banks and flow velocities of 0.3 m/s at the surface are typical.

2.2 Freudenau

The Upper Danube at Vienna is intensively regulated for navigation (Jungwirth *et al.*, 2014). The hydropower plant Freudenau (Figure 2) was constructed between 1992 to 1998 on the downstream edge of Vienna at river-km 1 921.05. It creates a reservoir that contains 55 million m³ of water on a length of 28 km. Being one of Austria's Danube hydropower plants, six Kaplan turbines generate a power output of 172 MW. For ship passage, two sluices were built on the right side, whereas on the left side four weir fields are located, each with a width of 24 m. During construction works, a nature-like fish pass was implemented on the Danube Island, which should provide a passage corridor around the dam for migrating fish species. Downstream, in the direct vicinity of the dam, strong currents from the turbines and fluctuating discharge with weir spillover during flood events created a heterogeneous landscape of the river bottom with deep holes and adjacent accumulations of sediment (Figure 3). From the impoundment at Jochenstein, sterlets are known to occupy the deepest parts directly below the dam (Ratschan *et al.*, 2017). At the same time, other authors attribute a diverse range of habitats to the sterlet such as flooded floodplains or brackish areas (Holčík, 1989). Therefore, due to its heterogeneous bottom structure and the vicinity of the mouth of the fish pass, including sand and clayey substrate, the area below the hydropower plant was the chosen sampling site for net fishing.

The Danube downstream of Vienna is part of the National Park Donauauen on the

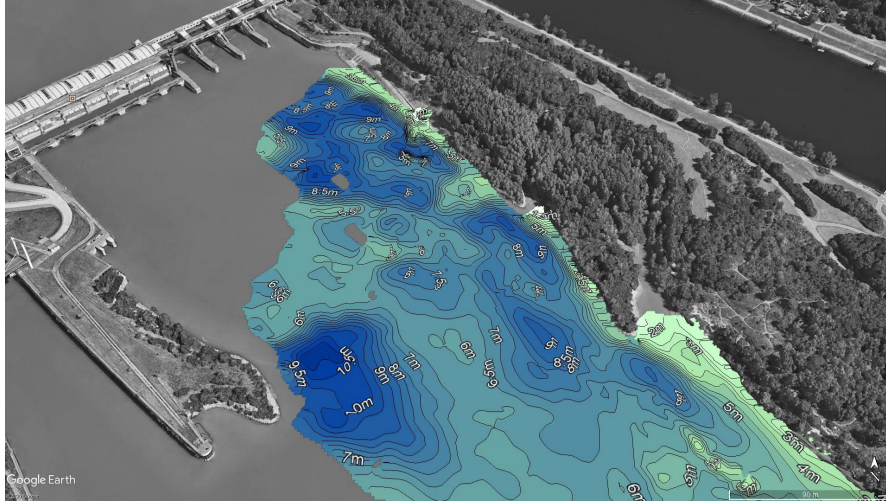


Figure 3: Depth map below the hydropower plant Freudenau. The map of the area was retrieved from Google Earth (earth.google.com) and the overlaid depth chart was made using an echo sounder (see section 3.2.1).

left bank, which was found in 1996 and extends until the mouth of the Morava river with a length of 36 km along the river and an area of 9 600 ha. On the right bank, two tributaries join the Danube, namely the rivers Schwechat and Fischa. In the course of the Interreg Slovakia-Austria program and the Alpen Karpaten Fluss Korridor project, the mouth of the latter river underwent a renaturation where riprap was removed to enable a more dynamic environment. Furthermore, several restoration projects aiming to reconnect cut-off oxbows in Austria and Slovakia are being implemented along the stretch, like the reconnection of the Spittelauer oxbow in the course of the Dynamic LIFE Lines Danube project. In the example of the Spittelauer oxbow, barriers at the upper and lower end as well as traverses inside the oxbow will be removed in order to allow for water supply during the whole year and sediment exchange with the Danube.

3 Material and Methods

3.1 Telemetry

In this section, used materials and methods to test the feasibility of acoustic telemetry in the Danube are described. The test design was chosen in regard to the monitoring of migration and habitat use of juvenile sterlets using fixed listening stations and mobile tracking. Four different receivers were tested, three operate in the boundaries of the Juvenile Salmonid Acoustic Telemetry System (JSATS) and one of Lotek's Mobile Acoustic Processor (MAP) series. At the beginning, only the WHS4250 was tested, but due to its unsatisfying performance two more JSATS and one MAP receiver were added to exclude the possibility of malfunctioning of the WHS4250 receiver and also to set the performance of different receivers and systems in relation to each other.

3.1.1 JSATS

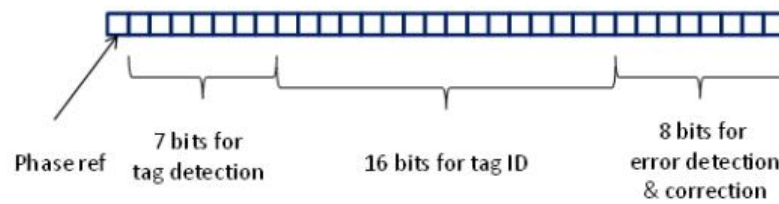


Figure 4: Structure of a JSATS signal (see Steig (2017)).

Due to declining stocks of Pacific salmon (*Oncorhynchus spp.*) and especially the lack of information about juveniles, the Portland District of U.S. Army Corps of Engineers initiated the development of an acoustic tracking system, the JSATS, which meets the requirements of working with small sized fish. Before its development, no acoustic telemetry system that meets the needs to work with small fish which migrate over long distances was available (McMichael *et al.*, 2010). Currently, the smallest available tags are just a bit larger than 1 cm and weigh around 0.28 g. Also tags with the same shape and size as PIT tags are available. Since the monitoring program of the Life Sterlet project aims to examine migration behavior and habitat use of juvenile sterlets, the JSATS is the system of choice due its tag sizes.

Uniquely, all compartments of the JSATS are non-proprietary and sufficiently specified to allow for competitive procurement between manufacturers. Therefore, the vendor with

the best product at an acceptable cost gets a contract for production (McMichael *et al.*, 2010).

The JSATS operates at a frequency of 416.7 kHz and sends signals with a typical source level of +158 dB and message length of 744 μ s. Each tag transmission is encoded in a 31 bit binary phase-shift keying (BPSK) code containing 7 synchronization bits, 16 ID bits and 8 cyclic redundancy check bits, resulting in 65 536 possible tag IDs (Weiland *et al.*, 2011) (Figure 4). Its BPSK code bares advantages as well as disadvantages. In comparison to a pulse interval coding (PIC) signal, in which the time between pulses is used to identify a unique tag code, the BPSK technology is more robust to background noise and is much less susceptible to tag collision problems due to the short duration of each transmission of the complete tag code (McMichael *et al.*, 2010; Weiland *et al.*, 2011). The short transmission of a single complete tag code decreases the likelihood of signal collision due to multipath signals (Jung *et al.*, 2015). Furthermore, does each signal contain the tag ID therefore an animal can be identified by the first signal reception. However, detections of a tag ID are usually only taken as valid if they meet certain criteria such as a minimum of four detections in 60 seconds (McMichael *et al.* (2010) take this time window for a burst interval of 5 s) and time spacing between detections has to match the burst rate or be a multiple of it (McMichael *et al.*, 2010). Another approach used by Ammann (2020) is that at least four detections of a specific tag code with time difference between first and fourth detection less than 16.6 times the burst rate have to be received. For a burst rate of 5 s this time window is 83 s. Since the signal is divided into different sections for tag detection and identification, each bit of the section has to be decoded correctly to get a proper signal. Containing 16 bits, the section for tag ID is the longest which makes it most prone to error (Steig, 2017).

3.1.2 MAP Series

The MAP series from Lotek is a complete different system than the JSATS. Unlike the JSATS it is not a non-proprietary environment but completely owned and manufactured by the company. Furthermore, coding and decoding works with a different system called Code Division Multiple Access (CDMA), which operates at a frequency of 76 kHz and can carry over 80 000 unique IDs. An advantage is that a large number of users (transmitter-receiver pair) can be supported and they can also easily be added or removed without disrupting the system (Proakis and Salehi, 2008). At lower frequencies, signals can generally be received at larger distances (McMichael *et al.*, 2010). On the other hand, do lower frequencies need larger transducers to be emitted and, hence, tag size and with it their use for small fish is limited (Stasko and Pincock, 1977; McMichael *et al.*, 2010; Cooke *et al.*, 2013). The smallest MAP-based tags available have a length of around 4 cm and weigh more than 5 g.

CDMA allows multiple users to operate simultaneously over the entire frequency band to transmit information (Sozer *et al.*, 2000; Proakis and Salehi, 2008). Operating on the same channel bandwidth, each user gets an individual signature sequence which is used to modulate and spread the information-bearing signal. When the receiver receives signals of multiple simultaneous users they appear as an additive interference with a varying

level of interference depending on the number of users. Therefore, the receiver uses the signature sequence to demodulate the signal whereas overlapping signals are separated via cross correlation of the received signal with each of the possible user codes (Proakis and Salehi, 2008). Additionally, signals can reliably be detected with a low Signal to Noise Ratio (SNR) allowing that signal strength of the received signal can even be lower than noise power (Niezgoda *et al.*, 2002).

3.1.3 Receivers

Table 1: Used receivers and their properties.

	WHS4250	WHS4350	SR3017	WHS3250
Manufacturer	Lotek	Lotek	ATS	Lotek
System	JSATS	JSATS	JSATS	MAP
Encoding	BPSK	BPSK	BPSK	CDMA
Operating Frequency	416.7 kHz	416.7 kHz	416.7 kHz	76 kHz
Operating Temp (°C)	0-50	0-50	0-50	0-50
Hydrophone Sensitivity			174 dB re 1 μ Pa/V	
Piezo form	cylindrical	spherical	cylindrical	cylindrical
Frequency Shift Immunity	no	yes	yes	

In this study, four receivers from two manufacturers, namely Lotek and ATS, were used (Table 1). The WHS4250, WHS4350 and WHS3250 are all manufactured by Lotek. The WHS4350 is the improved version of the WHS4250 and was not sold yet during the time of this study. Hence, for this study a prototype provided by Lotek in order to test its performance was used. The SR3017, another JSATS receiver, is a product from ATS.

The technical specifications of all receivers are presented in Table 1. On the very left the properties of the WHS4250 are shown. When compared to the WHS4350 and SR3017, the other JSATS based receivers, there are no differences in the encoding, operating frequency and temperature and depth rating. However, there are differences in the shape of the transducer, which is cylindrical in the WHS4250 and SR3017 but spherical in the WHS4350. A cylindrical transducer operates in the form of a "big donut" leaving a deaf spot directly below the tip (Lotek, pers. comm.), whereas the spherical transducer also covers this deaf spot. The second difference can be found in the frequency shift immunity, which means the receiver covers a larger frequency range and is able to decode the signal correctly even though the source moves. This is the case for the WHS4350 and the SR3017. About latter it is safe to say that it decodes tags at least in normal fish swimming speed (ATS, pers. comm.). The WHS4250 has no frequency shift immunity, at least not in the same extent as the other two receivers. No information about the hydrophone sensitivity of the receivers manufactured by Lotek is available, for the SR3017 it is given with 174 dB re 1 μ Pa/V.

The WHS3250, on the other hand, is a completely different device which operates at a lower frequency and with a different encoding system. Therefore, it cannot be compared to the JSATS receivers per se. However, like the WHS4250 and the SR3017, it also

has a cylindrical shaped transducer and the operating temperature is identical as for all JSATS receivers. For the WHS3250 no information about hydrophone sensitivity and frequency shift immunity is available.

3.1.4 Tags

Table 2: Used tags and their properties.

	L-AMT-8.2	ATS tag	MM-M-11-45
Manufacturer	Lotek	ATS	Lotek
System	JSATS	JSATS	MAP
Encoding	BPSK	BPSK	CDMA
Operating Frequency	416.7 kHz	416.7 kHz	76.8 kHz
Signal Strength	+158 dB (re 1 μ Pa @ 1 m)	+158 dB (re 1 μ Pa @ 1 m)	+76 dB (re 1 μ Pa @ 1 m)
ID Message Length	744 μ s	744 μ s	200 ms
Nr. of possible ID codes	65 536	65 536	>80 000
Size (mm)	9x23		12x73
Dry Weigth (g)	3.5		15

The properties of three different tags used for testing of the receivers in this study are described in Table 2. The L-AMT-8.2 and MM-M-11-45 tags are provided by Lotek. ATS provided a test tag (hereinafter referred to as ATS tag) with a big battery installed, which cannot be attached to fish but is only used for testing. The L-AMT-8.2 and ATS tag are operating in the boundaries of the JSATS and their specifications are, therefore, identical except of the size and weight. As mentioned above, size and weight of the ATS tag are irrelevant and the L-AMT-8.2 was designed to be used for fish with >175 g to match the 2 %-rule. The MM-M-11-45 is designed to operate in the boundaries of the MAP system. It works on a different frequency and with a different encoding technology. With 80 000 possible ID codes, the CDMA encoding gives access to a higher number of IDs. The MM-M-11-45 was designed to be used in larger fish of >750 g to match the 2 %-rule.

3.1.5 Test Design

3.1.5.1 Detection Range

Detection range was tested at 13 days. For the first five tests, only the WHS4250 receiver was available and used. Due to its unsatisfying performance, two further receivers, the WHS4350 and the SR3017, were made available. Subsequently, all three receivers were used for testing in order to compare their performance. For the last two tests in the impoundment also the MAP based WHS3250 receiver was tested, to set the JSATS in relation to the MAP system in an impoundment of the Danube. Testing was carried out in all three habitats, namely the free flowing section, the head of the impoundment and the impoundment section (Table 3). Detection range was tested during summer only for the WHS4250 receiver because the others were not available before autumn. Hence, the WHS4350 and SR3017 were tested during autumn and winter, the WHS3250 only in winter. No tests were carried out in spring.

Table 3: Test days and associated locations with values for discharge (Q, in m^3/s), water temperature (T, in $^{\circ}C$) and Secchi depth (Sd, in cm). Used receivers for testing detection range are marked with big crosses, whereas small crosses indicate test sessions where detection efficiency was tested.

date	section	Q	T	Sd	WHS4250	WHS4350	SR3017	WHS3250	DE test
05.02.2019	himp	1 390	3.1		X				
22.03.2019	imp	2 405	7.3		X				
12.07.2019	imp	1 510	18.1	48	X				
25.07.2019	imp	1 290	20.7	84	X				
20.08.2019	ff	1 380	19.1	25	X				
18.09.2019	ff	1 160	16	62	X		X		
15.10.2019	himp	1 300	12.5	91	X	X	X		x
17.10.2019	ff	1 230	12.4	88	X	X	X		x
14.11.2019	himp	1 290	8.3	112	X	X	X		x
29.11.2019	imp	1 050	7	64	X	X			
10.12.2019	ff	943	5	130	X	X	X		
17.01.2020	imp	1 010	3.6	202	X	X	X	X	x
21.01.2020	imp	977	3.8	210	X	X	X	X	x

For testing the detection range, test tags were attached with duct tape in a horizontal position on a rope at depths between 1-10 m, but mostly between 3-5 m. The rope was fixed to a buoy with a weight on its lower end to ensure it is vertically stretched. To get the locations of the tags, a GPS device was fixed to the buoy as well. The boat was equipped with an additional GPS device, which was used to subsequently determine the distance between boat and buoy with an accuracy of 3-4 m.

To test detection range, different distances between the receivers on the boat and the tags on the buoy had to be kept in order to see if signals can still be detected. Hence, the distance between boat and buoy was changed simply through drift or with the use of the engine. In order to avoid impacts through engine noise on the detectability of signals, drifting was the preferred way of increasing the distance. When boat and buoy drifted, the boat was always downstream of the buoy due to a faster drift. Low flow velocities in the head of the impoundment and the impoundment section necessitated the use of the engine in order to increase the distance between boat and buoy. After driving several meters, the engine was switched off again.

For analysis, the maximum, mean and median distances between boat and buoy were retrieved for each test session and receiver. Additionally, data of detection efficiency tests during the last two test sessions was used to get information about detection range performance of the WHS3250 receiver.

3.1.5.2 Detection Efficiency

As mentioned above, DE could only be tested in autumn and winter due to the availability of receivers. Hence, data for spring and summer is missing. Three JSATS receivers were available during all test sessions, whereas the WHS3250 was only used during the last two sessions in the impoundment.

Detection efficiency (DE) was tested during five test sessions, which are indicated with small crosses in Table 3. Tests were undertaken twice in the head of the impoundment, twice in the impoundment and once in the free flowing section. During the second test in the free flowing section (December 10th, 2019), anchoring did not work for neither the boat nor the buoy. Therefore, no reliable data could be collected and this test was excluded for further analysis.

Detection efficiency was tested with two different approaches. For tests in the impoundment a static approach was chosen. Therefore, tags were fixed with duct tape to a rope on a buoy at depths between 2-5m. The buoy was secured to the river bottom with an anchor. The boat anchored at different distances (25m, 50m, 75m, 100m, 150m, 200m, 400m) for five minutes each (compare with (McMichael and Kagley, 2015)).

In the free flowing section and the head of the impoundment, anchoring in sufficient distance off the bank, to avoid signal reflection, at the same clearly distinguishable distances as for the static approach, was not possible. Therefore, a floating approach was chosen with the same setup as for detection range testing (compare with section 3.1.5.1).

3.1.6 Abiotic Parameters

For the tests in the Wachau valley, abiotic data for discharge (Q), water temperature (T) and Secchi depth (Sd) as indication of turbidity were collected. Data for discharge and water temperature were retrieved from the eHYD online platform of the Austrian Federal Ministry of Agriculture, Regions and Tourism (www.ehyd.gv.at), while Secchi depth was measured in the field using a Secchi disc. The applied procedure was the same as in Green *et al.* (1996). The Secchi disc was lowered at the shady side of the floating boat until it disappeared. At this depth a measurement was taken. The second measurement was taken for the depth at which the Secchi disc reappeared after being lowered until it was not visible anymore. Then the mean value of both measurements was taken.

Figure 5 shows the discharge (blue) and water temperature (red) during the test period at the gauging station Kienstock, which is representative for the Wachau valley. The dashed, vertical lines mark all test days during the study period. Measurements for turbidity are only available for the test days, but not for the periods in between.

For analysis, all test days were used, except for Secchi depth, where no measurements for the first two sampling days (February 5th, 2019 and March 22nd, 2019) are available (compare with Table 3). Since the WHS4250 was the only receiver available during all test days, it was the only receiver used for analysis of possible effects of abiotic parameters on receiver performance. Hence, changes of measured mean distances were

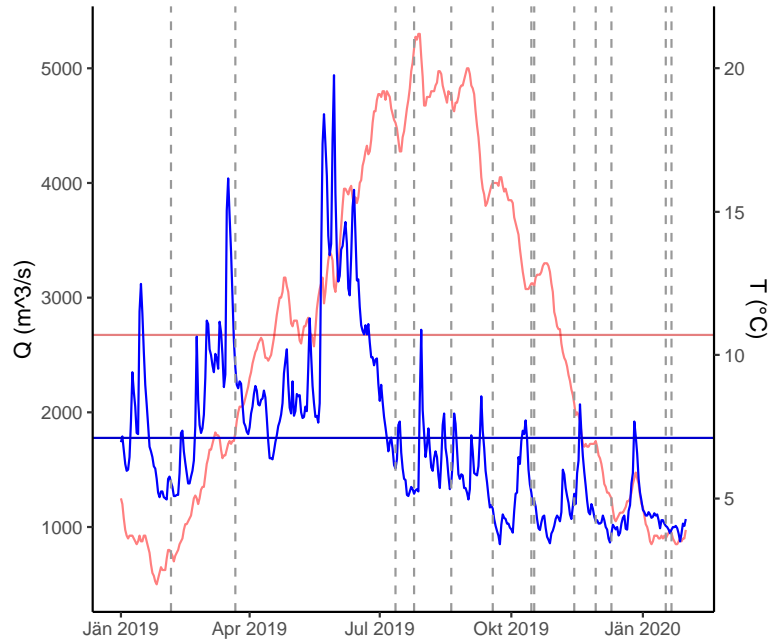


Figure 5: The discharge (blue) and daily mean water temperature (red) during the study period at the gauging station Kienstock. The blue horizontal line marks the mean discharge ($1\,777\text{ m}^3/\text{s}$), whereas the red horizontal line marks the mean water temperature (10.7 °C) during the study period. The gray dashed, vertical lines mark all test days.

analyzed for each parameter (Figure 12). The low amount of measurements in the head of the impoundment (two for Secchi depth and three for discharge and water temperature) made it necessary to exclude it from analysis.

Relationships between all parameters were analyzed with Spearman rank correlations.

3.1.7 Data Analysis - Telemetry

Collected data was analyzed using Microsoft Excel[®] and IBM[®] SPSS[®] version 26.

Detection range was analyzed for all habitats together and separately and for each receiver by calculating maximum, mean and median distances. To set receiver performance in relation to each other and between habitats, actual detections were transformed into detections per hour (n/h). For further analysis and due to its skewed distribution to the right, distance data was grouped into three homogenous groups with the cut points at ≤ 35 , 36-86 and ≥ 87 m (Table 18 in the appendix). Further analysis is focused on those groups.

Detection efficiency was calculated using Equation 1, by dividing actual tag detections (*detections*) through possible tag detections (*detections_{pos}*).

$$DE = \frac{detections}{detections_{pos}} \quad (1)$$

For example a tag with a programmed burst interval of 5 s sends 12 signal in one minute and 60 signals in five minutes, respectively. If the receiver detects 30 signals in 5 min, the detection efficiency is 0.5 which corresponds to a successful decoding of 50 % of emitted signals.

To calculate detection efficiency for the floating approach, time windows between 30 s and 6 min were chosen, in which signals could be received. It was necessary to exclude small time windows because detection efficiencies were often unrealistically high. Occasionally, two or three signals were detected in a row, but before and after this short time window no signals were detected for sometimes several minutes. Since this happened mainly at large distances, high values of DE would wrongly be attributed to those distances. Thus, the large bias of high DE values for short time windows had to be smoothed (Figure 19 in the Appendix).

With those time windows, data for all receivers out of all three habitats is available and can be analyzed. Time windows of e.g. 1 - 6 min or higher result in data loss of whole habitats. Subsequently, the results of drift tests were grouped in 25, 50 and 100 m windows, so they can be put in relation to the static tests (compare with (Ingraham *et al.*, 2014)).

The data base for detection efficiency analysis shows a significant relationship between passed seconds and DE, but the variance of DE cannot be well explained ($R^2=0.045$, $p < 0.05$, Figure 19 in the appendix). However, the slope is very low (-0.0005) so that DE is affected in a range which is acceptable for further analysis.

The distribution of DE data requires a non-parametric analysis approach. Hence, to explore the data and interpret receiver performance, a classification and regression tree (CRT) was used. The CRT analysis tries to separate the data into homogenous groups based on predictor variables (Hayes *et al.*, 2015) and their importance, starting with the most important one. Since variables are used repeatedly, complex interdependencies can be revealed. In order to include the habitats into the analysis and avoid a multitude of different decision trees, a split among habitats at the first node was set as default. CRT analysis is also well suited for smaller samples, which is the case in this study.

Due to the lack of a normal distribution, DE data was classified into three groups (trichotomous) with the categories ≤ 0.36 , $0.361-0.727$ and ≥ 0.728 . With those values as cut points, the data points are evenly distributed among groups (Table 18 in the appendix). The model performance is indicated in Table 6. For the sake of completeness, the metric approach based on all data points is added to the appendix (Figure 21). Its model performance is indicated by η^2 in Table 20 in the appendix. For a CRT based decision tree, η^2 functions as coefficient of determination (Eckstein, 2016). The calculation was done based on the manual for decision trees for SPSS[®] (IBM Corporation, 2011) using Equation 2. The risk estimate of the model can be found in Table 20 and the standard deviation (Std.Dev.) of the dependent variable is indicated in Node 0 in Figure 21.

$$\eta^2 = 1 - \left(\frac{Risk\ Estimate}{Std.Dev.^2} \right) \quad (2)$$

In order to give an overview and to compare the performance of all receivers among habitats, the mean and 95 % confidence intervals for DE were plotted. Actual measurements of DE for each receiver and habitat can be found in the appendix (Figure 20). Furthermore, the median and 95 % confidence intervals for DE were plotted to analyze receiver performance among habitats and in relation to distance. Confidence intervals were used to describe the results and show distinct differences rather than testing for statistical significance based on the articles by Rothman (1978) and Gardner and Altman (1986).

At last, an attempt to set measured DE of this study in relation to values for DE of other studies that used the JSATS was made. Therefore, the distance at which a DE of 20 % (20DE) occurs was calculated, using the same approach as applied by Ingraham *et al.* (2014). The authors assume a DE of 100 % at 0 m and then use a linear regression to calculate the value of 20DE.

3.2 Net Fishing

3.2.1 Net Deployment and Fish Handling



Figure 6: Net locations below the hydropower plant Freudenuh. Colors indicate the different seasons whereas winter, spring, summer and autumn are shown in black, green, red and orange, respectively (source: google earth).

Net fishing for sterlets was carried out in the area directly below the hydropower plant Freudenuh. Initially the aim was to extend the broodstock for the rearing project (see chapter 1), but net fishing was extended to gather information about the sterlet population in this area during all seasons.

For this purpose, trammel nets with a length of 25 m were used to catch fish as gentle as possible in order to minimize damage and subsequent death. It consists out of three layers of nets with two different mesh sizes between an upper swimming line and a lower lead line, whereby the close meshed inner net (40 mm) is flanked by two wide meshed outer nets (100 mm). The nets were secured to the river bottom by anchors and weights and a long rope connected the swimming line to a buoy to mark the nets at the surface. When a fish swims through, it drags the inner net through an outer and a pocket is formed from which it can be retrieved (Figure 7).

In the nearby area of the dam, the strong current of the turbines dug a diverse landscape with deep holes and adjacent elevations. A depth chart of the area was made using an echo sounder (Simrad GO9). According to literature (see chapter 1), nets were deployed in holes and deeper areas (Figure 6) to maximize the chance of catching sterlets due to their suspected movement patterns. Figure 6 shows that the nets were mainly located below the weir fields as well as in front of the lower fish pass entry.

Net fishing was carried out between March 2018 to June 2020, details about dates, number of deployed nets and respective duration are shown in Table 4. Sampling days were distributed over the year and always conducted over night to avoid any interference

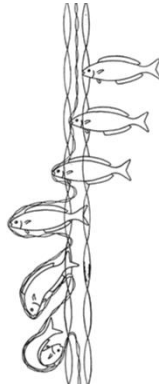


Figure 7: Operating principle of a trammel net (Nédélec and Prado, 1990).

of shipping. Caught sterlets were checked for PIT-tags and if no tag was present they were tagged. The further procedure included measuring, weighing, taking pictures for optical identification and genetic samples for genetic identification. If wounds occurred, they were treated with antiseptic. After the protocol of each fish was complete, the sterlets were released immediately. During spring, potential broodstock fish (ripe fish which were not used for artificial reproduction before) were transferred to the hatchery and released after eggs and sperm were obtained. Other fish species were recorded and released.

Table 4: Number of nets and duration of deployment.

Date	Nets (n)	Time per Net (h)	Time total (h)
29.03.2018	1	12	12
20.07.2018	3	13	39
25.07.2018	2	12	24
29.11.2018	3	11	33
15.01.2019	2	11	22
07.03.2019	3	9	27
02.04.2019	2	11	22
04.07.2019	1	8	8
17.07.2019	2	9	18
23.07.2019	3	11	33
07.08.2019	2	9	18
04.09.2019	3	10	30
01.10.2019	3	12	36
15.11.2019	3	11	33
18.12.2019	5	11	55
30.01.2020	2	13	26
13.03.2020	4	4	16
20.03.2020	3	5	15
25.03.2020	3	4	12
28.03.2020	6	4	24
03.04.2020	4	5	20
04.04.2020	4	7.5	30
16.04.2020	3	13	39
23.06.2020	3	5	15

3.2.2 Data Analysis - Net Fishing

Net fishing data was analyzed using Microsoft Excel[®] and R software version 3.6.3 (R Core Team, 2020) using the package FSA (Ogle *et al.*, 2020) for length-weight regression analysis and the population estimation after the Jolly-Seber method (Jolly, 1965; Seber, 1965). Description of caught sterlets includes length-frequency analysis, length-weight relationships and the calculation of two different condition factors. Equation 3 shows Fulton's condition factor (K_F) (Ricker, 1975), which assumes the value $b=3$ and, therefore, isometric growth. It measures the deviation from a hypothetical ideal fish (Le Cren, 1951).

$$K_F = \frac{W}{L^3} \quad (3)$$

- K_F = Fulton's condition factor
- W = weight in gram
- L = length in cm

Equation 4, on the other hand, shows the relative condition factor (K_n) (Le Cren, 1951), which measures the deviation from an individual of the average weight for lengths and ideally requires a length-weight regression analysis.

$$K_n = \frac{W}{W'} \quad (4)$$

- K_n = relative condition factor
- W = weight in gram
- W' = predicted length specific weight

Furthermore, a rough estimation of the population in the monitored area was calculated, using the mark-recapture method, which can be done because all caught sterlets were PIT-tagged. To estimate the population size, two different approaches were applied for comparison. The Chapman estimator (Equation 5) assumes a closed population without immigration or emigration, as well as without deaths and births. Given the current status of sterlet populations in Austria, in addition to a small monitored area, also a small population size is assumed. Therefore, the Chapman estimator, which is likely to be less biased for small samples than other estimators (Pollock, 1991; Borchers *et al.*, 2002), is used in this case. The population estimation was done for the years 2018 and 2019.

Due to a higher sampling effort in 2019 (302 h) than in 2018 (108 h) (see Table 9), the numbers of caught fish and recaptures were adapted based on netting duration with a factor of 0.36 ($=108/302$). Thus, real numbers of 2019 were multiplied by 0.36 to match the effort of 2018. The reason that the numbers are adapted based on the effort of 2018 is that an adaption based on 2019 would add fish to 2018 which were never caught.

$$N = \frac{(n_2 + 1)(n_1 + 1)}{n_M + 1} - 1 \quad (5)$$

- N = estimated population size
- n_1 = number of animals captured at the first visit
- n_2 = number of animals captured on the second visit
- n_M = number of recaptured animals that were marked

The second approach is the Jolly-Seber method (Jolly, 1965; Seber, 1965), which assumes an open population with occurring immigration and emigration as well as deaths and births of individuals. On the one hand, the sampling years 2018 and 2019 are taken to estimate the population. On the other hand, all sampling days between 2018 to 2020 are taken for an estimation of the population size as well. With the Jolly-Seber method, the population size at each sampling day (except the first and the last), as well as the increase in individuals at the next sampling day and residence time between sampling days can be estimated (Pfeifer, 2005).

4 Results

4.1 Telemetry

4.1.1 Detection Range

Table 5: Number of detections per hour (n/h) and detection range of all receivers. Maximum, mean and median values of measured distance (in m) are shown.

model	n/h	max	mean	median
WHS4250	134	150	24	18
WHS4350	402	220	53	39
SR3017	621	400	78	66
WHS3250	759	400	130	100

Table 5 shows the results of detection range testing for all receivers. As mentioned above, receivers were used during different test sessions (compare with Table 3). The number of detections per hour is given to set all receivers in relation. Since the receivers were used during different test sessions and different abiotic conditions, those values should be treated as rough trends and not as direct comparison.

The WHS4250 was used during all 13 test sessions, the WHS4350 and SR3017 during seven each and the WHS3250 only during two tests and only in the impoundment. In the impoundment, measurements were taken at fixed distances and not from a floating boat as during the other tests (see section 3.1.5.2). Nevertheless, the trend visible in Table 5 shows that the WHS4250 tends to show the worst performance in all parameters followed by the WHS4350 and the SR3017. The MAP based WHS3250 shows the highest values.

Since measured distances for all receivers are skewed to the right, the median distance is lower than the mean distance in all cases.

4.1.2 Detection Efficiency

Figure 8 shows the mean of detection efficiency and associated 95 % confidence intervals (CI) for all receivers among habitats. The distance is grouped as mentioned in section 3.1.7, in order to focus analysis on three homogenous groups of different distance classes. Figure 20 in the appendix shows all data points for DE and initial distances.

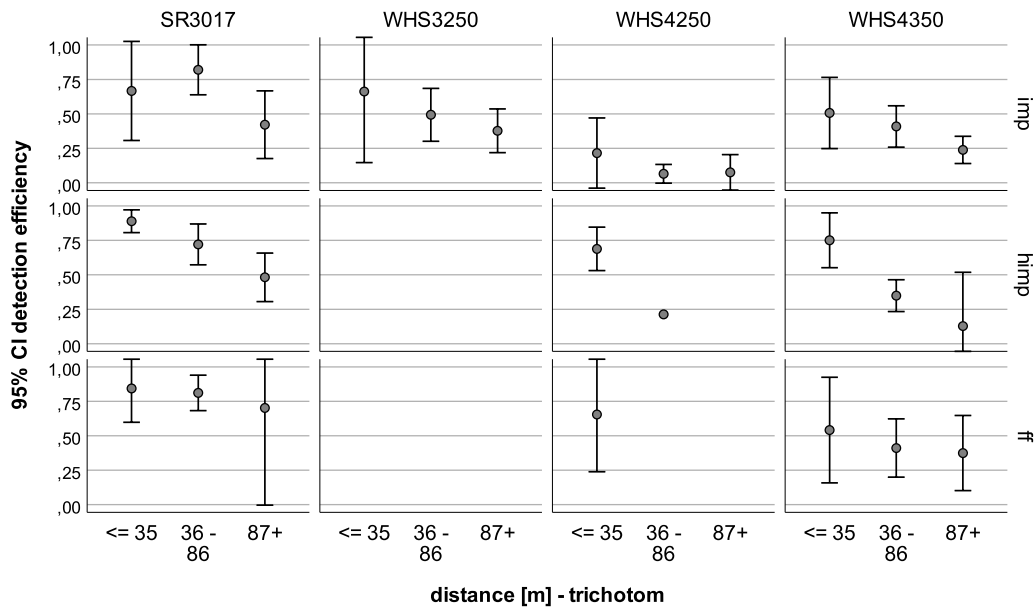


Figure 8: The mean and 95 % confidence intervals of DE for all receivers in each habitat based on grouped distances. ff = free slowing section, himp = head of the impoundment, imp = impoundment

In general, individual performances between models and among habitats are different, but DE is decreasing with increasing distance in all cases. The SR3017 tends to show highest detection efficiencies overall. Among habitats it performs similarly, except the vast scattering above 87 m in the free flowing section. The 95 % confidence intervals of the mean reveal distinctively higher values for DE at 36-86 m for the SR3017 than for both other JSATS receivers in all habitats. This difference is strengthened by the close link between confidence intervals and hypothesis tests, whereby the result of the hypothesis test can be inferred at an associated level of statistical significance (Gardner and Altman, 1986). This result is also indicated in Figure 20. While the SR3017 maintains a high DE until around 100 m to drop immediately thereafter, other receivers shows a rather uniform decrease of DE with distance.

In the head of the impoundment, the mean and associated 95 % confidence intervals show a similar difference with distinctively higher values for DE at distances below 35 m than at 87 and above regardless of the receiver model.

The WHS3250 was only used in the impoundment section and shows a high scattering of DE at low distances.

The WHS4250 shows low values for DE except in the head of the impoundment. In the free flowing section, DE scatters vastly. Notable is that in both, the head of the impoundment and the free flowing section, only measurements for low distances are available with one single measurement above 35 m (compare with Table 19 in the appendix).

The WHS4350 shows a very similar performance in all habitats, only in the head of the impoundment a sharp drop in DE at more than 35 m occurs.

4.1.3 Overall Performance

In general, the CRT did well in classifying cases into the first (≤ 0.36) and the third (≥ 0.728) class, only one third were classified correctly into the second class (0.361-0.727) though (Table 6). Overall, two thirds of all cases could be classified into the correct class, which indicates that the CRT is well suited to predict trends of DE based on habitat, receiver model and distance.

The first split indicates that DE tends to be generally higher in the head of the impoundment and in the free flowing section (node 1) than in the impoundment (node 2). The next split for both nodes was based on distance, whereby generally a distance of around 120 m tends to be decisive if DE tends to be higher or lower (node 3-6) in all habitats. For distances above 120 m, DE tends to be classified as ≤ 0.36 for all receivers in the impoundment and only slightly better in both other habitats, but no further distinction improves the explanatory value. At distances less than 120 m, further variables tend to influence DE.

In the head of the impoundment and the free flowing section below a distance of 120 m, a further separation between the SR3017 (node 7), on the one hand, and the WHS4250 and WHS4350 together (node 8), on the other hand, can be made. The SR3017 tends to have higher values for DE than both other JSATS based receivers. Until 120 m, at least every third signal tends to be successfully decoded. For the WHS4250 and the WHS4350

detection efficiency - trichotom

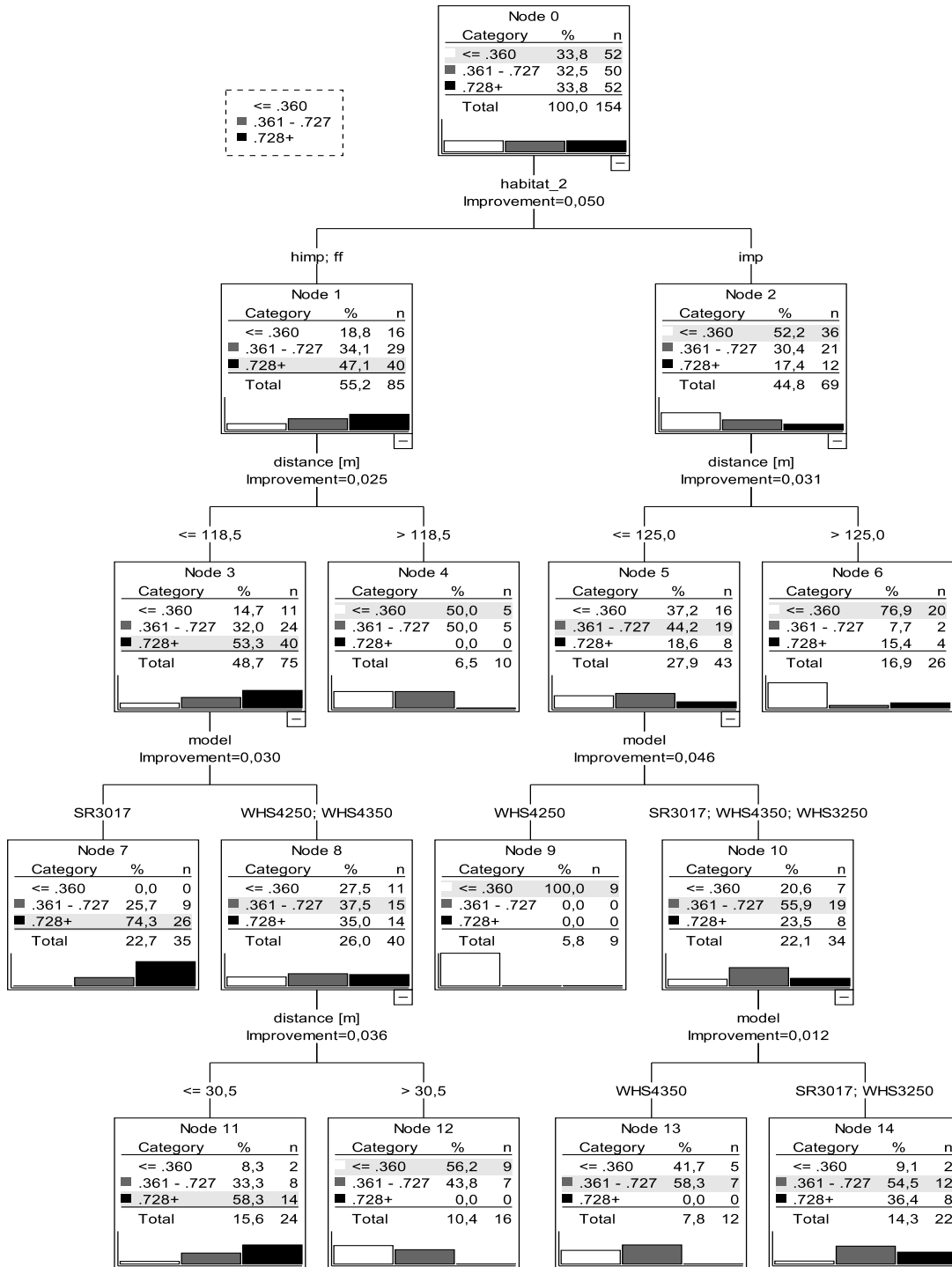


Figure 9: Decision tree based on grouped values of DE.

the classification is weak and another split is necessary. Nodes 11 and 12 indicate that both receivers tend to have higher values for DE until 30 m and a tendency to lower values at 30 m or more. The model does not distinguish between both receivers though.

In the impoundment section, a further distinction between receiver models can be made, whereas all cases of the WHS4250 are classified in the category ≤ 0.36 (node 9). Hence, one third or less of all signals tend to be decoded at distances below 120 m. For all other receiver models (including the MAP based WHS3250), DE tends to be around 50 %, but the classification in node 10 can further be improved. The last split distinguishes between the WHS4350 (node 13), which tends to decode between one and two thirds or less of all signals in most cases, on the one hand, and the SR3017 and the WHS3250 together (node 14), on the other hand. No distinction between the JSATS based SR3017 and the MAP based WHS3250 is made. Both receivers tend to decode between one to two thirds or more of all signals until 120 m in the impoundment section.

Table 6: Classification table for the decision tree based on grouped values of DE.

Observed	Predicted			Percent Correct
	≤ 0.36	0.361-0.727	≥ 0.728	
≤ 0.36	43	7	2	82.7 %
0.361-0.727	14	19	17	38 %
≥ 0.728	4	8	40	76.9 %
Overall Percentage	39.6 %	22.1 %	38.3 %	66.2 %

The metric approach of the CRT analysis (Figure 21) shows partially different results with a high validity ($\eta^2=0.604$, Table 20). The classification for the head of the impoundment and the free flowing section (left branch in Figure 9) is the same. The impoundment, however, is split up differently. In Figure 21, the first criterion to split node 2 is the receiver model, whereas the WHS4250 shows a low mean DE in general (node 5). Node 6 contains all other receivers and is further split at a distance of 175 m. Above this distance (node 10), only every fourth signal tends to be successfully decoded. Below 175 m, still every second signal tends to be decoded (node 9). However, a last split by receiver model reveals that the SR3017 (node 13) tends to decode more signals than both, the WHS4350 and WHS3250 (node 14) do.

4.1.4 Performance among Habitats

Table 7: Overview of detection range for all habitats, including number of detections per hour (n/h) and measured maximum distance. Calculated mean and median distance are shown and all distances are in m.

model	free flowing				head of the impoundment				impoundment			
	n/h	max	mean	median	n/h	max	mean	median	n/h	max	mean	median
WHS4250	78	138	18	12	133	81	26	23	155	150	24	18
WHS4350	216	220	74	69	433	200	54	43	479	200	47	25
SR3017	466	242	62	54	566	229	80	77	833	400	85	75
WHS3250									759	400	130	100

Table 7 shows trends of performance parameters for all receiver types among all habitats. Trends are similar as in Table 5 for all JSATS based receivers. Notable are the low values for mean and median distances of the WHS4250 in general and especially in the free flowing section.

An interesting trend are the increasing distances from the free flowing section, to the head of the impoundment and towards the impoundment section for the WHS4250 and the SR3017 in number of detections per hour and mean and median distance. The WHS4350, on the other hand, increased in number of detections per hour but the trend for mean and median distance is converse. The WHS3250, which was only tested in the impoundment, received signals at high distances in the mean and median. Again, these values are only trends because receivers were tested at different days in each habitat and are, therefore, not comparable.

Maximum distances at which signals were decoded successfully indicate no clear pattern. Except for the WHS4350, which received signals at the highest distance in the free flowing section, other receivers did so in the impoundment. The measured maximum distance of 400 m in the impoundment was concurrently the maximum distance at which measurements were taken. Hence, if the receivers would receive signals at higher distances is unknown. At the same time were measurements at 200 m and above uncommon events with only few exceptions (compare with Figure 20).

As already indicated in Figure 9, there is a difference in the performance among habitats. In the decision tree, no distinction between the head of the impoundment and

the free flowing section occurs though. Figure 10 and Figure 11 further unravel the performance of JSATS based receivers among habitats. Both the median and 95 % CI, Figure 10 for DE and Figure 11 for distance.

DE tends to be highest in the free flowing section and lowest in the impoundment for all receivers. For the WHS4250, the 95 % confidence intervals of DE in the impoundment do not overlap with those from both other habitats and, hence, describe a clearly worse ability to to decode signals in the impoundment. In all other cases 95 % confidence intervals overlap and no clear differences but rather trends are indicated.

Regarding the distances at which signals were decoded, an opposite trend than for DE is indicated. Successful decoding takes place at the lowest distances in the free flowing section and at highest distances in the impoundment. A missing overlap of the 95 % confidence intervals of the median of the WHS4250 between the free flowing section and the impoundment shows that it detected signals at lower distances in the former than in the latter . Both other receivers do not show a clear distinction.

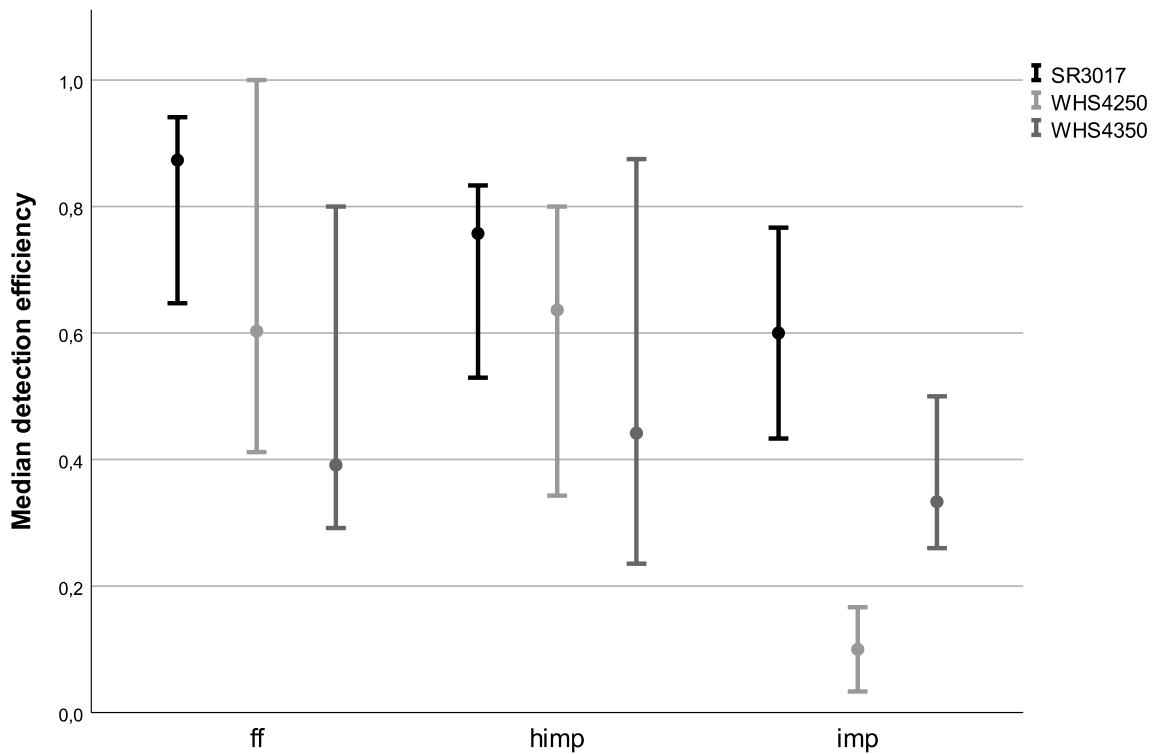


Figure 10: The median and 95 % confidence intervals of DE for all JSATS based receivers in each habitat.

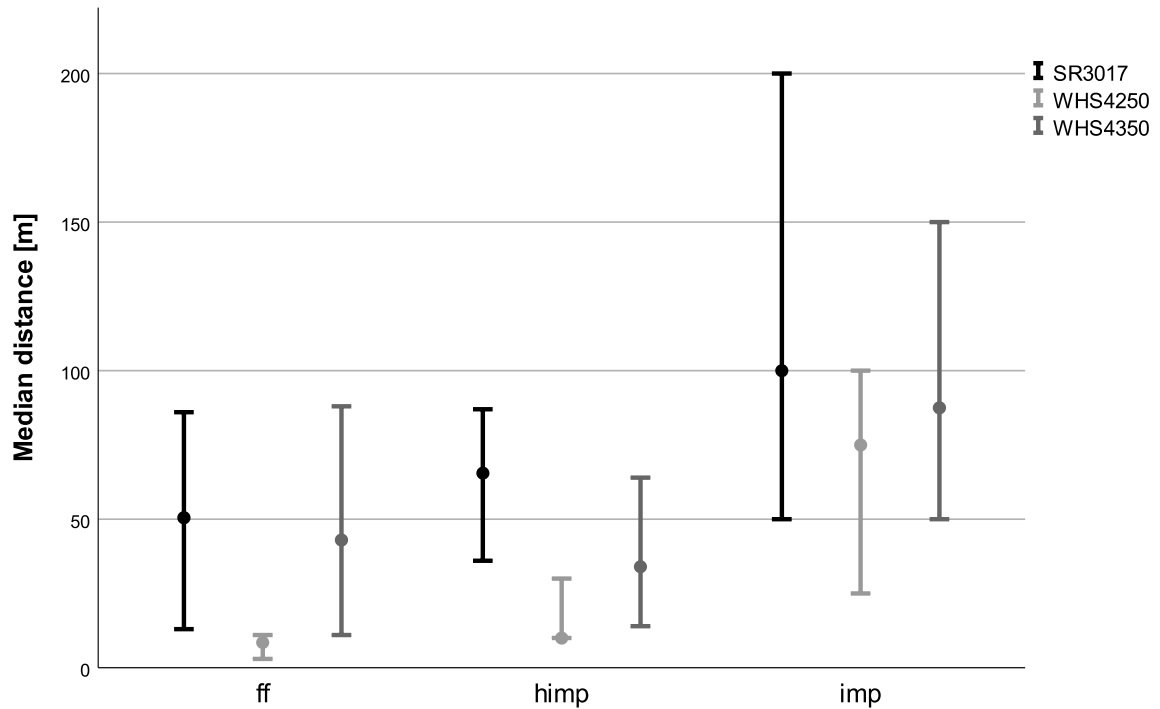


Figure 11: The median and 95 % confidence intervals of the distance for all JSATS based receivers in each habitat.

4.1.5 Abiotic Parameters

A list of all test days and corresponding values for discharge, water temperature and Secchi depth is given in Table 3. Discharge ranges between 943 to 2 405 m^3/s . However, twelve events fit into the boundaries up to 1 510 m^3/s and only one test was conducted during a higher discharge. Water temperature ranges from 3.1 to 20.7 °C, which reflects the normal range of the Danube well (Figure 5). Values for Secchi depth are missing for the first two tests, for the rest they range between 25 to 210 cm, representing very turbid to very clear water.

In Figure 12, the effects of all abiotic parameters on the WHS4250 receiver are shown. Since no data for Secchi depths is available for the first two sampling days, only eleven sampling days were considered. For discharge and water temperature, data for all 13 sampling days is available. In detail, discharge measurements are available for four days in the free flowing section, three in the head of the impoundment and for six days in the impoundment. For water temperature data is available for the same amount of days in all habitats and for Secchi depth, data is available for four days in the free flowing section, only for two in the head of the impoundment and for five days in the impoundment

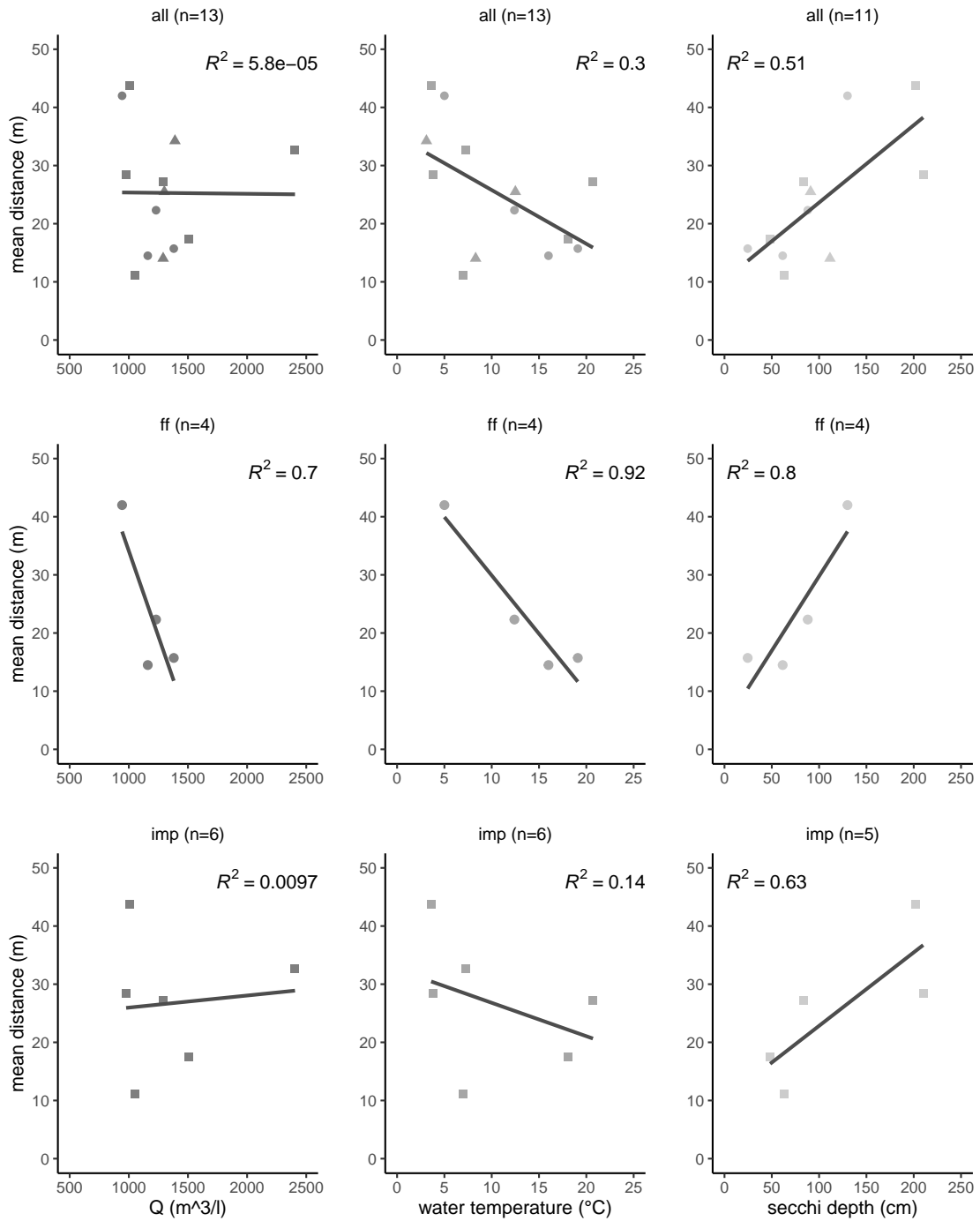


Figure 12: The mean distance at which the WHS4250 decoded signals is plotted for Q, water temperature and Secchi depth for all test days in all habitats together and in the free flowing section and the impoundment separately. Habitats are marked by symbols, whereas \circ = free flowing section, \triangle = head of the impoundment and \square = impoundment.

(Table 3). Due to the low amount of data available for the head of the impoundment, it was not analyzed alone, but it was considered for the analysis of all habitats together.

In general, discharge seems to have the least effect on the mean distance across habitats. When analyzed separately, the effect in the free flowing section is quite strong, but in the impoundment discharge seems not to affect the mean distance at which signals are decoded.

Water temperature, on the other hand, indicates a slightly negative effect on the mean distance across habitats. The mean distance tends to be lower when water temperatures are higher. This effect seems to be especially strong in the free flowing section, but weak in the impoundment.

The Secchi depth indicates the strongest effect on the mean distance at which signals are decoded, while the signal penetrates further when the Secchi depth is higher, thus, when the water is clearer.

Due to the low amount of measurements, especially in the free flowing section, these results indicate rough trends. To further explore the effects of abiotic parameters, further testing to achieve a reasonable amount of data points is recommended.

The relationships between Secchi depth, discharge and water temperature were analyzed using Spearman rank correlations (Figures 22, 23 and 24 in the appendix). According to Rasch and Kubinger (2006), Secchi depth and discharge show a weak negative monotonic relationship ($\rho=0.67$, $n=11$, $p=0.024$, Figure 22), while Secchi depth and water temperature show a moderate negative monotonic relationship ($\rho=0.81$, $n=11$, $p=0.05$, Figure 23). Since the significance level of $p > 0.05$, no monotonical relationship between discharge and water temperature is indicated ($\rho=0.5$, $n=13$, $p=0.085$, Figure 24).

4.1.6 Performance of JSATS in other studies

Table 8 shows different performance parameters from published literature and those from the field tests during this study. Apparently, different parameters were collected among studies, which makes a comparison difficult. Most authors mention a max DR in their publications, however, but the range of distances is immense.

McMichael *et al.* (2013) and McMichael and Kagley (2015) state a max DR of around 250 m, which fits to the values of the WHS4350 and SR3017. Values for the WHS4250 are generally lower. McMichael *et al.* (2010) state a max DR of 800 m, which is close to the max DR under ideal conditions ((Weiland *et al.*, 2011)). Weiland *et al.* (2011) states a lower max DR in the impoundment and Steig (2017) presents different values based on the background noise.

Ingraham *et al.* (2014) calculated the distance at which DE is 20 % and reports varying results, which are in between those of this study and are similar to those of the WHS4350. The SR3017 shows higher values, whereas the WHS4250 shows lower values.

The DE at 100 m in McMichael and Kagley (2015) are similar as for the SR3017 and slightly higher as for the WHS4350. The WHS4250 was able to decode signals at this distance only occasionally and has, therefore, lower values. At 200 m the DE reported by McMichael and Kagley (2015) is similar as for the WHS4350 but lower than for the

Table 8: Values for maximum detection range (max DR, in m), the distance at which the detection efficiency is at 20 % (20DE) and the detection efficiency at 100 and 200 m (DE100m, DE200m) from literature and field tests during this study.

source		max DR	20DE	DE100m	DE200m	comment
WHS4250	ff	138	58			
	himp	81	71			
	imp	150	79	6-13 %		
WHS4350	ff	220	116	35 %		
	himp	200	111	24-27 %		
	imp	200	148	33-40 %	3-20 %	
SR3017	ff	242	276	65-89 %		
	himp	229	229	44-79 %	26-42 %	
	imp	400	286	53-60%	33-74 %	
(McMichael <i>et al.</i> , 2010)		800	300			
(McMichael <i>et al.</i> , 2013)		250		20 %		in saltwater
(McMichael and Kagley, 2015)	imp	200		70 %	10 %	
	tailrace	300		40 %	2 %	
(Steig, 2017)	50 dB	210				
	60 dB	120				
	70 dB	55				
(Ingraham <i>et al.</i> , 2014)	dam		113-184			
	downstream		148-154			
	array		75-100			
(Weiland <i>et al.</i> , 2011)	ideal	1 000				
	imp	122		53-76 %		
WHS3250	ff					
	himp					MAP based system
	imp	400	296	33-87 %	15-45%	

SR3017. McMichael *et al.* (2013), on the other hand, measured low detection efficiencies at 100 m. Their array was deployed in saltwater, however, where detection ranges are assumed to be lower in general (compare with section 5.1.3).

Interestingly, despite operating at a lower frequency range, the WHS3250 performs similar as other JSATS based receiver, except for a higher value for 20DE.

4.2 Net Fishing

4.2.1 Catch Per Unit Effort

Table 9: Total duration of nets deployed (in h), number of caught sterlets and CPUE (in Ind/h/net) per season and year.

		spring	summer	autumn	winter	total
2018	duration	12	63	33		108
	sterlets	8	3			11
	CPUE	0.67	0.05	0.00		0.10
2019	duration	49	107	69	77	302
	sterlets	11	5		3	19
	CPUE	0.22	0.05	0.00	0.04	0.06
1.-6. 2020	duration	156	15		26	197
	sterlets	10	2			12
	CPUE	0.06	0.13		0.00	0.06
total	duration	217	185	102	103	607
	sterlets	29	10		3	42
	CPUE	0.13	0.05	0.00	0.03	0.07

Catch per Unit Effort (CPUE) was calculated for caught sterlets split off by season and year as well as for the whole sampling time (Table 9). In general, effort was highest in spring and summer and, therefore, both seasons are slightly overrepresented. However, most sterlets were caught in spring, yielding the highest CPUE value of 0.13 Ind/h/net. CPUE values in summer and winter are rather low due to the low number of caught sterlets in relation to a high number of fishing time. In autumn no sterlet was caught.

When comparing the years separately, total CPUE was highest in 2018 and decreased every year. Sampling in 2020 only involves the first six months though and no sampling took place in winter 2018. Apparently total sampling time increased from 2018 to 2019 and is already very high (182 h) in 2020 as did the number of caught sterlets increase with years. Higher sampling effort did not yield more captures to the same extend, which would explain the decreasing CPUE over the years.

When comparing the CPUE per season, values are highest in spring, followed by summer and winter with no sterlet caught in autumn in any year. However, in 2020 no sampling data for autumn is available yet. The explanation for the very high value of 0.67 in spring 2018 is that only one net caught eight sterlets, which was sufficient for the hatchery and, therefore, no further sampling was conducted in spring this year. On the other hand, the very high effort of 156 h in spring 2020 - even though ten sterlets were caught - can be explained by the high amount of recaptures (compare with Table 10), which did not qualify as broodstock fish and the availability of only one ripe male (fish 8020). Hence, net fishing was continued in order to catch different animals.

4.2.2 Total Catches

In Figure 13, a summary of all net catches is shown. In sum, 219 individuals of 18 species were caught, whereas barbel (*Barbus barbus*) and silver bream (*Blicca bjoerkna*) were most abundant with 43 individuals each. In total 42 sterlets could be caught, whereby ten of them were recaptures (see chapter 4.2.4). Additionally, vimba (*Vimba vimba*) and pikeperch (*Sander lucioperca*) were common bycatch with 24 and 20 individuals, respectively. The remaining species were caught occasionally. However, some of them are very interesting and rare species in the Austrian Danube like the Danube roach (*Rutilus rutilus*), the Volga pikeperch (*Sander volgensis*) or the rudd (*Scardinius erythrophthalmus*) (Haunschmid *et al.*, 2010).

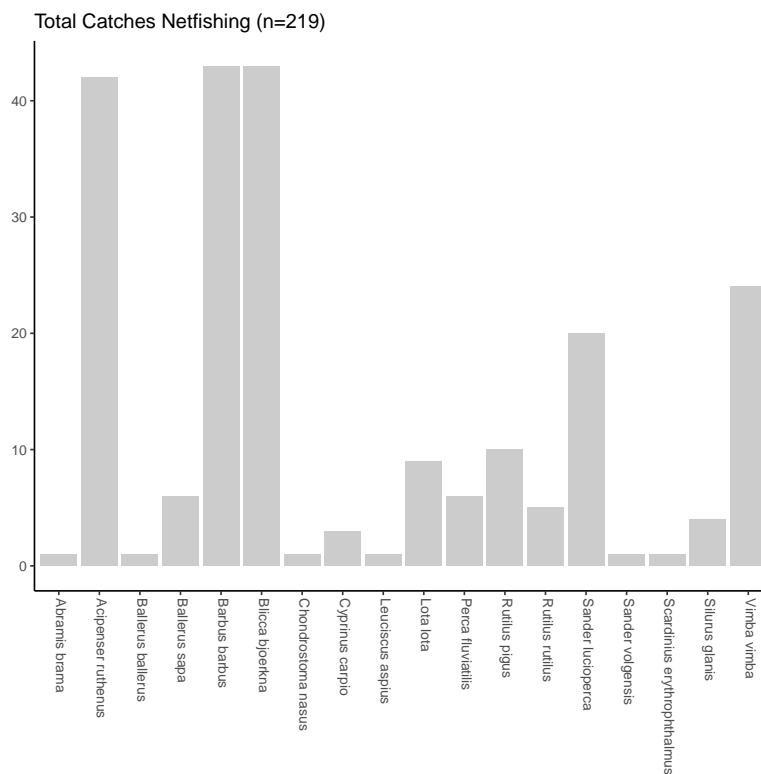


Figure 13: A summary of all caught fish during net fishing.

Table 10: List of caught sterlets (n=42) showing catch date, the full PIT-ID, sex, TL (in mm) and W (in g), K_n and K_F of each fish and if it was a recapture (yes) or not.

Catch Date	PIT-ID	sex	TL	W	K_n	K_F	recapture
29.03.2018	226000178081	?	880	3 700	0.79	0.54	
29.03.2018	226000178065	f	800	4 200	1.30	0.82	
29.03.2018	226000178086	f	680	1 500	0.87	0.48	
29.03.2018	226000178072	?	740	2 200	0.92	0.54	
29.03.2018	226000178037	f	830	2 100	0.56	0.37	
29.03.2018	226000178099	f	790	2 300	0.75	0.47	
29.03.2018	226000178018	f	820	2 400	0.67	0.44	
29.03.2018	226000178020	m	660	1 600	1.05	0.56	
20.07.2018	226000915264	f	860	4 200	0.98	0.66	
25.07.2018	226000177321	f	840	4 200	1.07	0.71	
25.07.2018	226000177377	f	810	3 800	1.12	0.72	
07.03.2019	226000741278	f	770	3 800	1.36	0.83	
07.03.2019	226000741282	m	630	1 400	1.10	0.56	
07.03.2019	226000741324	f	670	2 600	1.60	0.86	
07.03.2019	226000915264	f	860	6 000	1.40	0.94	yes
07.03.2019	226000741295	f	780	4 200	1.43	0.89	
02.04.2019	226000178020	m	660	2 000	1.31	0.70	yes
02.04.2019	226000177377	f	810	4 800	1.41	0.90	yes
02.04.2019	126053536313	m	700	1 700	0.88	0.50	
02.04.2019	126053536348	f	920	6 300	1.13	0.81	
02.04.2019	126053536372	f	860	4 400	1.02	0.69	
02.04.2019	126053536304	f	800	4 400	1.36	0.86	
23.07.2019	226000915487	f	690	1 819		0.55	
23.07.2019	226000915300	f	840	3 920		0.66	
23.07.2019	226000915490	f	880	4 701		0.69	
04.09.2019	226000915264	f	860	4 298		0.68	yes
04.09.2019	043000125526	?	280	54		0.25	
18.12.2019	126053536352	f	770	2 760	0.99	0.60	
18.12.2019	126053536397	m	620	930	0.78	0.39	
18.12.2019	126053536383	m	540	760	1.09	0.48	
13.03.2020	126053536352	f	790	3 085		0.63	
20.03.2020	126053536319	f	740	2 400	1	0.59	
20.03.2020	226000915487	f	680	1 700	0.99	0.54	yes
20.03.2020	226000178065	f	810	3 500	1.03	0.66	yes
20.03.2020	226000741324	f	750	2 200	0.87	0.52	yes
20.03.2020	226000178020	m	670	1 200	0.74	0.40	yes
20.03.2020	126053536376	m	700	1 500	0.78	0.44	
20.03.2020	226000178086	f	680	1 718		0.55	yes
20.03.2020	043000125694	?	570	923	1.07	0.50	
20.03.2020	126053536345	f	740	1 500	0.63	0.37	
23.06.2020	226000177304	f	860	4 900	1.14	0.77	
23.06.2020	226000177321	f	840	3500	0.89	0.59	yes

4.2.3 Sterlets

As mentioned earlier, a total of 42 sterlets were caught, ten of them more than once, amounting to 32 different individuals. They range in total length (TL) between 280 to 920 mm with a mean of 750 mm and their weight (W) ranges between 54 to 6 300 g with a mean weight of 2 885 g. Fulton’s condition factor (K_n) ranges between 0.25 and 0.94 with a mean of 0.61, whereas the relative condition factor (K_r) is generally higher, ranging between 0.56 and 1.60 with a mean of 1.03. Analysis of weights and condition factors is done in more detail below.

In sum, 30 females (Figure 14), eight males (Figure 15) and four individuals whose sex remains unknown were caught (Table 10). Sexing was done based on the presence of ripe gametes during spawning season, body shape and rostrum and scute formation.

In general, caught sterlets were rather large, shown in their size distribution (Figure 16). Even though the mesh size should be sufficiently fine to capture small individuals, only one smaller fish (280 mm) was caught. This fish was quite certainly one from the hatchery, which was stocked the day before net fishing. Not all released sterlets are PIT-tagged and this fish might have been one of them.

Table 11: Comparison of total length (in mm) and weight (in g) of sterlets separated by sex.

sex	TL			W		
	min	max	mean	min	max	mean
f	670	920	794	1 500	6 300	3 440
m	540	700	648	760	2 000	1 386
?	280	880	618	54	3 700	1 719

At a closer look, female fish appear to be larger and heavier than males and those whose sex is unknown (Table 11). Females have a mean total length of 794 mm and a mean weight of 3 440 g, respectively. Males are smaller with a mean total length of 648 mm and a mean weight of 1 386 g. Length and weight of unsexed fish lie in between, with a mean total length of 618 mm and a mean weight of 1 719 g. The same trend can be observed in Figure 16, where females (red) cluster at larger total lengths than males (blue) do. Unsexed fish (white) show no clear trend. Sex determination for one individual of 880 mm could not successfully be done, regardless of its length, due to a high amount of intestinal fat, which was observed during the implantation of a radio telemetry tag in 2018.

The assumption that weight differences are partially due to the presence of female gametes is strengthened by Figure 17, which shows that females with ripe gametes during spring (f.r, pink) tend to have higher weights than females, whose gametes were not identified as ripe during spring, or which were caught during any other season (f, red). Moreover, except of one individual, all females with ripe gametes have weights lying at or above the simulated trend line for all fish. The calculated b-value based on the length-weight regression analysis for all sterlets caught during net fishing corresponds to 3.91 and shows allometric growth.



Figure 14: Female sterlet, note the round belly. This picture was made during spawning season, where this individual carried many eggs.



Figure 15: Male sterlet, note the elongated rostrum and thin body shape.

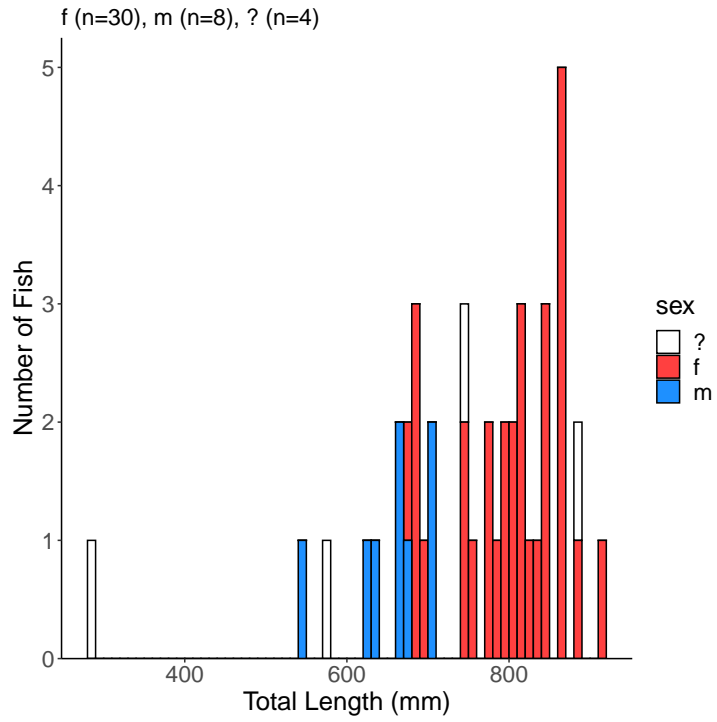


Figure 16: Length Frequency diagram of caught sterlets separated by sex.

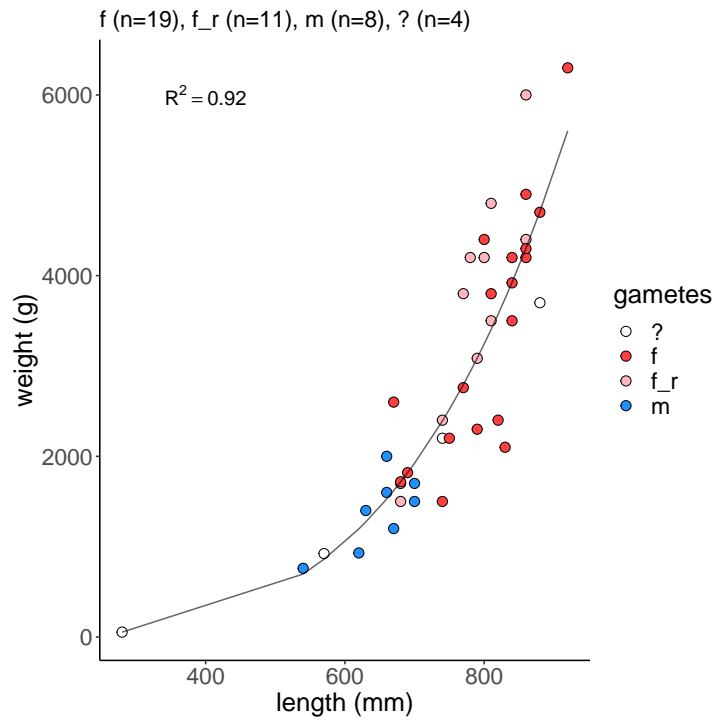


Figure 17: Length-Weight regression separated by sex, whereby f = females, f_r = females with ripe gametes, m = males, ? = unknown sex.

4.2.3.1 Condition Factors

Table 12 shows the values for the relative condition factor and Fulton’s condition factor for females, males and unknown fish in all seasons and the general differences between sexes. For seven fish no weight measurement was available (compare with Table 10), hence, they are not included in this analysis. In Table 12 some values are missing due to missing data because in autumn no sterlet was caught and during the other seasons not all sexes (see CPUE (Table 9)). Overall, females show higher values for both condition factors than males do. Unsexed sterlets show the lowest K_n but their K_F is in between those of males and females. However, values for unsexed fish were calculated from only four individuals.

In spring, values for all fish are available and again values for both condition factors are highest for female sterlets, indicating a slightly better condition than in males and unknowns. However, some females carried a good amount of eggs, which contributes to a temporarily increased weight. The fact that K_n of females is higher in spring could be due to the same reason. Condition factors in winter are lowest in males and females than during any other season. In general, the relative condition factor attributes an overall better condition to all fish than Fulton’s condition factor does.

Table 12: Condition factors K_n and K_F for all season and separated by sex.

sex	mean K_n					mean K_F				
	overall	spring	summer	autumn	winter	overall	spring	summer	autumn	winter
f	1.07	1.08	1.04		0.99	0.67	0.67	0.69		0.60
m	0.97	0.98			0.94	0.50	0.53			0.44
?	0.93	0.93				0.53	0.53			

In Table 13, the mean values for K_n and K_F in spring of the years 2018, 2019 and 2020 are shown for all females and separated based on the maturity of their gametes. As in Table 12, the relative condition factor attributes higher values to all fish than Fulton’s condition factor does. In 2018 and 2020, both condition factors show higher values for females with ripe gametes, but not in 2019, where all females seemed to be in an overall better condition. However, since the scale used in 2019 was very imprecise, those values and subsequent interpretations have to be taken with caution.

Table 13: Condition factors K_n and K_F for all females, ripe females (f_r) and unripe females (f_u) in spring of 2018, 2019 and 2020.

sex	2018			2019			2020		
	n	K_n	K_F	n	K_n	K_F	n	K_n	K_F
f	5	0.83	0.52	8	1.34	0.85	5	0.90	0.54
f_r	2	1.08	0.65	5	1.32	0.85	3	1.01	0.60
f_u	3	0.66	0.43	3	1.36	0.84	2	0.75	0.45

4.2.3.2 Recaptures

Table 14: Initial capture and recapture events of eight different individuals including their TL, W and K_n at each capture event if available.

		29.03.2018	20.07.2018	25.07.2018	07.03.2019	02.04.2019	23.07.2019	04.09.2019	20.03.2020	23.06.2020
8086	TL	680							680	
	W	1 500							1 718	
	K_n	0.9								
8020	TL	660				660			670	
	W	1 600				2 000			1 200	
	K_n	1				1.3			0.7	
8065	TL	800							810	
	W	4 200							3 500	
	K_n	1.3							1	
5264	TL		860		860			860		
	W		4 200		6 000			4 298		
	K_n		1		1.4					
7377	TL			810		810				
	W			3 800		4 800				
	K_n			1.1		1.4				
1324	TL				670				750	
	W				2 600				2 200	
	K_n				1.6				0.9	
5487	TL						690		680	
	W						1 819		1 700	
	K_n								1	
7321	TL			840						840
	W			4 200						3 500
	K_n			1.1						0.9

All recaptures are shown in Table 14 and for simplification only the last four digits of their PIT-ID (compare with Table 10) are used for identification. The first appearance relates to the initial catch of the fish and all further appearances are recaptures. Thus, two fish (8020 and 5264) were caught three times and five fish were caught twice (8086, 8065, 7377, 1324 and 5487). Additionally, length, weight and K_n for each fish are displayed.

Sterlet 8020 was caught three times between 2018 to 2020 and always in spring. It is a male that was used for reproduction each year - in the third year due to the lack of other males. The fish grew only 10 mm in two years, its weight varied each time when it was caught and with it K_n . Even though K_n at the last catch was 0.7 suggesting the fish was in poor condition, it made a very lively impression though.

The second fish which was caught three times is a female with the code 5264. It was initially caught in summer 2018 where it was in good condition. After it was caught for the second time in spring 2019, it was used as broodstock because it carried many eggs which is indicated by its weight of 6 kg. This fish was caught for the third time in summer 2019, where weight was not measured and, therefore, no K_n is available. Since the fish always had the same size and, according to the calculated weight, a K_n of around 1 can be assumed.

Sterlet 8086 is a female and was caught in spring 2018 as well as in spring 2020. Both times it was kept as temporary broodstock. In 2018, it carried eggs, but in 2020 it did not and the fish was in bad condition. Apparently, it did not grow over the course of two years and no data for K_n is available for 2020 because fish weight was not measured.

Therefore, the weight for spring 2020 displayed in Table 14 was calculated based on the calculated b-value.

Sterlet 8065 is a female and was caught twice in spring 2018 and 2020. It was used for reproduction because it was ripe in both years. It grew 10 mm over two years and its weight was less in 2020 than in 2018, which can be explained by the big amount of eggs the fish carried in 2018. K_n always suggests the fish being in good condition.

The sterlet 7377, which is a female, was caught in summer 2018 and in spring 2019, where it was used for reproduction. Again, it had the same total length at both events but its weight and with it K_n was quite different and indicates the vast amount of eggs it carried in 2019.

Sterlet 1324 is a female which was caught twice, first in spring 2019 and almost exactly one year later in spring 2020. Interesting about this fish is that it grew eight cm in one year. Since this is not very likely to happen at this size, it could be due to a measuring mistake at the first capture. In 2019, it weighed more than in 2020 and since the length measurement is likely to be wrong, the value for the K_n might have the same error. This fish was not used as broodstock in either year. In 2020, it did not carry eggs and in 2019 the only remark is that the eggs might have been unripe. The higher weight suggests that it carried at least a small amount of eggs in 2019.

The fish 5487 is a female that was kept for reproduction in 2020. At the first catch in summer 2019, no weight measurement was taken and, therefore, no value for K_n is available. At the second catch in spring 2020, K_n indicates that the fish is in good condition. Apparently, the length measurement was carried out imprecisely because the fish shrank between first and second capture. The low weight in 2020 can be explained by the fact that the fish carried eggs but ovulation was not finished at the time of the weight measurement.

The last fish which was caught more than once is the female 7321, which was caught in summer 2018 and in summer 2020. Over two years the fish remained at 840 mm length but the weight changed from 4 200 g to 3 500 g and with it did K_n drop from 1.1 to 0.9, which still indicates the fish is in good condition. Since it was always caught in summer, this fish was never used as broodstock.

4.2.4 Population Estimation

In Table 15, the population estimation for the sampling area based on sampling years 2018 and 2019 is shown. The real catch approach takes into consideration all real captures in both years. Hence, in 2018 eleven sterlets were captured (n_1 - number of animals captured at the first visit) and 18 sterlets were caught in 2019 (n_2 - number of animals captured at the second visit), three among them were tagged (n_M - number of recaptured animals that were marked, compare with equation 5). Since sterlet 5264 was caught twice in 2019, it has been removed once, which gives 18 total captures and three recaptures in 2019 (instead of 19 and four respectively, compare with Table 10). For this approach, the estimated population size (N) is 56 individuals and with a 95 % confidence interval (CI) between 27-140 individuals.

As described in section 3.2.2, the sampling effort was around three times higher in

Table 15: Population estimation based on the sampling years 2018 and 2019 using the Chapman estimator.

	real catch		adapted	
	2018	2019	2018	2019
n_1	11		11	
n_2		18		6
n_M		3		1
N	56		41	
95 % CI	27-140		18-145	

2019 than in 2018. Hence, it was adapted to match the sampling effort of 2018. This approach reduces the number of caught fish in 2019 to 6 and the recaptures to one. With this approach, the estimated population size is 41 individuals with a 95 % confidence interval between 18-145.

Table 16: Population estimation (N) based on the sampling years 2018-2019 and 2018-2020 using the Jolly-Seber estimator. Upper and lower 95 % confidence intervals are displayed in the table.

sampling day	2018-2019			2018-2020		
	lower CI	N	upper CI	lower CI	N	upper CI
1						
2	0	2	Inf	0	6	Inf
3	0	9	Inf	0	12	Inf
4	0	21	71	0	33	95
5	0	21	Inf	0	46	140
6	0	16	Inf	0	48	Inf
7		2		0	29	Inf
8				0	48	Inf
9				0	13	Inf
10				0	25	Inf
11						

The second method used to calculate the population size in the sampling area is the Jolly-Seber-model (JS-model) which results are shown in Table 16. With this approach, population sizes are calculated for each sampling day except the first and the last including an upper and lower confidence interval of 95 %. In the years 2018 and 2019, sterlets were caught at 7 different sampling days. Depending on the number of new captures and recaptures, the population size varies between two to 21 individuals. Only at sampling day four a confidence interval which is not infinite could be calculated. The lower confidence interval is zero for all sampling days.

In 2020, sterlets were caught at three more days, therefore, at ten days between 2018-

2020. Population estimations for all sampling days range between six to 48 individuals. Lower CI is zero for all sampling days and except for sampling days four and five all upper CI values are infinite. For sampling days four and five they are 95 and 140, respectively.

5 Discussion

5.1 Telemetry

Beforehand has to be mentioned that the need to test the equipment evolved, after the performance of the receiver in use - the WHS4250 - appeared to be unsatisfying due to the low amount of signals it decoded and the short distance at which successful decodes were achieved (compare with Table 5 and Table 7). In regard to mobile tracking by boat, results for mean and median distance at which signals were decoded by the WHS4250 in the free flowing section are discouraging, but reflect the impressions in the field. They are as low as 18 and 12 m, respectively. Given the size of the Danube, reasonable tracking of fish is almost impossible. Thus, after initial testing of the WHS4250 during active tracking sessions and based on the results from those sessions, it became apparent that more accurate and detailed testing is necessary, also in regards to further studies using acoustic telemetry. For a better overview, other JSATS based receiver models and one MAP based receiver were included. Especially, to evaluate if the impressions obtained from the WHS4250 in a large and fast flowing river reflect the overall performance of the JSATS in such a system, or if there are differences between receivers and also between technologies.

Owed to the inexperience of working with acoustic telemetry, the available equipment and the conditions and character of the sampling area, the testing method was developed successively towards the methods which were ultimately used and can be used for future testing. The applied testing methods worked and suffice to describe trends of the performance of the receivers in focus and across habitats, but there is still room for further gains.

5.1.1 Overall Performance

The main result in regards to answering the question if the tested JSATS based receivers are suitable for sterlet monitoring in the study area, is the fact that 120 m seems to be the crucial distance at which a clear difference of detection efficiency becomes apparent. This result was achieved across all habitats and regardless of the receiver model (Figure 9). Since the width of the Danube in the study area is between 300 to 400 m and above, a detection range of 120 m - or 240 m because the receiver detects tags at 360° - is not enough to cover the whole river width. Furthermore, it has to be mentioned that the DE below 120 m is usually lower than 100 % (Figure 9), hence, not all signals emitted by a tag can be expected to be decoded. Therefore, the chosen burst interval at which the tags emit their signals becomes a crucial factor. If the burst interval is too high and the tag leaves the area in which the receiver is able to detect its signal, the tag remains

unnoticed. During mobile tracking, this effect might be stronger in the free flowing section than it would be in an impoundment because of the higher velocity at which the tag moves through the area in which it can be detected (Steig, 2017). Moreover, a detection range of 240 m is only given, if the tag travels exactly through the center of the detection area of the receiver. If the tag is displaced and travels through the detection area at some distance off the center, the effective detection range is smaller. This effect is well explained by Steig (2017), who uses the more conservative criterion that four signals must be detected in a row to count as a valid detection (compare with section 3.1.1 and Figure 18). When a tag passes through the center, it has a higher chance of being detected because more signals are emitted. The scenario in which the tag does not travel through the exact center seems to be more likely during mobile tracking and during tracking with fixed listening stations, however.

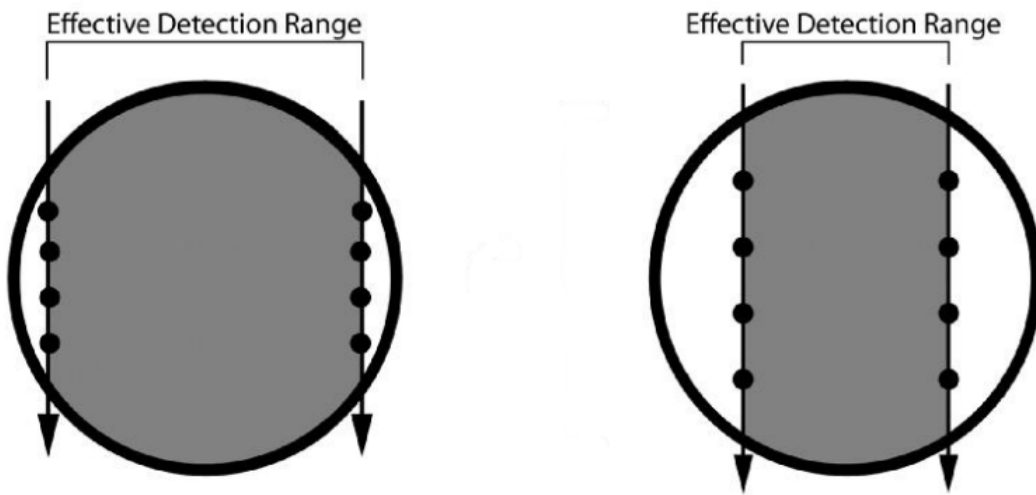


Figure 18: Effective detection range of a signal emitted at a low burst interval (left) and at a high burst interval (right). Modified from Steig (2017).

Furthermore, clear differences between receiver models became apparent regarding their detection range and efficiency. That said, the WHS4250 receiver shows a very low detection range overall and especially in the mean and median (Table 5 and Table 7). In relation to all other receivers, the WHS4250 received the lowest amount of signals in general and across all habitats. Due to the fact that the receivers were used during different test days and, hence, abiotic conditions, the values presented in Table 5 and Table 7 cannot be compared per se. Nevertheless, both tables indicate a trend which is strengthened by the subsequent results in section 4.1.

In the impoundment section, only every third signal or less is decoded by the WHS4250 below 120 m (Figure 9). Moreover, Figure 21 in the appendix reveals a mean DE of 0.113 for the same terminal node, which corresponds to 11.3 %. Figure 20 further reveals that the WHS4250 was able to detect more than every 10th signal only at a distance of 25

m but not at higher distances. At this point, one weakness of classifying the data into categories becomes apparent, since some information loss occurs regarding the precise performance of the WHS4250 in the impoundment.

In both other habitats, the detection efficiencies of both, the WHS4250 and the WHS4350, are low at distances above already 30 m. In the impoundment, the latter receiver tends to miss many signals as well (Figure 9). Figure 20 further reveals that only six out of ten signals are decoded below 75 m.

The SR3017 showed the best performance among all JSATS based receivers and across habitats. Figure 21 reveals high mean detection efficiencies of 80.3 % in the free flowing section and the head of the impoundment below 120 m and 71.1 % below even 175 m in the impoundment. In this case Figure 20 strengthens those results and reveals that the SR3017 keeps a high DE until 100 to 150 m with a steep decrease thereafter. All other receiver models show a more uniform decline in DE.

What all receivers have in common is the vast scattering of data points at each distance (Figure 20). This might result from the use of two different tags (see section 3.1.4) and the merging of two test days with different abiotic circumstances in the head of the impoundment and the impoundment. Only one test from the free flowing section was considered in data analysis. This scattering seems to be especially strong for the WHS3250 receiver. Interestingly the test at January 17th yielded higher detection efficiencies than at January 21st for the WHS3250, but vice versa for the SR3017. DE is known to vary with time due to environmental conditions (Kessel *et al.*, 2014), but since abiotic conditions in the water were similar during both days (compare with Table 3), they might not explain this variability entirely. Both tests were conducted in the same area but during the first test it was windier. This still does not explain why not both receivers worked better during the second test. Another approach might be the depth at which the test tags were deployed at. During the first test in the impoundment, the tags readable by the well working WHS3250 were deployed at a depth of 4 m, whereas those belonging to the SR3017 were deployed at a depth of 3 m. During the second test, the tags belonging to the well working SR3017 were deployed at depths of 4 and 5 m, whereas the tags belonging to the WHS3250 were deployed depths of 4.5 and 3 m. At both test days, the tags deployed at 3 m performed worst, which might be an indication for a higher amount of multipath interference due to the vicinity to the water surface as discussed below.

In summary, it becomes apparent that neither the WHS4250 nor the WHS4350 can reliably detect signals at distances of around 50 m in the study area. Even the ability of the SR3017 to reliably detect signals to a distance of around 100 m might not be sufficient for the study area, given the width of the Danube. As mentioned above, it depends on the burst interval which is used and on the monitoring design. In order to monitor long distance migrations, receivers are usually positioned along possible routes the target species might chose (McMichael *et al.*, 2010; Acolas *et al.*, 2012; Ratschan *et al.*, 2017). Thereby, depending on the number of receivers available, either a receiver line (McMichael *et al.*, 2010; Acolas *et al.*, 2012) or single receivers (Ratschan *et al.*, 2017) are deployed to detect passing fish. Hence, if a single receiver is used, it should cover the whole river width in order to exclude the possibility that fish pass the receiver

in an area, where it cannot be detected. With the receivers tested in this study, a whole coverage of width in the study area can only be achieved with a line of at least two (for the SR3017) or more receivers. Subsequently, a large number of receivers is necessary. A different approach was chosen by Kubala *et al.* (2019). The authors defined an area of interest, which was confined with two receivers at both ends. The area in between was sampled via mobile tracking. However, in this example the authors captured the fish in this area and knew they tend to stay there (Pekarik, pers. comm.). Given the performance of the receivers in this study, this approach might be feasible in theory, using the SR3017. Detection range and corresponding detection efficiencies of both other receiver are likely to be unsuitable. However, since little is known about habitat requirements of sterlets (Friedrich *et al.*, 2014) and one goal of the Life Sterlet project is the identification of habitats (Friedrich, 2017), such an approach would be restricted in space and other potential habitats could be overlooked.

The JSATS was successfully used to observe fish in the vicinity of dams (McMichael *et al.*, 2010; Jung *et al.*, 2015; Li *et al.*, 2015a, 2018) and during their migration at bridges (McMichael *et al.*, 2010; Li *et al.*, 2015b). All sites have in common that the areas where fish can pass are confined and, additionally, a high number of hydrophones was used to cover these confined areas. Since already low detection ranges would suffice, high detection rates could be observed. In contrast, lower detection efficiencies in the plume array in McMichael *et al.* (2013) are attributed to generally lower detection ranges in saltwater (the effect is even stronger at frequencies above 300 kHz (Pincock and Johnston, 2012)), but also to larger spacing of the receiver array. The research goals of the studies varied strongly, consequently did array designs. Goals were to quantify survival rates (McMichael *et al.*, 2010), to assess how juvenile salmonids approach and pass dams (Jung *et al.*, 2015; Li *et al.*, 2015b,a, 2018) and to monitor the migratory behavior of juvenile salmonids once they arrived at the sea (McMichael *et al.*, 2013). Moreover, did all studies have access to very high numbers of receivers for deployment, which is not the case in the current Life Sterlet project. Since the aim is to gather information about the migratory behavior and habitat use of juvenile sterlets with restricted access to receivers, mobile tracking will be an important part of the monitoring. As already mentioned, not many receivers to cover the whole river width at one point are available, but as few receivers as possible need to cover the whole width to observe the migration at several points in the study area. Thus, high detection ranges and efficiencies are needed.

Table 1 reveals that both, the WHS4350 and SR3017 have an improved frequency shift immunity compared to the WHS4250. Hence, movement of the tag, the receiver or both likely affect latter more and interfere with successful decoding of signals. Considering the flow velocity alone, this effect should be highest in the free flowing section and lowest in the impoundment. In general, all receivers were able to successfully decode signals at higher distances in the impoundment than in the free flowing section (Figure 11). This effect could be attributed to a faster moving boat and, therefore, the Doppler effect. During mobile tracking, either the fish, the boat or in most cases both are expected to move, which could limit the tracking success. Moreover, do Pincock and Johnston (2012) comment on the results in Weiland *et al.* (2011) that the major issue for the performance of the telemetry system, is likely to be the small range of distortion through multipath

interference and Doppler effects that is tolerated by the decoding system.

Hence, signals are detectable at further distances, but successful decoding is only possible at smaller distances (compare with results of decoding efficiency vs detection efficiency from (Weiland *et al.*, 2011) above). The trend in Figure 11 indicates that all JSATS based receivers tend to decode signals at higher distances in deeper water than in the shallower environment of the free flowing section. Acoustic telemetry systems typically work better at higher depths (McMichael *et al.*, 2010; Ingraham *et al.*, 2014) because signal collisions are reduced (McMichael *et al.*, 2010; Weiland *et al.*, 2011; Pincock and Johnston, 2012; Ingraham *et al.*, 2014; Jung *et al.*, 2015). One general problem for both, the JSATS and the MAP decoding, is its aggressiveness in decoding to generate a high number of individual codes, which reduces the maximum range tags can be reliably detected at (Pincock and Johnston, 2012). If only one bit is not decoded correctly, the proper ID of the tag cannot be obtained (Steig, 2017). It would be possible to reduce the number of individual codes and at the same time provide more than other decoding technologies do, without reducing the detection range by the same extent, however, such products are not on the market yet (Pincock and Johnston, 2012). Lu *et al.* (2016) presented a tag directly addressed to long-term monitoring (up to one year) of juvenile sturgeons, which operates at the same frequency as the JSATS. The published detection distance of 500 m is reached through a more powerful signal emission, but is currently based on calculations and, at most, valid for quiet reservoir type locations, where the data base for their calculations was gathered. Thus, research on achieving high detection distances and at the same time keeping tags small and tag life high, will be of major importance in order to answer yet unanswered questions about long-term behavior of small taxa.

5.1.2 Performance among Habitats

All JSATS based receivers received the most detections per hour in the impoundment and, in contrast, the lowest amount in the free flowing section (Figure 7). This indicates that signals are easiest received in the impoundment and worst in the free flowing section.

From literature it is known that high flow velocities and associated higher noise levels, as well as the structure of the substrate, can interfere with the performance of acoustic telemetry systems (Bergé *et al.*, 2012; Cooke *et al.*, 2013; DeCelles and Zemeckis, 2014). A shift from smooth to turbulent river flow may cause a drop of detection range from several 100 to less than 10 m (Melnychuk, 2012). Higher flow velocities and a harder substrate in the free flowing section could cause an increased scattering of signals due to multipath reflections and, therefore, limit the amount of successfully decoded signals (Ingraham *et al.*, 2014). On the one hand, these assumptions are strengthened by the fact that the free flowing section is the shallowest habitat (compare with section 2.1.1). On the other hand, mindful of the low amount of data points, does Figure 12 show a negative correlation of mean distance and discharge in the free flowing section. An effect of discharge on the mean distance in the impoundment is missing. In general, it can be assumed that the effect of a higher discharge on flow velocity is larger in the free flowing section than in the impoundment. This means that, during high discharge events, in the

free flowing section flow velocities increase stronger than in the impoundment because the latter is well buffered due to its depth and amount of water. Moreover, does the spillover of the dam usually open only at a certain discharge. Even though the exact threshold at which it is opened is unknown for the hydropower plant Altenwörth, the spillover at the comparable Freudenuau opens at $2\,800\text{ m}^3/\text{s}$ as a reference. This value was not reached during any test in the impoundment and the spillover gates were always closed. Hence, during the tests a higher discharge was well buffered and probably did not affect the performance of the receivers in the impoundment due to higher flow velocities.

However, the hydrograph from the closest gauging station Kienstock reveals that only during one test (March 22nd, 2019 - impoundment), the discharge was above the mean discharge for the study period. During all other tests it stayed well below (Figure 5). Hence, in the free flowing section, only a very small range of possible situations regarding the discharge of the Danube is covered. The tests only reflect low water levels in the Danube, which are usually expected during summer and winter. The narrow range of discharge and corresponding wide range of mean distances could represent variability in receiver performance rather than an influence of discharge as well, which reasons that no real trend can definitely be identified. To comprehensively cover the influences of discharge on receiver performance and the scattering of signals, tests focusing on these questions are necessary and should cover a wide range of possibly occurring situations in the area of interest, as mentioned by several authors (McMichael *et al.*, 2010; Kessel *et al.*, 2014; Steig, 2017).

In Figures 8, 10 and 11 the 95 % confidence intervals for the mean in the former and the median in both others are given. A confidence interval represents a range of values that are considered to be plausible for the population and, hence, provides a description of differences between populations rather than showing that there is any based solely on statistical significance (Gardner and Altman, 1986). The confidence interval summarizes the results clearly and interpretation can confidently be done based on the position of the interval on its scale of measurement (Rothman, 1978). The close link between the use of a confidence interval and a two-sided hypothesis test and the fact that the result of the hypothesis test can be inferred at an associated level of statistical significance (Gardner and Altman, 1986), helps to distinguish clear differences of results and at the same time describe those differences based on confidence intervals.

An interesting result is the converse trend of DE and distance among habitats. While DE tends to decrease from the free flowing section towards the impoundment (Figure 10), distance tends to increase along the same path (Figure 11). Since DE decreases with distance (Figure 20 and compare with (Weiland *et al.*, 2011; Ingraham *et al.*, 2014; Kessel *et al.*, 2014; McMichael and Kagley, 2015)) and signals were decoded at lowest distances in the free flowing section and vice versa in the impoundment, these results are unsurprising. Reasons for the capability of decoding signals from higher distances in the impoundment are discussed above and include signal scattering from reflective surface such as the river bottom or the water surface, which is reduced in deeper water (Bergé *et al.*, 2012; Ingraham *et al.*, 2014; Jung *et al.*, 2015). Additionally, turbulent flows negatively impact detection range (Melnychuk, 2012).

At this point, the data base for DE calculations (Figure 19 in the appendix) has to be

discussed. Even though the R^2 -value is very low, a significant relationship between DE and passed s exists. This affects especially the tests in the free flowing section and the head of the impoundment because in those habitats the majority of DE data comes from shorter time windows up to 90 s. In the impoundment, all data points come from time windows of 300 s because in this part of the river anchoring of both, the boat and the buoy, was no problem. Since DE tends to be higher at shorter time windows, it tends to be overestimated in the free flowing section and the head of the impoundment. An application of the test design used in the impoundment (and by (McMichael and Kagley, 2015)) in all parts of the river might have yielded different and even better comparable results. To perform tests in a large, fast flowing river, a design matching those rough environments including heavier gear has to be applied for future testing.

Depending on the study aim and method how fish are to be monitored, Melnychuk (2012) suggests considering different definitions of DE. One definition by the author is the "probability of detecting a tag moving past a specific location (DE_{mig})" for surveys using stationary listening stations. The author points out that DE_{mig} can be high even though DE (the author refers to it as DE_{single}) is low because already one valid detection proofs the presence of the fish. Contrary, could DE_{mig} be low even though DE is high if the burst rate of the tag is too high to be detected while moving through the area where it could be detected. Tags transmitting at higher burst rates could, therefore, improve detection probability in areas where fish move quickly (McMichael *et al.*, 2010). DE_{mig} varies with background noise and flow velocity and subsequent swimming speed of fish and should be estimated for various conditions. Despite those exceptions, DE is considered as reasonable index of DE_{mig} (Melnychuk, 2012). In terms of mobile tracking, the author defines DE_{mobile} as "probability of detecting tags present within the area sampled by mobile surveys". In order to design mobile sampling patterns, it is crucial to understand detection ranges of mobile sampling gear and how they change with environmental conditions and boat speed. However, to know DE_{mobile} is especially important if the number of tagged fish present in the sampled area during mobile tracking is of interest, but not necessarily to assess migration patterns.

Lastly, the question why the WHS4350 shows a converse trend of mean and median distances among habitats than both other JSATS receivers do (Table 7) needs some clarification. This question might not be entirely solved, but it is quite certainly a problem with the testing procedure itself. As mentioned in section 3.1.5.1, the low flow velocity in the impoundment made it necessary to use the engine to increase or decrease the distance between receiver and tag. Especially, when the boat went upstream towards the buoy, signals were only received below 10 to 15 m. Maybe due to a combination of an occurring Doppler effect and increased noise at the hydrophone during driving. That is what happened during the test at November, 29th, when only the WHS4350 and the WHS4250 but not the SR3017 were available. The SR3017 was, therefore, not affected by this mistake and the effect on the WHS4250 was low because it did not decode signals at high distances anyway. The exceptionally well performance in the free flowing section cannot be explained, but indicates that the receiver copes well with some degree of movement between the tag and the receiver itself.

5.1.3 Performance of JSATS in other studies

From literature different values for distances at which the JSATS successfully decode signals are documented. All available values of different metrics are collectively presented in Table 8.

The performance of the JSATS based receivers can be summarized as being similar to slightly worse in the Danube than in other studies published. The big exception is the WHS4250, which did strikingly worse than both other receivers tested and the telemetry systems in consulted literature. The WHS4350 used in this study was only a prototype, therefore the results obtained during the tests might be different than those the final product might obtain. The fact that the WHS4350 is the successor of the WHS4250 also suspects that the latter is not a product of fullest satisfaction.

As a benchmark Weiland *et al.* (2011) tested the performance of a JSATS hydrophone under ideal conditions in a laboratory experiment. The signal was emitted with different output power to simulate signal attenuation with distance from the source. For analysis, the authors distinguish between decoding efficiency, which is the number of correctly decoded detections by the number of transmissions, and detection efficiency, which is the number of detections divided by the number of transmissions. In the laboratory tank, the simulated threshold for a decoding efficiency of 100 % was 316 m and at 562 m still 59 % were achieved. At 1 000 m only very few signals were decoded, which further decreased with increasing distance. No signals were decoded at a simulated distance of 1 778 m. At a field experiment at the Bonneville Dam in the Columbia River, both, the decoding efficiency and the detection efficiency, were evaluated. While detection efficiency includes multipath signals in this study decoding efficiency does not. Hence values for former are higher with 99.5 % up to 107 m and 71.3 % at 122 m than for latter with 53 and 76 % up to 107 m. No values are given for further distances.

In McMichael *et al.* (2010) a DR of 300 m is quoted but with additional information that at this distance still 20 % of the signals were received, which complies with a DE of 20 % at 300 m. Additionally, the authors point out that transmitters have also been detected at 800 m. The only additional information is that those distances were measured in freshwater, but no information about the nature of the waterbody or abiotic conditions at the time of measurement is provided. However, since the study was conducted in the Columbia and Snake River, it is likely those values come from the same area. The authors also address the problem of changing environmental conditions and state that this range data should be viewed with caution.

McMichael and Kagley (2015) present DE tests for the JSATS in the study area of McMichael *et al.* (2010). The impoundment of the Ice Harbor Dam in the Snake River shows a similar flow velocity (0.2 m/s) as the impoundment of Altenwörth, but with 28 m it is deeper. The tailrace below the dam has a flow velocity of 0.5 m/s and is 7 m deep which are similar conditions as in the head of the impoundment of Altenwörth (compare with section 2.1). The patterns of the declining DE with distance in the impoundment and in the tailrace are very similar to the decline of DE with distance from the SR3017 in the impoundment and in the head of the impoundment during this study, respectively. This is especially interesting because McMichael and Kagley (2015) used a receiver from

the company ATS as well. Unfortunately, the exact model is not mentioned.

McMichael *et al.* (2013) received signals at a maximum distance of 250 m in their array in the plume of the Columbia river in saltwater, where receivers were deployed at 55 m below the water surface. The authors indicate DE values for 100 and 150 m with 20 % and between 5-10 % respectively and refer to a reduction of the JSATS detection range of approximately the half in saltwater compared to freshwater.

In Steig (2017), maximum and effective detection ranges for a JSATS type tag are published. For effective detection range, the author uses the more conservative criterion that four signals must be detected in a row to count as a valid detection as mentioned above. Hence, it corresponds to the distance from the center of the receiving circle of a receiver, to the line at which a tag can pass this receiving circle and at the same time stays long enough to emit four signals. This implies that the effective detection range is shorter than the maximum detection range, depending highly on the burst rate interval of the tag and on the velocity with which the tag passes through the detection circle. All values for maximum and effective DR are given for scenarios of two different water velocities (1 and 3 m/s for low and high) in three background noise environments (50, 60, 70 dB for low, medium and high noise environments respectively). The results for maximum DR are 210, 120 and 55 m for low, medium and high noise environments. The flow velocity has no influence in this case. Conversely, flow velocity has an effect on the effective DR because it influences the time the tag stays in the receiving circle. In a low noise environment, effective DR is 209.66 and 206.89 m, in a medium noise environment it is 119.4 and 114.47 m and in a high noise environment effective DR is 53.67 and 41.58 m for low and high water velocities, respectively (compare with Steig (2017)). However, all values are calculated taking into account the source level of the tag, absorption in freshwater (55 dB/km) and the minimum required signal to noise ratio (SNR) for tag identification as threshold. The SNR should be a difference of at least 5 dB between tag signal and background noise for successful decoding. The flow velocities stated above are once again comparable to velocities present in the study area, whereas 1 m/s matches the head of the impoundment and 3 m/s the free flowing section (compare with section 2.1). Since no background noise levels for any site in the Wachau valley are available, a comparison per se is not reliable. However, those results show how detection range can vary depending on the surroundings and, especially, the maximum DR which decreases with an increasing noise level.

At the Ice Harbor Dam in the Snake River, range tests for the JSATS were conducted directly at the dam, 500 m downstream by boat and with an array of autonomous receivers (Ingraham *et al.*, 2014). Additionally, the authors recorded ambient noise levels, which were greatest close to the spillway at high flow events. However, in this paper values for noise levels are published as Sound Pressure Level (SPL), whereas Steig (2017) uses the Power Spectrum Level (PSL) format (which is SPL in a 1 Hz band (Ingraham *et al.*, 2014)). For better comparability, background noise levels measured at the Ice Harbor Dam vary between 50 to 60 dB in PSL format, which corresponds to a low or medium noise environment as defined in Steig (2017). Ingraham *et al.* (2014) define detection range as "the distance at which detection efficiency drops to 20 %", which is less than the maximum detection range achievable. Directly at the

dam, noise levels ranged between 104 - 114 dB re 1 μ Pa depending on their distance to the spillway. Noise levels decreased with increasing distance to the spillway. The noise level 350 m downstream of the dam was 106 dB re 1 μ Pa. Associated detection ranges for receivers attached to the dam are 113 m for tags and 136 m for beacons mounted to a remote controlled boat and between 166 and 184 m for beacons mounted on the dam. The authors explain lower detection ranges of tags and beacons mounted to the remote controlled boat with a changing orientation due to a high current and because of the shallower water further away from the dam (3 m) than directly at the dam (8 m) where the beacons were attached. In shallower water, multipath interference due to more reflections can limit the detection range. The tests by boat 500 m downstream of the dam were conducted from a floating, as well as from a moored boat. Detection ranges are 154 m for the stationary test and 148 m for the drift test. Those higher distances are explained by the authors with their distance to the spillway and the accompanying lower noise level. The detection range of the array was lowest with distances between 75 and 100 m. Ingraham *et al.* (2014) attribute these distances to the low depth (6 m) the receivers were deployed at and the corresponding higher multipath interference.

The results of Weiland *et al.* (2011), Ingraham *et al.* (2014) and Steig (2017) all have in common that noisier environments limit the detectability of JSATS tags with increasing distance to the source. For successful decoding, the SNR between the signal and background noise is crucial. In environments with higher background noise levels, SNR is smaller at shorter distances given signal attenuation stays the same. Even though the presented metrics are very different, measured detection ranges coincide with those measured in the Wachau valley.

Of particular interest are the results of Ingraham *et al.* (2014), which were measured 500 m downstream of the dam. The Snake River is somewhat comparable to the Danube, whereas the distance to the dam and, hence, no direct noise pollution through dam operation create an environment similar to the free flowing section in the Wachau valley. Similar conditions regarding the noise level can be found at 50 and 60 dB in Steig (2017). Also the results of McMichael and Kagley (2015) were collected at sites in the Snake River, which are similar to the head of the impoundment and the impoundment at Altenwörth in regard to flow velocity and depth.

Unfortunately, no data for noise levels, especially in the frequency range the JSATS operates at, are available for the study area. Amoser and Ladich (2010) recorded ambient noise levels in the Danube at two sites, namely the impoundment at Vienna and in the free flowing section at Orth an der Donau south of Vienna, although at low frequencies between 1 - 80 kHz. Noise levels in the impoundment range between 104.7 - 114.8 dB and between 129.3 - 137.8 dB in the free flowing stretch at Orth and show only minimal variability throughout the year. Values for PSL are only available for frequencies up to 5 kHz and vary around 60 dB in the impoundment and around 95 dB in the free flowing section. Since the frequencies analyzed in this paper are considerably lower than the operating frequency of the JSATS (416.7 kHz), no direct comparison to noise levels in the Wachau can be drawn. Nevertheless, those results indicate that noise levels between both parts of the river are likely to be very different. In general, background noise is significantly greater at lower frequencies than at higher (Ingraham *et al.*, 2014; Jung

et al., 2015). Especially man made noise is usually not a significant factor above 200 kHz and main noise sources above 100 kHz are mainly from inherent thermal noise (i.e. by random vibration of water molecules), while other environmental noise sources have only a negligible effect (Pincock and Johnston, 2012).

Looking at the free flowing section in the Wachau valley, a maximum DR for the WHS4250 of 138 m was measured and 58 m as 20DE were calculated. Ingraham *et al.* (2014) calculated values for 20DE between 148-154 m during the boat tests and 75-100 m with the array in the stretch below the dam. Steig (2017) calculated 120 and 210 m as maxima for noise levels matching those measured in former study. In comparison, the WHS4250 has a lower value for 20DE but the maximum DR is between those calculated by Steig (2017). The WHS4350 shows a maximum DR of 220 m, which is a little bit higher than the values calculated by Steig (2017) and a 20DE of 116 m, which is lower than values reported by Ingraham *et al.* (2014). The SR3017 has a max DR of 242 m and a 20DE value of 276 m. Both values are higher than those published in literature and the calculated value of 20DE is even higher than the measured max DR. This indicates a weakness of using a linear regression line and of assuming a DE of 100 % at 0 m to model DE. Figure 20 reveals that the SR3017 shows high detection efficiencies until 100 m with a subsequent rapid decline. Hence, a linear regression line tends to model unrealistically high values for DE at further distances.

The head of the impoundment in the Wachau valley is most comparable to the tailrace below the Ice Harbor Dam in the Snake River in terms of flow velocity and water depth. McMichael and Kagley (2015) tested for DE with the same "fixed" method as was used in the Wachau valley in the impoundment. During their tests, the authors yielded better results than both the WHS4250 and WHS4350 in the head of the impoundment, but not than the SR3017, which showed higher values for DE at each distance up to 200 m, but no values for DE were measured at 300 m.

The impoundment of Altenwörth is best comparable to the impoundment of the Ice Harbor Dam in terms of flow velocity, but with 28 m the latter is deeper. Values measured by McMichael and Kagley (2015) are higher than those of the WHS4250 and WHS4350 and also than the SR3017 up to 100 m but at further distances the SR3017 measured higher values up to 400 m. The general better performance at the Ice Harbor Dam could be attributed to the higher depth of its impoundment and hence less multipath interference (Ingraham *et al.*, 2014).

At this point, it has to be mentioned that maximum DR might not be a good metric to consider when evaluating the performance of a telemetry system. The reason is that these values are only detected once in a while, but the majority of detections are made at distances well below. One example is the maximum DR of 242 m of the SR3017 in the free flowing section. Out of all detections, only one signal was detected at this distance and just five more were detected above 200 m. This relationship is also well described by the median values available for the Wachau valley, which are always lower than their respective means, which indicates distributions that are skewed to the right.

Hence, the metric of 20DE (the distance at which a DE of 20 % is achieved) could be better suited to set system performance in relation to each other between different studies. The drawback here is that this value is calculated based on the regression line

of the measured DE values and is, therefore, not an actual measurement. Moreover, does this value depend on how it was calculated. As shortly mentioned above, different methods are applied in literature. While Ingraham *et al.* (2014) use a linear regression with the assumption that at 0 m the DE must be 100 % (hence, the regression line intersects the y-axis at 1, this was also used for the Wachau data), Kessel *et al.* (2014) suggest presenting DE metrics with use of a logistic regression (Huvneers *et al.* (2016) use it to estimate the distance at which DE equals 50 %) and McMichael *et al.* (2010) do not mention how they collected their result for 20DE at all. Accordingly, comparison between published detection ranges is not always easy and should only be made with caution. The calculation method as suggested by Ingraham *et al.* (2014) might not be the best fitting model for the present data from the Wachau valley because a linear regression line does not describe the decline of DE with distance for any combination of receiver model and habitat as the best fitting model. Furthermore, the assumption that at 0 m the DE has to be 100 % and the subsequent intersection of the regression line through the y-axis has to be criticized as well. Through this assumption, the model loses accuracy and the values might be far off those which can be expected in the field. Good examples for a bad fit are the values of 20DE for the SR3017 in the head of the impoundment and the free flowing section, which are as high or higher as the value for max DR which were both only measured once (Table 8). Thus, a DE of 20 % at these distances seems to be unrealistic. Due to those peculiarities in performance, a better practice seems to be choosing the best fitting model for each receiver on its own. This indication is strengthened by the pattern of how DE declines with distance. While the WHS4250 and WHS4350 show a uniform decline the SR3017 shows high detection efficiencies until 100 to 150 m (depending on the habitat), to decrease abruptly thereafter in all habitats (compare with Figure 20). The WHS3250 shows a rather uniform decline (although vast scattering) at a higher level than the JSATS based receivers. It was only tested for its DE in the impoundment.

In summary, it gets obvious that many different values for detection range and a vast amount of different metrics, definitions and collecting methods for its identification were published in literature so far (Melnychuk, 2012; Kessel *et al.*, 2014). This supports confusion between results with negative impacts on their comparability. Thus, the establishment of a comparable range testing culture among the scientific community is strongly recommended as pointed out already by Kessel *et al.* (2014). Due to the demonstrated difference in performance depending on the habitat and environmental conditions, it is recommended to test telemetry systems especially in the most representative sites of the study area (Pincock and Johnston, 2012; Kessel *et al.*, 2014). If differences between these areas of interest occur in regards of their abiotic parameters and, hence, in the expected performance of the telemetry system, the worst scenario should be taken as benchmark (Hobday and Pincock, 2011), if all parts are of same interest regarding tracking of animals. Moreover, it has to be considered that internally placed tags could have lower detection ranges due to signal attenuation through the fish body (Brownscombe *et al.*, 2019) than those used during performance tests.

Even though the JSATS based receivers performed similar in the Danube as during other studies in terms of their detection range and detection efficiency, its successful

performance in those studies is highly dependent on the way it was used. As discussed above, detection ranges in consulted studies were of minor importance because the areas where fish could pass were either confined in space at dams or in fish ladders (Jung *et al.*, 2015; Li *et al.*, 2015a, 2018) or the receivers were spread across the river at bridges creating bottlenecks, which are narrow and monitored by two receivers from both sites (McMichael *et al.*, 2010; Li *et al.*, 2015b). Since the circumstances for the sterlet monitoring do not allow for any of those options and detection ranges are too low to cover the whole river width, the JSATS is not the right system for a long-term monitoring of juvenile sterlets with fixed listening stations due to the low amount of receivers available.

5.1.4 Abiotic Parameters

Abiotic data for tests in the Wachau valley are available for all seasons only for the WHS4250 receiver. The other receivers were used during a small amount of tests, which makes the data base insufficient for any interpretations of abiotic parameters (compare with Table 3). Moreover, even though the WHS4250 operates in the boundaries of the JSATS like the WHS4350 and the SR3017, it might not be comparable as already shown by the results and discussion above. The WHS3250 is a completely different system and cannot be compared either. Hence, the following discussion only refers to the WHS4250.

While water temperature and Secchi depth represent a wide range of situations occurring in the Danube, only a small range of possible discharge situations was covered as already discussed above. Since all tests were conducted in the course of tracking sessions, the small range of (low) discharge situations over a whole year can easily be explained because tracking during high discharge was too dangerous and, therefore, not conducted. During less favorable conditions, the performance of telemetry systems could be considerably lower (Hobday and Pincock, 2011) than during favorable conditions, which may lead to an overestimation of the results (Melnychuk, 2012). A negative impact of increased discharge on signal detection, as observed by Ratschan *et al.* (2017) in the Danube, is also indicated by the tests in the free flowing section despite the small number of samples.

In general, Secchi depth shows the strongest effects on receiver performance among all abiotic parameters (Figure 12). Turbid water can act as a barrier for telemetry signals (Niezgoda *et al.*, 2002) through acoustic scattering (Gjelland and Hedger, 2013) and noise production when particles hit the hydrophone (Shroyer and Logsdon, 2009). In the study area, Secchi depth shows significantly negative correlations with both, discharge and water temperature (Figure 22 and Figure 23 in the appendix). During high discharge events, water is generally more turbid than during periods with low discharge in winter and during hot months without precipitation in summer. Hence, even though high discharge events show no effect on receiver performance through flow velocity or increased noise production in the impoundment, the increased transport of suspended materials might affect it. Additionally, in slower flowing water in the impoundment, higher primary production during warmer months can be expected, which increase turbidity and potentially the scattering of telemetry signals (Shroyer and Logsdon, 2009).

No significant monotonic relationship between discharge and water temperature exists (Figure 24), which is not unexpected since both, high and low discharge situations, can occur during all seasons and, thus, water temperatures.

Water temperature affects telemetry signals through changing densities and, therefore, different signal propagation and distortion (Pincock and Johnston, 2012). In the Wachau valley, higher distances were measured when water temperatures were low. How and De Lestang (2012) observed the same effect during telemetry tests at the West coast of Australia. The authors discuss this effect being contrary to acoustic theory because acoustic signals are more likely to be absorbed in denser water. They attribute lower detection rates at higher water temperatures to increased noise production through faunal activity among other explanations, which are not relevant in a river. As mentioned above, Pincock and Johnston (2012) state inherent thermal noise, which is produced partly by vibrations of molecules, as the dominant noise source at high frequencies. Higher water temperatures could increase molecule movements and subsequently reduce detection ranges. Biofouling, as discussed by Simpfendorfer *et al.* (2008), is another possible reason limiting receiver performance over time, although of more importance for passive tracking and irrelevant for the Wachau tests because receivers were deployed at each test separately.

Looking at the different habitats, the effects are strongest and behave as expected in the free flowing section. In the impoundment, effects of discharge and water temperature are low, but Secchi depth seems to have an influence on the mean distance at which signals are decoded (Figure 12). Due to the very low amount of data available for the head of the impoundment, reasonable interpretation of the results is impossible and it was, therefore, not analyzed as separate habitat, but was included in the analysis of all habitats. Overall, only a small amount of data is available, which strengthens the need of more testing and even perhaps continuously over a longer period because effects of abiotic parameters can vary over time (Kessel *et al.*, 2014) and interactions between parameters might exist (Simpfendorfer *et al.*, 2008), which could remain undetected when analyzed separately. Since the tests in the Wachau valley were conducted in different habitats, but pooled for the sake of analysis of abiotic parameters, the important effect of depth (Ingraham *et al.*, 2014; Pinter *et al.*, 2019) is not taken into account at all and could be excluded through continuous testing at one location. Moreover, Shroyer and Logsdon (2009) remark that modeling acoustic detection distances by using other potentially relevant variables without accounting for ambient noise would be misleading because in their study all other variables were confounded with ambient noise level. Hence, future testing should include recordings of ambient noise levels preferably during a wide range of occurring abiotic situations.

5.1.5 WHS3250

The WHS3250 operates in a different system, working at a lower frequency of 76 kHz (Table 1) and is, therefore, not comparable to the JSATS based receivers. As in the JSATS, the lower frequency used in the MAP system has strengths and weaknesses in regards to the monitoring of juvenile sterlets. On the one hand, it is likely to achieve higher detection distances through the use of a lower frequency (McMichael *et al.*, 2010), but on the other hand the transmitter needs a larger acoustic element and more power resulting in a larger and heavier tag (McMichael *et al.*, 2010; Pincock and Johnston, 2012). This limits the size of fish which can be monitored. As discussed above, background noise is considered to be higher at lower frequencies (Ingraham *et al.*, 2014; Jung *et al.*, 2015), while it is negligible at higher frequencies, except from inherent thermal noise (Pincock and Johnston, 2012). In the vicinity of dams, however, background noise is high enough even at high frequencies in order to impact system performance than further away (Ingraham *et al.*, 2014), but it is still considered being higher at lower frequencies (Ingraham *et al.*, 2014; Jung *et al.*, 2015). This explains the common use of JSATS in the vicinity of dams, but for monitoring fish in a stretch which is not affected by dams at the biggest part, the advantage of achieving higher detection distances could be of higher importance. Niezgodna *et al.* (2002) demonstrated that the MAP system works in shallow water environments, where many reflections of different surfaces can be assumed. However, the system was used in a pond, which shows drastically different characteristics than a fast flowing river.

Since only tests in the impoundment are available for the WHS3250, no conclusions can be drawn in terms of detection efficiency for other habitats. In the impoundment, the receiver showed high scattering of DE over distance and no further split between the WHS3250 and SR3017 occurred in the decision tree (Figure 9). However, single events of high detection efficiencies were measured at further distances than the JSATS based receivers did (Figure 20 in the appendix). In combination with the use of a high burst interval (McMichael *et al.*, 2010; Melnychuk, 2012), higher detection distances than with the JSATS receivers could, therefore, be realized. Especially in the context of DE_{mig} (compare with Melnychuk (2012)), which might be among the most important metrics when sterlets shall be identified in a fixed receiver setup, as is planned for the monitoring in the Danube. In contrast, the SR3017 performed similar (if not better) at shorter distances, but showed a rapid decline after 150 m. Given the width of the Danube varies between 300 to 400 m, this might not be sufficient to cover it reliably also considering that detection ranges decrease in faster flowing water which occurs through the biggest part of the sampling stretch. However, due to changing environmental conditions and missing test results for the free flowing section and the head of the impoundment, more tests should be conducted to judge the suitability of the WHS3250 in the study area more accurately.

In the course of a feasibility study for a 2D-array below the hydropower plant Freudenau, this system proved its ability to locate tags in a fast flowing part of the Danube with sufficient distance to the dam. In this study, the depth of the receivers was a crucial factor in regards to the number of detections, showing a positive correlation with depth

(Pinter *et al.*, 2019). Even though Pinter *et al.* (2019) proved the system to be working in the Danube, no actual tests for detection ranges or efficiencies are available.

The tags used for range tests in this study are suitable to be inserted to fish with >750 g in order to match the 2 % rule. Even though this rule is heavily discussed and fish were already tagged where tag weights exceeded 2 % of the fish weight (discussed in Bridger and Booth (2003) and Jepsen *et al.* (2005)), it might be advantageous to chose a conservative approach. However, since the longest part of the study area has a depth of 5 m or less, radio telemetry tags might be suitable as well and were already used in the study area with success (Wagner, 2010). Due to the occurrence of shallow stretches as well as deep areas in the impoundment, also the use of combined radio and acoustic telemetry tags could yield satisfying results and should be considered for future studies in areas where both, shallow and deep water, occurs.

5.2 Net Fishing

5.2.1 Catch Per Unit Effort

As can be seen in Table 9, sampling effort was not distributed evenly over the years and neither within single years. Due to the need of catching broodstock fish for the hatchery in spring, the effort is highest because net fishing was carried out until a satisfying amount of suitable fish was caught. Autumn and winter are slightly underrepresented. To improve comparability between years, the sampling effort should be similar in each year, and within years in each season. Even though CPUE is decreasing over the years, no plausible information about abundances of sterlets in the sampling area can be yielded. CPUE is considered as a poor measure regarding changes in abundance (Harley *et al.*, 2001; Maunder *et al.*, 2006).

The fact that sterlets were caught during winter, qualifies the sampling area as wintering habitat, as well as possible feeding habitat since sterlets could be caught almost all year round.

5.2.2 Sterlets

The gear used for sampling appears to be effective in targeting sterlets but a lot of bycatch ended up in the nets too. Even though the majority of caught sterlets consists out of larger fish (Figure 16), also one smaller specimen with a total length of 280 mm was caught. Despite the large number of stocked sterlets, it remained the only smaller sterlet which ended up in the nets. Since the mesh size seems to be sufficiently small to capture juvenile sterlets, the question why not more were captured remains open. Providing evidence for the occurrence of small specimen and, therefore, an evaluation of the Life Sterlet project, remains the aim of future research. Apparently, different methods to capture small specimen have to be applied or the sampling area has to be changed because the sampled area below the hydropower plant might simply not be suitable for the youngest age classes.

According to Friedrich (2013), caught sterlets could originate from a stocking program which was carried out between 2002 to 2005. However, despite one reproducing population at Aschach, all remaining sterlet populations in the Austrian Danube are considered extinct (Friedrich, 2013), but single catches of large sterlets and juveniles in the Wachau valley, as well as at Klosterneuburg and Vienna, indicate the existence of remnant fish (Friedrich *et al.*, 2014). Holčík (1989) further mentions that, in the Kuibyshev Reservoir of the Volga, the age structure of populations developed towards younger average age classes, with fish being between 4-7 years old, and also an increasing number of old fish, which do not take part in spawning. Sterlets caught below the hydropower plant Freudenuau were used as broodstock (8020 and 8065 even repeatedly) when they had ripe gonads. If they would have spawned naturally cannot be evaluated because no natural reproduction of sterlets in this part of the Danube was reported recently. As mentioned above, it is likely that those fish are very old.

Most fish were identified as females resulting in a deviation from an expected sex ratio of 1:1 (Holčík, 1989; Falahatkar *et al.*, 2013; Havasi *et al.*, 2018). However, in sturgeons

the distribution among individuals of each gender can vary between different water bodies and seasons (Holčík, 1989; Wheeler *et al.*, 2015). Wheeler *et al.* (2015) sampled Atlantic sturgeons (*Acipenser oxyrinchus* Mitchell, 1815) in the Saco River and observed the presence of more males during spring and autumn, but more females during summer. The authors used a combination of three different techniques for sex determination. Holčík (1989) summarizes several authors and concludes that males are predominant at spawning sites, whereas females tend to be predominant among fish spending the winter in deep water. At feeding grounds the proportions of sexes are equal. How sex was determined is unfortunately not mentioned. In farmed beluga sturgeons, Falahatkar *et al.* (2013) determined the sex via gonadal histology and reported the majority of examined fish being females.

Fish sampled for this study were sexed based on their body shape, belly shape and softness, sharpness of scutes and the presence of gametes during spawning season, or a combination of features based on expert judgement. Sex determination based on the gametes was only done for fish which were used as broodstock. For four fish sex determination was not possible, hence, their sex remains unknown. However, sex determination based on external morphological differences in sturgeons was often attempted but only partially successful (Chebanov and Galich, 2011), therefore, sex ratios in this study have to be treated with caution.

Nevertheless, given the sex ratios as they were determined, females appear to be larger fish in general as they have higher weights and total lengths than males, which becomes apparent in Figures 16 and 17, as well as in Table 11. The small sample size did not allow for reliable statistical testing though. Therefore, the results are only a rough description about a part of the sterlet population directly below the hydropower plant Freudenuau.

A look at Figure 17 indicates that females with ripe gametes (f.r) in spring tend to be heavier in relation to their total length than females with unripe gametes in spring and females during other season. For the simulation, weights of all captured fish of all genders were taken into account. Hence, it is unsurprising that females which carry eggs are heavier than the average in relation to their total length.

The results from different condition factors diverge quite a bit. According to Fulton's condition factor, fish are in better condition the higher the value for K_F is (Omogoriola *et al.*, 2011). Best condition is found in females in spring and worst in males in winter. However, K_F is suitable for comparing different individual fish of the same species and it will also indicate differences related to sex, season, or place of capture (Ricker, 1975). Thus, even though it might not reflect the actual condition of the fish, information about changing conditions between sex and seasons might be gained. That said Fulton's condition factor shows a change in fish condition during the seasons with worst condition in winter, as well does it assign a better overall condition to females. For latter it has to be considered that some females were weighted carrying a good amount of eggs. The condition factor can be used for measuring gonad development (Le Cren, 1951).

The fact that Fulton's condition factor uses the value $b=3$ lets assume that small and large fish show an isometric growth, which means they increase their weight to the same extent as length increases. In other words small specimen have the same form as large specimen (Le Cren, 1951; Froese, 2006). The calculated b -value for sterlets caught

below the hydropower plant Freudenuau equals 3.91, which lets assume a higher increase in height and/or width with increasing length (Froese, 2006). Allometric growth in different sturgeon species and even at different life stages was already reported several times (Gisbert, 1999; Gisbert and Doroshov, 2006; Gisbert *et al.*, 2014) and might also explain low values for K_F and, therefore, supposed bad condition.

While K_F measures the deviation from a hypothetical ideal fish ($b=3$, isometric growth), K_n measures the deviation from an individual of the average weight for lengths (Le Cren, 1951) and is suitable for comparing condition within a sample (Froese, 2006). Latter also has the advantage that the average fish of all lengths has a value of 1, therefore the influence of length is removed (Blackwell *et al.*, 2000).

The relative condition factor for sterlets in the sampling area ranges between 0.56-1.60 for females and between 0.74-1.31 for males (Table 10), with mean values of 1.08 and 0.97, respectively (Table 12). A $K_n > 1$ indicates good condition (Zubia *et al.*, 2014), therefore, females are in good condition and slightly better than males. In general, K_n produces similar results as K_F , as it assigns better overall condition to females and it shows a decline from spring to winter. Moreover, does K_n assign good condition to the majority of fish, which matches to the observations in the field.

The values for condition factors in Table 13 show a clear difference between females with ripe and with unripe gametes in the years 2018 and 2020. Ripe females show higher values for both condition factors than unripe females do. Hence, the overall better conditions of females than in males and unknowns might be attributed to the amount of eggs present. According to the calculated condition factors, unripe females appear to be in bad condition.

In 2019, the high values are indebted to a malfunctioning scale, which was used during spawning season. Therefore, the values have to be taken with caution and the big difference to both other years is likely to be distorted. Hence, no profound interpretation of the differences between ripe and unripe females for 2019 can be done at this point.

In total, eight sterlets were recaptured at least once. Only in three fish increasing lengths could be observed, whereby two fish (8020 and 8065) grew 1 cm and one fish (1324) grew 8 cm (compare with Table 14). However, all recaptures could originate from a stocking program conducted between 2002 to 2005 (Friedrich, 2013), as mentioned above. Hence, those fish are already very old and might have reached their maximum size. Fish weight and with it K_n showed some variation between capture events. Ripe female sterlets, which were used as broodstock, always showed a relatively high K_n . However, as mentioned above, values for weight measurements and, therefore, for K_n of 2019 have to be taken with caution. One example is the female 1324, which was unripe in 2019 despite having the highest K_n of all fish with 1.6. At the second capture in spring 2020, the same fish was unripe again with a K_n of 0.9 (compare with Table 14). Moreover, it is likely that an additional error at the initial length measurement in 2019 occurred, which would additionally increase the relative condition factor. On the other hand, the fish carried unripe eggs in 2019 and a slightly increased weight and with it a higher K_n would, therefore, be possible.

5.2.3 Population Estimation

In section 4.2.4, the results of the estimation of the sterlet population size directly below the hydropower plant Freudenuau are shown. In order to compare different approaches, both, an approach assuming a closed population (Chapman) and one assuming an open population (Jolly-Seber), were calculated. The difference is that in an open population it is assumed that immigration and emigration (births and deaths) occur whereas in a closed population those parameters are not considered (Seber, 1965). In detail the closed population approach has following assumptions (Pollock, 1991):

- the population is closed to additions and deletions
- all animals are equally likely to be captured in each sample
- marks are not lost or overlooked

Whereas the open population approach (Jolly-Seber-method) has following assumptions (Pollock, 1991):

- every animal present in the population has the same probability of survival until the next sampling time
- every animal present in the population at a particular sampling time has the same probability of capture
- marks are not lost or overlooked
- all samples are instantaneous and each release is made immediately after the sample

The results of both models used in this study are not far apart from each other. The Chapman estimator for closed populations estimates a population size of 56 individuals with a 95 % CI between 27-140 individuals for the real catch approach and 41 individuals with a 95 % CI between 18-145 individuals for the adapted approach. Since the effort varied greatly between the years 2018 and 2019, the presented results have to be treated with caution. The real population size might lie around both calculated estimations.

The JS-model for open populations estimates the population size for each sampling day considering immigration and emigration. For the years 2018-2019 the population size varies between 2-21 and for 2018-2020 between 6-48. The confidence intervals for both JS-model approaches are unsatisfying because in most cases they lie at zero and infinite. The JS-model tends to underestimate the population size because it is neither possible to estimate numbers for the first nor the last sampling day (Pfeifer, 2005).

In general, closed population models are used for studies covering a relatively short period of time (Pollock, 1980, 1991). Since netfishing for sterlets was carried out for more than two years, the open population model seems to be favored. However, according to the current status of sterlet populations in Austria (compare with Friedrich (2013) and Friedrich *et al.* (2014)), immigration is negligible as well as births. Emigration or deaths, on the other hand, cannot be excluded. Those restrictions qualify for a model

that allows only for losses (Pollock, 1991) to get a more realistic picture of the population below the hydropower plant Freudenau.

When using open population models, an important aspect when calculating the population size is the sampling intensity which is defined as the proportion of the population that is sampled at each trip and it is suggested to keep it high (more than 0.1) to get reliable results (Gilbert, 1973; Nichols *et al.*, 1981; Hightower and Gilbert, 1984). In general counts, the higher the sampling intensity and population size the more precise the estimates of population size will be (Nichols *et al.*, 1981). However, reliable estimates of the population size can also be made with lower sampling intensity but only if survival is high and sampling size is large (Hightower and Gilbert, 1984). Latter is not the case for the sterlet population in question. A look at Table 17 indicates that the sampling intensity (p_i) is above 0.1 except at sampling days six to nine and, therefore, the imprecise results for the confidence intervals in Table 16 are rather indebted by the small sample size (Gardner and Altman, 1986). Moreover, the calculation of confidence intervals for the JS-model after Seber (1965) is criticized because if parameters are underestimated its variance is underestimated as well, resulting in the confidence intervals being narrower than they should be (Manly, 1984). Subsequently, Manly (1984) formulated an alternative way to calculate confidence intervals for some parameters in question. However, quiet the contrary happens when applied on the sterlet population below the hydropower plant, since the newly calculated confidence intervals are narrower than before (Table 17).

Table 17: Number of caught sterlets (n_i), sampling intensity (p_i), population size (N_i) and both 95 % CIs after Manly (1984) for each sampling day (i).

date	sampling day (i)	caught sterlets (n_i)	p_i	population size (N_i)	lower CI	upper CI
29.03.2018	1	8				
20.07.2018	2	1	0.17	6	3	63
25.07.2018	3	2	0.17	12	6	161
07.03.2019	4	5	0.15	33	17	342
02.04.2019	5	6	0.13	46	23	501
23.07.2019	6	3	0.06	48	16	1002
04.09.2019	7	2	0.07	29	11	449
18.12.2019	8	3	0.06	48	16	1002
13.03.2020	9	1	0.08	13	7	117
20.03.2020	10	9	0.36	25	11	493
23.06.2020	11	2				

In summary, both ways to estimate the population size of the sterlet population below the hydropower plant Freudenau yield results which overlap to some extend. Maybe one option here could be a combined approach between a closed and open population approach (Pollock, 1980). Nevertheless, sampling was not designed to estimate the population size and the current estimations are rough attempts to get an idea about the population directly below the hydropower plant. Further recapture and telemetry results could help to improve or confirm those rough estimates (Friedrich *et al.*, 2016). However, as stated by Pollock (1980), "small studies may be little better than none at all". To improve results, an appropriate sampling design and model choice is crucial.

6 Conclusions

In the boundaries of the JSATS, small sized tags are available and suitable to monitor juvenile sterlets. However, due to their small size, battery life is restricted and the monitoring period of 0+ is very restricted. Since the aim of the monitoring in the course of the Life Sterlet project is to gather information about the habitat use of juvenile sterlets over the course of a year, monitoring of this age class for the time span of interest might not be possible with the material currently available. Monitoring of 1+ fish and older (before maturity) is possible, taking into account tag size and battery life. Tags available in the MAP system are too large for 0+ sterlets, but could be used for the age classes 1+ and older under consideration of the tag burden on the fish.

The performance of all receivers indicate that tracking fish in the study area is basically possible. However, receivers performed differently and the size of the Danube further restricts their application. Especially the WHS4250 and WHS4350 receivers are not able to detect tags at distances of more than 30 m in the free flowing section and the head of the impoundment reliably. The SR3017 reliably detects tags until 120 m, but given the size of the Danube and the availability of only a small amount of receivers, this does not suffice to monitor the migration of juvenile sterlets because receivers need to be deployed in pairs or more to cover the whole width. The MAP based WHS3250 showed a similar performance as the SR3017, but with a high variability and at the same time the potential to achieve high detection efficiencies at high distances. Since only two tests in the impoundment were conducted, more tests are necessary to evaluate its overall performance in other habitats. This is especially relevant because receiver performance varies among habitats and sterlets are expected to reside in the whole study site. The worst performance from the free flowing section should be taken as benchmark for designing the actual monitoring.

Detection ranges and efficiencies of the SR3017 would suffice for mobile tracking, since areas potentially used by sterlets can be observed in detail. However, fast currents, as present in the free flowing section, could limit tracking success through increased background noise and unsuccessful decodings caused by the Doppler effect. Changing abiotic conditions have been identified to interfere with the performance of telemetry systems and should, therefore, be considered in the monitoring design. Mindful of the prevailing range of abiotic parameters, an adequate functionality during unfavorable environmental conditions should be the goal.

Supporting the telemetry monitoring, net fishing could be valuable to help gather additional information about the sterlet population. Through net fishing in the Danube, insights into the sex ratio and condition of a part of the population below the hydropower plant Freudenu were gathered. Attempts of calculating the population size yielded rough estimations. For more precise estimations, the whole sampling has to be designed

for the method that fits best and is ultimately used. In order to maximize the ecological value gained from the monitoring, an approach combining telemetry and net fishing should be chosen.

List of Figures

1	The study site Wachau with the hydropower plants Melk and Altenwörth (red) and the different habitats (blue). The map is based on maps retrieved from Google Earth (earth.google.com).	10
2	Hydropower plant Freudenau South-East of Vienna. This picture was retrieved from Verbund AG (www.verbund.com).	11
3	Depth map below the hydropower plant Freudenau. The map of the area was retrieved from Google Earth (earth.google.com) and the overlaid depth chart was made using an echo sounder (see section 3.2.1).	12
4	Structure of a JSATS signal (see Steig (2017)).	13
5	The discharge (blue) and daily mean water temperature (red) during the study period at the gauging station Kienstock. The blue horizontal line marks the mean discharge ($1\,777\text{ m}^3/\text{s}$), whereas the red horizontal line marks the mean water temperature ($10.7\text{ }^\circ\text{C}$) during the study period. The gray dashed, vertical lines mark all test days.	19
6	Net locations below the hydropower plant Freudenau. Colors indicate the different seasons whereas winter, spring, summer and autumn are shown in black, green, red and orange, respectively (source: google earth).	22
7	Operating principle of a trammel net (Nédélec and Prado, 1990).	23
8	The mean and 95 % confidence intervals of DE for all receivers in each habitat based on grouped distances. ff = free slowing section, himp = head of the impoundment, imp = impoundment	28
9	Decision tree based on grouped values of DE.	30
10	The median and 95 % confidence intervals of DE for all JSATS based receivers in each habitat.	33
11	The median and 95 % confidence intervals of the distance for all JSATS based receivers in each habitat.	34
12	The mean distance at which the WHS4250 decoded signals is plotted for Q, water temperature and Secchi depth for all test days in all habitats together and in the free flowing section and the impoundment separately. Habitats are marked by symbols, whereas \circ = free flowing section, Δ = head of the impoundment and \square = impoundment.	35
13	A summary of all caught fish during net fishing.	39
14	Female sterlet, note the round belly. This picture was made during spawning season, where this individual carried many eggs.	42
15	Male sterlet, note the elongated rostrum and thin body shape.	42

16	Length Frequency diagram of caught sterlets separated by sex.	43
17	Length-Weight regression separated by sex, whereby f = females, f.r = females with ripe gametes, m = males, ? = unknown sex.	43
18	Effective detection range of a signal emitted at a low burst interval (left) and at a high burst interval (right). Modified from Steig (2017).	50
19	Data base for DE analysis.	86
20	Performance and all values of DE for each receiver in all habitats separately.	87
21	Decision tree based on the metric values of DE.	89
22	Relationship between Secchi depth and discharge with the 95 % CI in light gray. Spearman's ρ (R), the significance level (p) and the number of observations (n) are shown.	90
23	Relationship between Secchi depth and water temperature with the 95 % CI in light gray. Spearman's ρ (R), the significance level (p) and the number of observations (n) are shown.	91
24	Relationship between discharge and water temperature with the 95 % CI in light gray. Spearman's ρ (R), the significance level (p) and the number of observations (n) are shown.	92

List of Tables

1	Used receivers and their properties.	15
2	Used tags and their properties.	16
3	Test days and associated locations with values for discharge (Q, in m^3/s), water temperature (T, in °C) and Secchi depth (Sd, in cm). Used receivers for testing detection range are marked with big crosses, whereas small crosses indicate test sessions where detection efficiency was tested.	17
4	Number of nets and duration of deployment.	24
5	Number of detections per hour (n/h) and detection range of all receivers. Maximum, mean and median values of measured distance (in m) are shown.	27
6	Classification table for the decision tree based on grouped values of DE.	31
7	Overview of detection range for all habitats, including number of detections per hour (n/h) and measured maximum distance. Calculated mean and median distance are shown and all distances are in m.	32
8	Values for maximum detection range (max DR, in m), the distance at which the detection efficiency is at 20 % (20DE) and the detection efficiency at 100 and 200 m (DE100m, DE200m) from literature and field tests during this study.	37
9	Total duration of nets deployed (in h), number of caught sterlets and CPUE (in Ind/h/net) per season and year.	38
10	List of caught sterlets (n=42) showing catch date, the full PIT-ID, sex, TL (in mm) and W (in g), K_n and K_F of each fish and if it was a recapture (yes) or not.	40
11	Comparison of total length (in mm) and weight (in g) of sterlets separated by sex.	41
12	Condition factors K_n and K_F for all season and separated by sex.	44
13	Condition factors K_n and K_F for all females, ripe females (f.r) and unripe females (f.u) in spring of 2018, 2019 and 2020.	44
14	Initial capture and recapture events of eight different individuals including their TL, W and K_n at each capture event if available.	45
15	Population estimation based on the sampling years 2018 and 2019 using the Chapman estimator.	47
16	Population estimation (N) based on the sampling years 2018-2019 and 2018-2020 using the Jolly-Seber estimator. Upper and lower 95 % confidence intervals are displayed in the table.	47

17	Number of caught sterlets (n_i), sampling intensity (p_i), population size (N_i) and both 95 % CIs after Manly (1984) for each sampling day (i). . .	69
18	Frequency table for grouped values of DE and distance.	86
19	Crosstabulation of the count for classified DE and distance by habitat and receiver model.	88
20	Risk estimate, standard error and η^2 of the metric decision tree.	90

References

- Acolas, M. L., Le Pichon, C., and Rochard, E. (2017). Spring habitat use by stocked one year old European sturgeon *Acipenser sturio* in the freshwater-oligohaline area of the Gironde estuary. *Estuarine, Coastal and Shelf Science*, 196:58–69.
- Acolas, M. L., Rochard, E., Le Pichon, C., and Rouleau, E. (2012). Downstream migration patterns of one-year-old hatchery-reared European sturgeon (*Acipenser sturio*). *Journal of Experimental Marine Biology and Ecology*, 430-431:68–77.
- Ammann, A. J. (2020). Factors affecting detection probability and range of transmitters and receivers designed for the Juvenile Salmon Acoustic Telemetry System. *Environmental Biology of Fishes*, 103:625–634.
- Amoser, S. and Ladich, F. (2010). Year-round variability of ambient noise in temperate freshwater habitats and its implications for fishes. *Aquatic Sciences*, 72:371–378.
- Bemis, W. E., Findeis, E. K., and Grande, L. (1997). Part 1: Diversity and evolution of sturgeons and paddlefishes - An overview of Acipenseriformes. *Environmental Biology of Fishes*, 48:25–71.
- Bemis, W. E. and Kynard, B. (1997). Sturgeon rivers: an introduction to acipenseriform biogeography and life history. *Environmental Biology of Fishes*, 48:167–183.
- Bergé, J., Capra, H., Pella, H., Steig, T., Ovidio, M., Bultel, E., and Lamouroux, N. (2012). Probability of detection and positioning error of a hydro acoustic telemetry system in a fast-flowing river: Intrinsic and environmental determinants. *Fisheries Research*, 125-126:1–13.
- Billard, R. and Lecointre, G. (2001). Biology and conservation of sturgeon and paddlefish. *Reviews in Fish Biology and Fisheries*, 10:355–392.
- Blackwell, B. G., Brown, M. L., and Willis, D. W. (2000). Relative Weight (W_r) Status and Current Use in Fisheries Assessment and Management. *Reviews in Fisheries Science*, 8(1):1–44.
- Bănăduc, D., Rey, S., Trichkova, T., Lenhardt, M., and Curtean-Bănăduc, A. (2016). The Lower Danube River-Danube Delta-North West Black Sea: A pivotal area of major interest for the past, present and future of its fish fauna - A short review. *Science of the Total Environment*, 545-546:137–151.

- Borchers, D., Buckland, S., and Zucchini, W. (2002). *Statistics for Biology and Health: Estimating Animal Abundance - Closed Populations*. Springer-Verlag London, 1. edition.
- Bridger, C. J. and Booth, R. K. (2003). The Effects of Biotelemetry Transmitter Presence and Attachment Procedures on Fish Physiology and Behavior. *Reviews in Fisheries Science*, 11(1):13–34.
- Brooks, J. L., Boston, C., Doka, S., Gorsky, D., Gustavson, K., Hondorp, D., Isermann, D., Midwood, J. D., Pratt, T. C., Rous, A. M., Withers, J. L., Krueger, C. C., and Cooke, S. J. (2017). Use of Fish Telemetry in Rehabilitation Planning, Management, and Monitoring in Areas of Concern in the Laurentian Great Lakes. *Environmental Management*, 60:1139–1154.
- Brownscombe, J. W., Lédée, E. J., Raby, G. D., Struthers, D. P., Gutowsky, L. F., Nguyen, V. M., Young, N., Stokesbury, M. J., Holbrook, C. M., Brenden, T. O., Vandergoot, C. S., Murchie, K. J., Whoriskey, K., Mills Flemming, J., Kessel, S. T., Krueger, C. C., and Cooke, S. J. (2019). Conducting and interpreting fish telemetry studies: considerations for researchers and resource managers. *Reviews in Fish Biology and Fisheries*, 29:369–400.
- Chebanov, M. S. and Galich, E. V. (2011). *Sturgeon Hatchery Manual*. FAO Fisheries and Aquaculture Technical Paper. No. 558, Ankara.
- Cooke, S. J., Hich, S., Lucas, M., and Lutcavage, M. (2012). Biotelemetry and Biologging. In Zale, A., Parrish, D., and Sutton, T., editors, *Fisheries Techniques*, chapter 18, pages 819–881. American Fisheries Society, Bethesda, Maryland, 3. edition.
- Cooke, S. J., Midwood, J. D., Thiem, J. D., Klimley, P., Lucas, M. C., Thorstad, E. B., Eiler, J., Holbrook, C., and Ebner, B. C. (2013). Tracking animals in freshwater with electronic tags: Past, present and future. *Animal Biotelemetry*, 1(5):19.
- DeCelles, G. and Zemeckis, D. (2014). Acoustic and Radio Telemetry. In Cadrin, S. X., Kerr, L. A., and Mariani, S., editors, *Stock Identification Methods: Applications in Fishery Science (Second Edition)*, pages 397–428.
- Eckstein, P. P. (2016). *Angewandte Statistik mit SPSS - Praktische Einführung für Wirtschaftswissenschaftler*. Springer Gabler, Berlin, Deutschland, 8. edition.
- Falahatkar, B., Akhavan, S. R., Tolouei Gilani, M. H., and Abbasalizadeh, A. (2013). Sex identification and sexual maturity stages in farmed great sturgeon, *Huso huso* L. through biopsy. *Iranian Journal of Veterinary Research*, 14(2):133–139.
- Friedrich, T. (2013). Sturgeons in Austrian rivers: Historic distribution, current status and potential for their restoration. *World Sturgeon Conservation Society: Special Publication*, 5:80.

- Friedrich, T. (2017). Actions and prerequisites for sturgeon conservation in the Danube River Basin - case study LIFE Sterlet. *8th International Symposium on Sturgeons (ISS8), September 2017, Vienna, Austria.*
- Friedrich, T., Pekarik, L., and Ratschan, C. (2016). Restoration programs for the Sterlet (*Acipenser ruthenus*) in the Upper and Middle Danube. *Danube News*, 18(33):4–5.
- Friedrich, T., Schmall, B., Ratschan, C., and Zauner, G. (2014). Die Störarten der Donau: Teil 3: Sterlet, "Stierl" (*Acipenser ruthenus*) und aktuelle Schutzprojekte im Donaauraum. *Österreichs Fischerei*, 67. Jahrga:167–183.
- Froese, R. (2006). Cube law, condition factor and weight-length relationships: History, meta-analysis and recommendations. *Journal of Applied Ichthyology*, 22:241–253.
- Gardner, M. J. and Altman, D. G. (1986). Confidence intervals rather than P values: Estimation rather than hypothesis testing. *British Medical Journal*, 292:746–750.
- Gessner, J., Arndt, G. M., Tiedemann, R., Bartel, R., and Kirschbaum, F. (2006). Remediation measures for the Baltic sturgeon: Status review and perspectives. *Journal of Applied Ichthyology*, 22(Suppl. 1):23–31.
- Gilbert, R. O. (1973). Approximations of the Bias in the Jolly-Seber Capture-Recapture Model. *Biometrics*, 29(3):501–526.
- Gisbert, E. (1999). Early development and allometric growth patterns in Siberian sturgeon and their ecological significance. *Journal of Fish Biology*, 54:852–862.
- Gisbert, E., Asgari, R., Rafiee, G., Agh, N., Eagderi, S., Eshaghzadeh, H., and Alcaraz, C. (2014). Early development and allometric growth patterns of beluga *Huso huso* (Linnaeus, 1758). *Journal of Applied Ichthyology*, 30:1264–1272.
- Gisbert, E. and Doroshov, S. I. (2006). Allometric growth in green sturgeon larvae. *Journal of Applied Ichthyology*, 22(Suppl. 1):202–207.
- Gjelland, K. Ø. and Hedger, R. D. (2013). Environmental influence on transmitter detection probability in biotelemetry : developing a general model of acoustic transmission. *Methods in Ecology and Evolution*, 4:665–674.
- Green, L., Addy, K., and Sanbe, N. (1996). Measuring Water Clarity. *Natural Resources Facts*, 96(1):4.
- Harley, S. J., Myers, R. A., and Dunn, A. (2001). Is catch-per-unit-effort proportional to abundance? *Canadian Journal of Fisheries and Aquatic Sciences*, 58:1760–1772.
- Haunschmid, R., Schotzko, N., Petz-Glechner, R., Honsig-Erlenburg, W., Schmutz, S., Spindler, T., Unfer, G., Wolfram, G., Bammer, V., Hundritsch, L., Prinz, H., and Sasano, B. (2010). Leitfaden zur Erhebung der biologischen Qualitätselemente - Teil A1 - Fische.

- Havasi, M., Lefler, K. K., Takács, D., and Rónyai, A. (2018). How do long-term effects of temperature influence sex ratio, somatic and gonadal development in juvenile sterlet (*Acipenser ruthenus* L.)—An additional climate change consequence? *Aquaculture Research*, 49:3577–3585.
- Hayes, T., Usami, S., Jacobucci, R., and McArdle, J. J. (2015). Using classification and regression trees (CART) and random forests to analyze attrition: Results from two simulations. *Psychology and Aging*, 30(4):911–929.
- Hensel, K. and Holčík, J. (1997). Past and Current Status of Sturgeons in the Upper and Middle Danube River. *Environmental Biology of Fishes*, 48:185–200.
- Hightower, J. E. and Gilbert, R. J. (1984). Using the Jolly-Seber Model to Estimate Population Size, Mortality, and Recruitment for a Reservoir Fish Population. *Transactions of the American Fisheries Society*, 113:633–641.
- Hobday, A. J. and Pincock, D. (2011). Estimating Detection Probabilities for Linear Acoustic Monitoring Arrays. *American Fisheries Society Symposium*.
- Holčík, J. (1989). *The Freshwater Fishes of Europe - Vol. 1, Part II General Introduction to Fishes/Acipenseriformes*. AULA-Verlag GmbH, Wiesbaden, Germany.
- Honsig-Erlenburg, W. and Friedl, T. (1999). Zum Vorkommen des Sterlets (*Acipenser ruthenus* L.) in Kärnten. *Österreichs Fischerei*, 52:129–133.
- How, J. R. and De Lestang, S. (2012). Acoustic tracking: Issues affecting design, analysis and interpretation of data from movement studies. *Marine and Freshwater Research*, 63(4):312–324.
- Huveneers, C., Simpfendorfer, C. A., Kim, S., Semmens, J. M., Hobday, A. J., Pederson, H., Stieglitz, T., Vallee, R., Webber, D., Heupel, M. R., Peddemors, V., and Harcourt, R. G. (2016). The influence of environmental parameters on the performance and detection range of acoustic receivers. *Methods in Ecology and Evolution*, 7:825–835.
- IBM Corporation (2011). IBM SPSS Decision Trees 20. page 129.
- Ingraham, J. M., Deng, Z. D., Martinez, J. J., Trumbo, B. A., Mueller, R. P., and Weiland, M. A. (2014). Feasibility of Tracking Fish with Acoustic Transmitters in the Ice Harbor Dam Tailrace. *Scientific Reports*, 4(4090):1–8.
- Jepsen, N., Schreck, C., Clements, S., and Thorstad, E. B. (2005). A brief discussion on the 2% tag/bodymass rule of thumb. *Aquatic telemetry: advances and applications. Proceedings of the Fifth Conference on Fish Telemetry held in Europe*, pages 255–259.
- Jolly, G. M. (1965). Explicit from estimates data with both death and immigration-stochastic. *Biometrika*, 52(1/2):225–247.

- Jung, K. W., Deng, Z. D., Martinez, J. J., Geist, D. R., McMichael, G. A., Stephenson, J. R., and Graf, P. J. (2015). Performance of an acoustic telemetry system in a large fishway. *Animal Biotelemetry*, 3(17):1–9.
- Jungwirth, M., Haidvoogl, G., Hohensinner, S., Waidbacher, H., and Zauner, G. (2014). *Österreichs Donau. Landschaft - Fisch - Geschichte*. Institut für Hydrobiologie und Gewässermanagement, BOKU Wien.
- Kalmykov, V. A., Ruban, G. I., and Pavlov, D. S. (2010). Migrations and resources of sterlet *Acipenser ruthenus* (Acipenseridae) from the lower reaches of the Volga River. *Journal of Ichthyology*, 50(1):44–51.
- Kessel, S. T., Cooke, S. J., Heupel, M. R., Hussey, N. E., Simpfendorfer, C. A., Vagle, S., and Fisk, A. T. (2014). A review of detection range testing in aquatic passive acoustic telemetry studies. *Reviews in Fish Biology and Fisheries*, 24:199–218.
- Krenmayr, H. G., Hofmann, T., Mandl, G. W., Peresson, H., Pestal, G., Pistotnik, J., Reitner, J., Scharbert, S., Schnabel, W., and Schönlaub, H. P. (2002). *Rocky Austria. Eine bunte Erdgeschichte von Österreich*. Geologische Bundesanstalt, Wien, 2. edition.
- Kubala, M., Farský, M., and Pekárik, L. (2019). Migration patterns of sterlet (*Acipenser ruthenus*, Linnaeus 1758) in the Middle Danube assessed by 1 year acoustic telemetry study. *Journal of Applied Ichthyology*, 35:54–60.
- Le Cren, E. D. (1951). The Length-Weight Relationship and Seasonal Cycle in Gonad Weight and Condition in the Perch (*Perca fluviatilis*). *Society Journal of Animal Ecology*, 20(2):201–219.
- Lenhardt, M., Jarić, I., Cvijanović, G., Smederevac - Lalić, M., Gačić, Z., Mićković, B., and Nikčević, M. (2010). Sterlet (*Acipenser ruthenus* L.) as an object of research, fishery and aquaculture in Serbia. *38th IAD Conference, June 2010, Dresden, Germany*, page 5.
- Lenhardt, M., Jarić, I., Kalauzi, A., and Cvijanović, G. (2006). Assessment of extinction risk and reasons for decline in sturgeon. *Biodiversity and Conservation*, 15:1967–1976.
- Li, X., Deng, Z. D., Brown, R. S., Fu, T., Martinez, J. J., McMichael, G. A., Skalski, J. R., Townsend, R. L., Trumbo, B. A., Ahmann, M. L., and Renholds, J. F. (2015a). Migration depth and residence time of juvenile salmonids in the forebays of hydropower dams prior to passage through turbines or juvenile bypass systems : implications for turbine-passage survival. *Conservation Physiology*, 3:1–17.
- Li, X., Deng, Z. D., Fu, T., Brown, R. S., Martinez, J. J., McMichael, G. A., Trumbo, B. A., Ahmann, M. L., Renholds, J. F., Skalski, J. R., and Townsend, R. L. (2018). Three-dimensional migration behavior of juvenile salmonids in reservoirs and near dams. *Scientific Reports*, 8(1):1–12.

- Li, X., Deng, Z. D., Martinez, J. J., Fu, T., Titzler, P. S., Hughes, J. S., Weiland, M. A., Brown, R. S., Trumbo, B. A., Ahmann, M. L., and Renholds, J. F. (2015b). Three-dimensional tracking of juvenile salmon at a mid-reach location between two dams. *Fisheries Research*, 167:216–224.
- Lu, J., Deng, Z. D., Li, H., Myjak, M. J., Martinez, J. J., Xiao, J., Brown, R. S., and Cartmell, S. S. (2016). A small long-life acoustic transmitter for studying the behavior of aquatic animals. *Review of Scientific Instruments*, 87(114902):6.
- Ludwig, A., Lippold, S., Debus, L., and Reinartz, R. (2009). First evidence of hybridization between endangered sterlets (*Acipenser ruthenus*) and exotic Siberian sturgeons (*Acipenser baerii*) in the Danube River. *Biological Invasions*, 11:753–760.
- Manly, B. F. J. (1984). Obtaining Confidence Limits on Parameters of the Jolly-Seber Model for Capture-Recapture Data. *Biometrics*, 40(3):749–758.
- Maunder, M. N., Sibert, J. R., Fonteneau, A., Hampton, J., Kleiber, P., and Harley, S. J. (2006). Interpreting catch per unit effort data to assess the status of individual stocks and communities. *ICES Journal of Marine Science*, 63:1373–1385.
- McMichael, G. A., Eppard, M. B., Carlson, T. J., Carter, J. A., Ebberts, B. D., Brown, R. S., Weiland, M., Ploskey, G. R., Harnish, R. A., and Deng, Z. D. (2010). The Juvenile Salmon Acoustic Telemetry System : A New Tool. *Fisheries*, 35(1):9–22.
- McMichael, G. A., Hanson, A. C., Harnish, R. A., and Trott, D. M. (2013). Juvenile salmonid migratory behavior at the mouth of the Columbia River and within the plume. *Animal Biotelemetry*, 1(14):15.
- McMichael, G. A. and Kagley, A. (2015). Field Tests of Two Acoustic Telemetry Systems to Examine Range and Detection Efficiency. *American Fisheries Society Annual Meeting 2015, Portland, Oregon*.
- Melnichuk, M. C. (2012). Detection Efficiency in Telemetry Studies: Definitions and Evaluation Methods. In Adams, N. S., Beeman, J. W., and H, E. J., editors, *Telemetry techniques: A user guide for fisheries research*, chapter 7.2, pages 339–357. American Fisheries Society.
- Nédélec, C. and Prado, J. (1990). Definition and classification of fishing gear categories. *FAO Fisheries Technical Paper*, 222(Revision 1. Rome, FAO):92.
- Nelson, T. C., Doukakis, P., Lindley, S. T., Schreier, A. D., Hightower, J. E., Hildebrand, L. R., Whitlock, R. E., and Webb, M. A. H. (2013). Research Tools to Investigate Movements, Migrations, and Life History of Sturgeons (*Acipenseridae*), with an Emphasis on Marine-Oriented Populations. *PLoS ONE*, 8(8):22.
- Nichols, J., Noon, B., Stokes, S., and Hines, J. (1981). Remarks on the use of mark-recapture methodology in estimating avian population size. *Studies in Avian Biology*, 6:121–136.

- Niezgoda, G., Benfield, M., Sisak, M., and Anson, P. (2002). Tracking acoustic transmitters by code division multiple access (CDMA)-based telemetry. *Hydrobiologia*, 483:275–286.
- Ogle, D. H., Wheeler, P., and Dinno, A. (2020). FSA: Fisheries Stock Analysis. R package version 0.8.30. <https://github.com/droglenc/FSA>.
- Omogoriola, H. O., Williams, A. B., Adegbile, O. M., Olakolu, F. C., Ukaonu, S. U., and Myade, E. F. (2011). Length- weight relationships, condition factor (K) and relative condition factor (Kn) of Sparids, *Dentes congoensis* (Maul, 1954) and *Dentes angolensis* (Maul and Poll, 1953), in Nigerian coastal water. *International Journal of Biological and Chemical Sciences*, 5(2):739–747.
- Pfeifer, M. A. (2005). Ein verbessertes Schätzverfahren für Gesamtpopulationsgrößen bei Tagfaltern und anderen Invertebraten. *Linzer biol. Beitr. = Verh.*, 37(1):113–128.
- Pincock, D. G. and Johnston, S. V. (2012). Acoustic Telemetry Overview. In Adams, N. S., Beeman, J. W., and Eiler, J. H., editors, *Telemetry Techniques: A User Guide for Fisheries Research*, chapter 7.1, pages 305–338. American Fisheries Society.
- Pinter, K., Sonten, L., and Meulenbroek, P. (2019). A Feasibility study for 2D telemetry as a means to monitor the migration behavior of potamodromous cyprinid species at the hydropower plant Freudenu, Vienna. page 16.
- Pollock, K. H. (1980). Capture-Recapture Models: A Review of Current Methods, Assumptions and Experimental Design. *Department of Statistics, North Carolina State University*, page 32.
- Pollock, K. H. (1991). Review papers: Modeling Capture, Recapture, and Removal Statistics for Estimation of Demographic Parameters for Fish and Wildlife Populations: Past, Present, and Future. *Journal of the American Statistical Association*, 86(413):225–238.
- Pollock, M. S., Carr, M., Kreitals, N. M., and Phillips, I. D. (2015). Review of a species in peril: what we do not know about lake sturgeon may kill them. *Environmental Reviews*, 23(1):30–43.
- Proakis, J. G. and Salehi, M. (2008). *Digital Communications*. McGraw-Hill, New York, 5. edition.
- R Core Team (2020). *R: A language and environment for statistical computing*. R Foundation for Statistical Computing, Vienna, Austria.
- Rasch, D. and Kubinger, K. D. (2006). *Statistik für das Psychologiestudium*. Elsevier GmbH, München, Deutschland, 1 edition.
- Ratschan, C., Zauner, G., and Jung, M. (2017). Der Sterlet im oberen Donautal – Identifikation der Laichhabitats mittels Telemetrie, Endbericht 2016. *ezb - TB Zauner GmbH, Technisches Büro für Gewässerökologie und Fischereiwirtschaft*, page 67.

- Ricker, W. E. (1975). *Computation and Interpretation of Biological Statistics of Fish Populations*. Bulletin of the Fisheries Research Board of Canada.
- Rothman, K. J. (1978). A Show of Confidence. *The New England Journal of Medicine*, 299(24):1362–1363.
- Sandu, C., Reinartz, R., and Bloesch, J. (2013). Sturgeon 2020 - A program for the protection and rehabilitation of Danube sturgeons. *Danube Sturgeon Task Force (DSTF) & EU Strategy for the Danube River (EUSDR) Priority Area (PA) 6 - Biodiversity*, page 24.
- Seber, G. A. F. (1965). A note on the multiple-recapture census. *Biometrika*, 52(1/2):249–259.
- Shroyer, S. M. and Logsdon, D. E. (2009). Detection Distances of Selected Radio and Acoustic Tags in Minnesota Lakes and Rivers. *North American Journal of Fisheries Management*, 29(4):876–884.
- Simpfendorfer, C. A., Heupel, M. R., and Collins, A. B. (2008). Variation in the performance of acoustic receivers and its implication for positioning algorithms in a riverine setting. *Canadian Journal of Fisheries and Aquatic Sciences*, 65:482–492.
- Sozer, E. M., Stojanovic, M., and Proakis, J. G. (2000). Underwater acoustic networks. *IEEE Journal of Oceanic Engineering*, 25(1):72–83.
- Stasko, A. B. and Pincock, D. G. (1977). Review of Underwater Biotelemetry, with Emphasis on Ultrasonic Techniques. *Journal of Fisheries Research Board Canada*, 34:1261–1285.
- Steig, T. (2017). Evaluation of Two Acoustic Telemetry Signal Types on Fish Passage Studies. *International Conference on Engineering and Ecohydrology for Fish Passage*.
- Strelnikova, A. P. (2012). Feeding of juvenile sterlet (*Acipenser ruthenus*, *Acipenseridae*) in the Danube River midstream. *Journal of Ichthyology*, 52(1):85–90.
- Tétard, S., Maire, A., Lemaire, M., De Oliveira, E., Martin, P., and Courret, D. (2019). Behaviour of Atlantic salmon smolts approaching a bypass under light and dark conditions: Importance of fish development. *Ecological Engineering*, 131:39–52.
- Wagner, C. (2010). Fischökologisches Monitoring im Rahmen des EU-LIFE-Projekts „Vernetzung Donau Ybbs“ mit Hilfe der Radiotelemetrie - Darstellung der Gesamtergebnisse von November 2007 bis Juni 2009 unter spezieller Berücksichtigung der saisonalen Migration und des Verhalt.
- Weiland, M. A., Deng, Z. D., Seim, T. A., LaMarche, B. L., Choi, E. Y., Fu, T., Carlson, T. J., Thronas, A. I., and Brad Eppard, M. (2011). A cabled acoustic telemetry system for detecting and tracking juvenile salmon: Part 1. Engineering design and instrumentation. *Sensors*, 11:5645–5660.

- Wheeler, C., Little, C., Wippelhauser, G., Zydlewski, G., Kinnison, M., and Sulikowski, J. (2015). Determining Sex Ratios and Sexual Maturities of Atlantic sturgeon (*Acipenser oxyrinchus oxyrinchus*) in the Saco River, ME. *Marine Sciences*.
- Wimmer, R., Wintersberger, H., and Parthl, G. A. (2012). Hydromorphologische Leitbilder - Fließgewässertypisierung in Österreich. Band 3: Große Flüsse.
- Wolfram, G. and Mikschi, E. (2007). Rote Liste der Fische (Pisces) Österreichs. pages 61–198.
- Zubia, M., Rehana, Y., Muhammad, S., Omer, M., e Zehra, L., , and Adeyemi, S. (2014). Length-Weight Relationship, Condition and Relative Condition Factor of Four Mugilid Species (Family mugilidae) from the Karachi Coast of Pakistan. *Journal Coastal Development*, 17(1):1–6.

Online References

- Elektronische hydrographische Daten (eHYD): www.ehyd.gv.at (retrieved at 24.03.2020)
- Google Earth: earth.google.com (retrieved at 10.02.2021)
- Navionics: navionics.com (retrieved at 10.02.2021)
- Verbund AG: verbund.com (retrieved at 10.02.2021)

Appendix

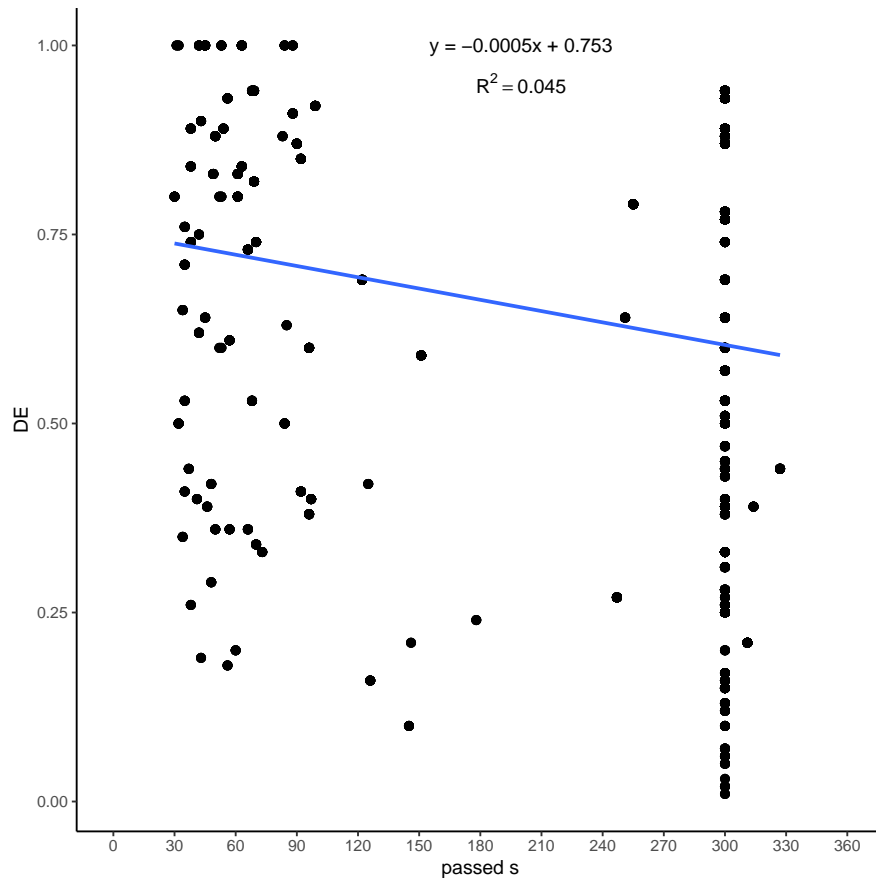


Figure 19: Data base for DE analysis.

Table 18: Frequency table for grouped values of DE and distance.

DE-trichotom		distance-trichotom	
group	frequency	group	frequency
≤ 0.36	52	≤ 35	52
0.361-0.727	50	36-86	51
≥ 0.728	52	≥ 87	51

Scale
 ○ 3,0
 ○ 2,5
 ○ 2,0
 ○ 1,5
 • 1,0

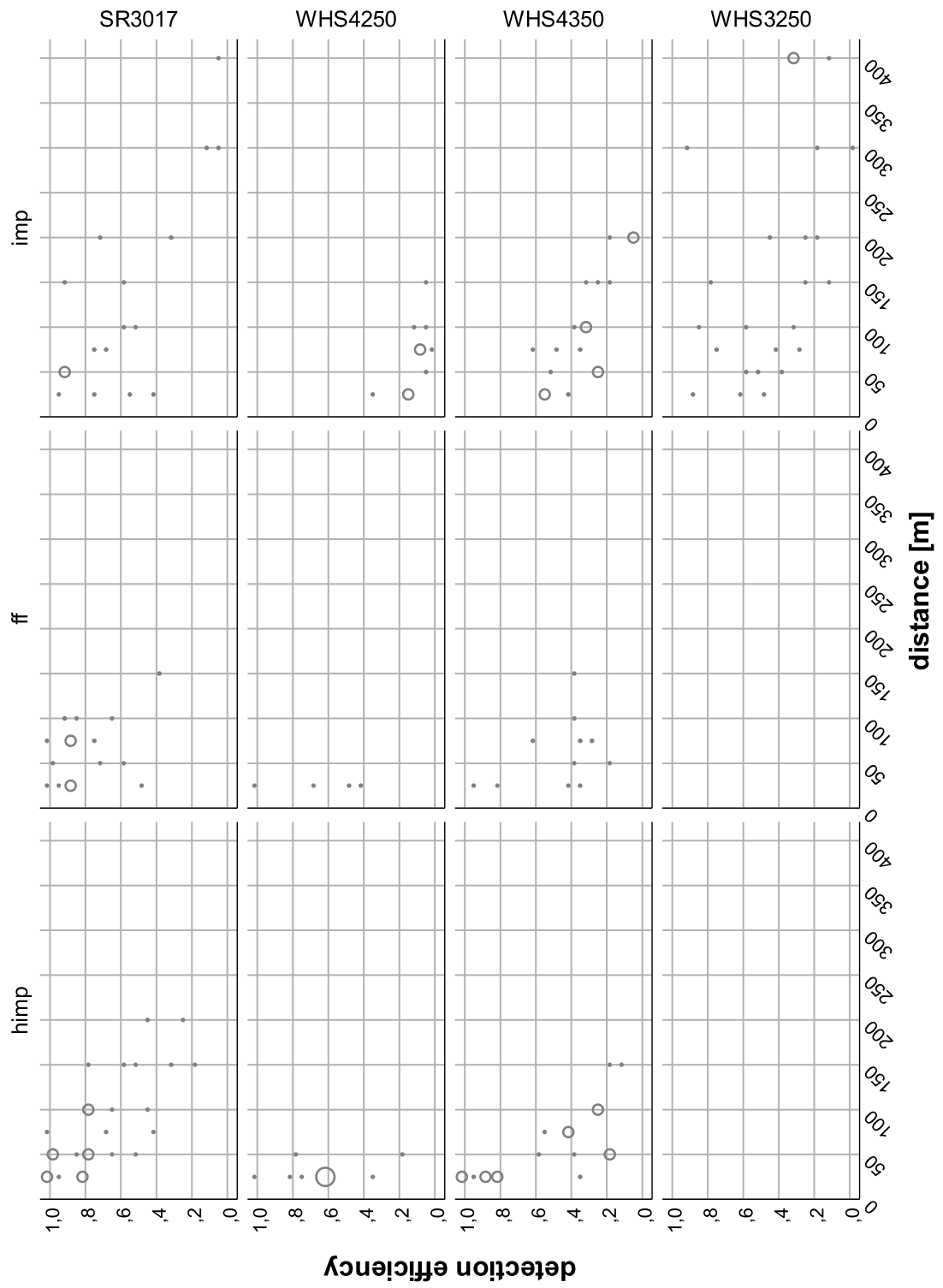


Figure 20: Performance and all values of DE for each receiver in all habitats separately.

Table 19: Crosstabulation of the count for classified DE and distance by habitat and receiver model.

receiver	habitat	DE-trichotom	distance-trichotom			Total	
			≤ 35	36-86	≥ 87		
SR3017	imp	≤ 0.36	0	0	4	4	
		0.361-0.727	2	1	3	6	
		≥ 0.728	2	3	2	7	
		Total	4	4	9	17	
	himp	≤ 0.36	0	0	3	3	
		0.361-0.727	0	6	3	9	
		≥ 0.728	7	5	2	14	
		Total	7	11	8	26	
	ff	0.361-0.727	1	2	1	4	
		≥ 0.728	4	6	2	12	
		Total	5	8	3	16	
	Total	≤ 0.36	0	0	7	7	
0.361-0.727		3	9	7	19		
≥ 0.728		13	14	6	33		
	Total	16	23	20	59		
WHS3250	imp	≤ 0.36	0	1	10	11	
		0.361-0.727	2	4	2	8	
		≥ 0.728	1	1	3	5	
		Total	3	6	15	24	
	Total	≤ 0.36	0	1	10	11	
		0.361-0.727	2	4	2	8	
		≥ 0.728	1	1	3	5	
		Total	3	6	15	24	
	WHS4250	imp	≤ 0.36	3	4	3	10
			Total	3	4	3	10
			himp	≤ 0.36	1	1	2
		0.361-0.727		3	0	3	6
≥ 0.728		4		0	4	8	
		Total	8	1	9	18	
ff		0.361-0.727	3	0	3	6	
		≥ 0.728	1	0	1	2	
		Total	4	0	4	8	
Total		≤ 0.36	4	5	3	12	
		0.361-0.727	6	0	0	6	
		≥ 0.728	5	0	0	5	
	Total	15	5	3	23		
WHS4350	imp	≤ 0.36	0	3	8	11	
		0.361-0.727	3	3	1	7	
		Total	3	6	9	18	
	himp	≤ 0.36	2	3	2	7	
		0.361-0.727	1	4	0	5	
		≥ 0.728	7	0	0	7	
		Total	10	7	2	19	
	ff	≤ 0.36	1	2	1	4	
		0.361-0.727	2	2	1	5	
		≥ 0.728	2	0	0	2	
		Total	5	4	2	11	
	Total	≤ 0.36	3	8	11	22	
0.361-0.727		6	9	2	17		
≥ 0.728		9	0	0	9		
	Total	18	17	13	48		
Total	imp	≤ 0.36	3	8	25	36	
		0.361-0.727	7	8	6	21	
		≥ 0.728	3	4	5	12	
		Total	13	20	36	69	
	himp	≤ 0.36	3	4	5	12	
		0.361-0.727	4	10	3	17	
		≥ 0.728	18	5	2	25	
		Total	25	19	10	54	
	ff	≤ 0.36	1	2	1	4	
		0.361-0.727	6	4	2	12	
		≥ 0.728	7	6	2	15	
		Total	14	12	5	31	
Total	≤ 0.36	7	14	31	52		
	0.361-0.727	17	22	11	50		
	≥ 0.728	28	15	9	52		
	Total	52	51	51	154		

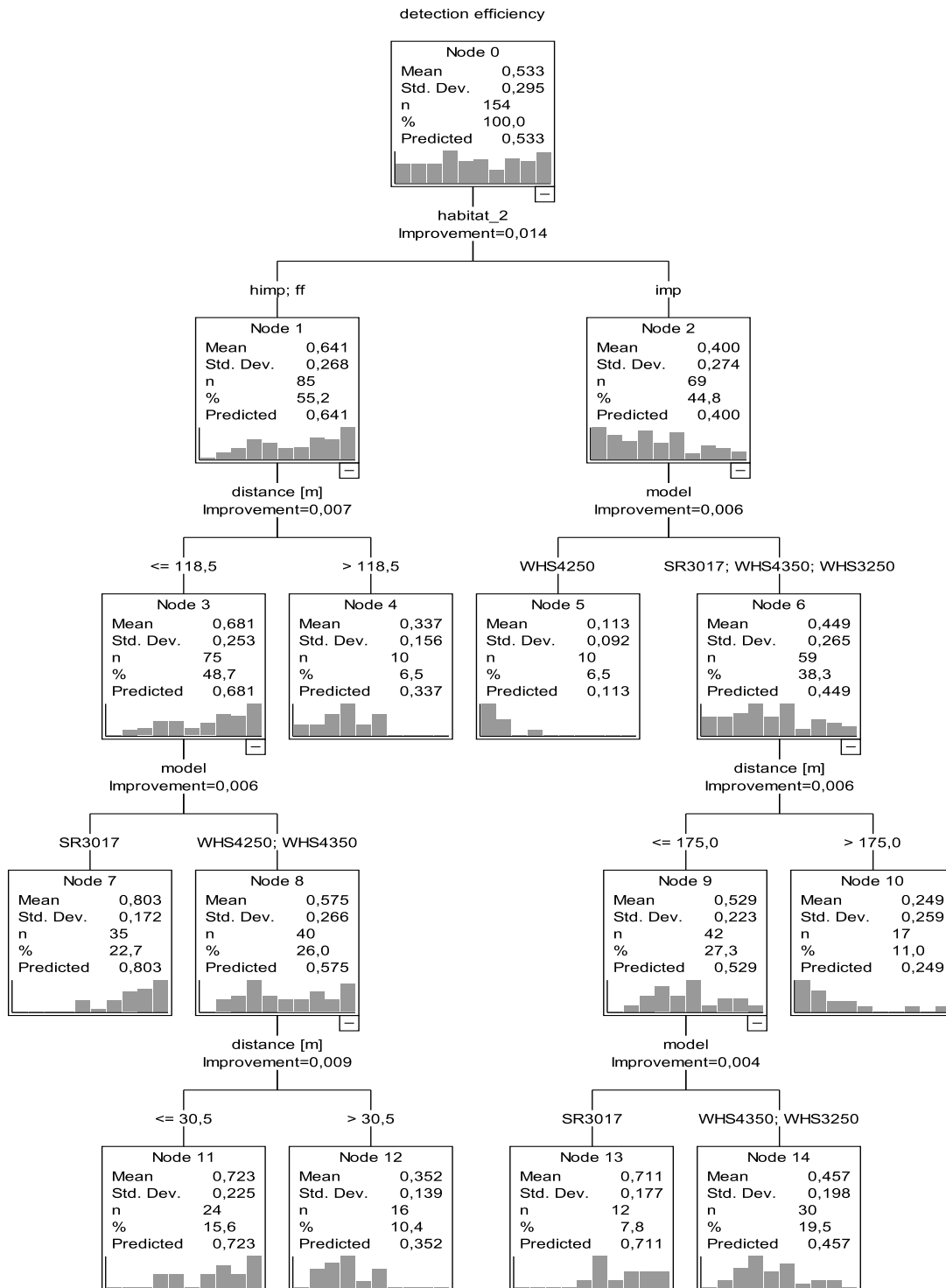


Figure 21: Decision tree based on the metric values of DE.

Table 20: Risk estimate, standard error and η^2 of the metric decision tree.

Risk		
Estimate	Std Error	η^2
0.03447	0.004	0.604

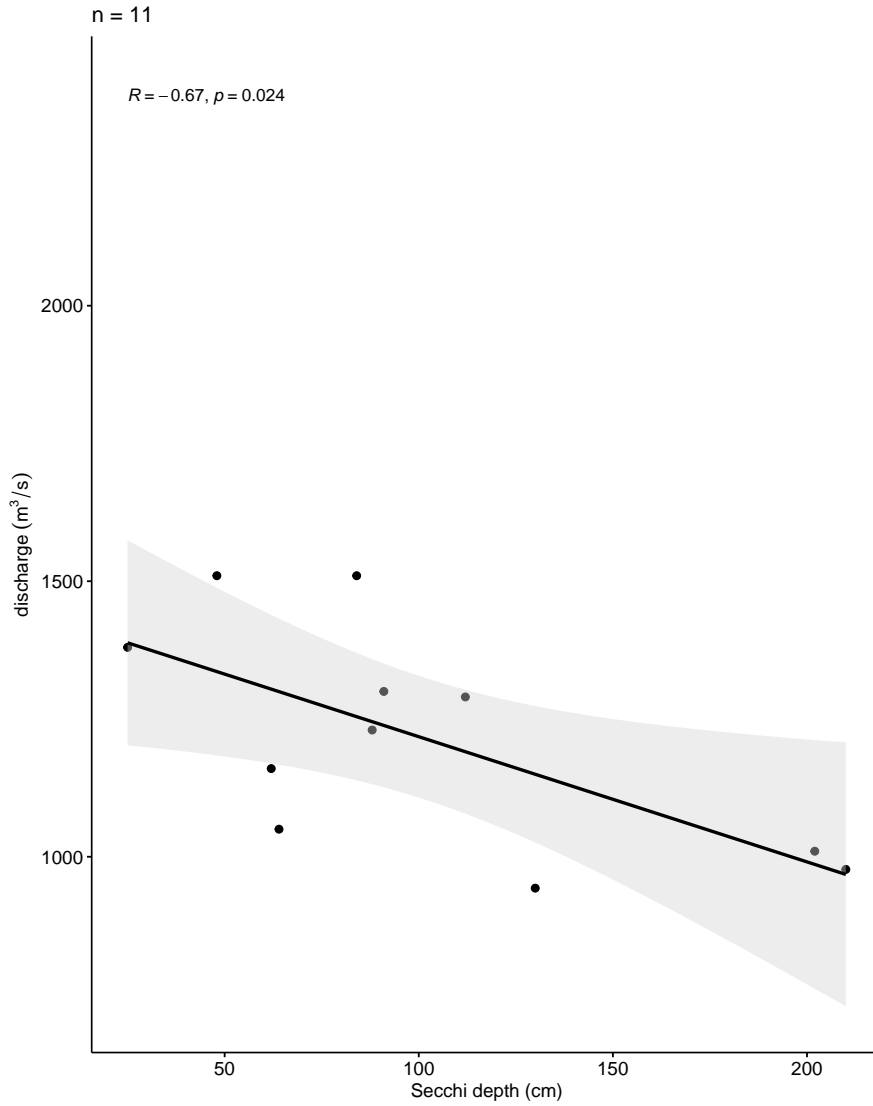


Figure 22: Relationship between Secchi depth and discharge with the 95 % CI in light gray. Spearman's ρ (R), the significance level (p) and the number of observations (n) are shown.

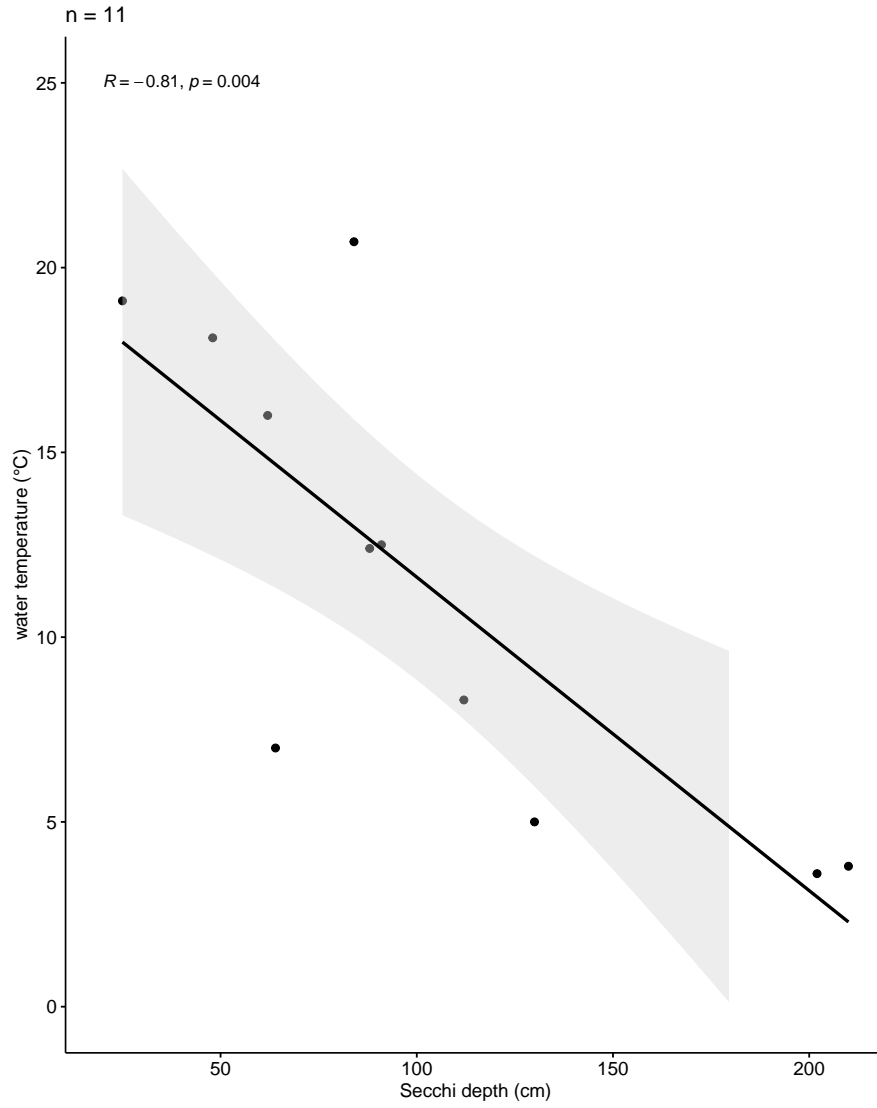


Figure 23: Relationship between Secchi depth and water temperature with the 95 % CI in light gray. Spearman's ρ (R), the significance level (p) and the number of observations (n) are shown.

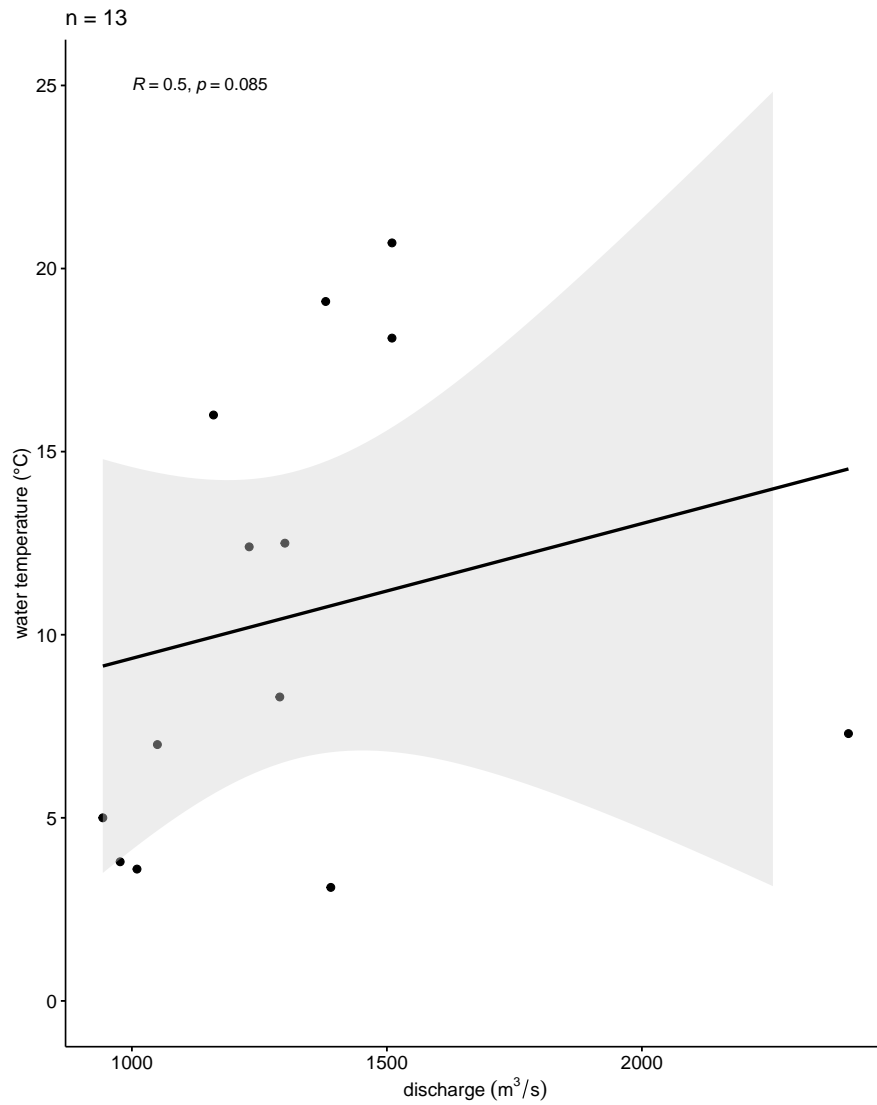


Figure 24: Relationship between discharge and water temperature with the 95 % CI in light gray. Spearman's ρ (R), the significance level (p) and the number of observations (n) are shown.